REPUBLIQUE DU CAMEROUN
Paix – Travail – Patrie
****
UNIVERSITE DE YAOUNDE I
FACULTE DES SCIENCES
DEPARTEMENT DE SCIENCES DE LA TERRE
****

Centre de Recherche et de Formation Doctorale en Sciences, Technologies et Géosciences
LABORATOIRE DE GEOSCIENCES DES FORMATIONS SUPERFICIELLES

REPUBLIC OF CAMEROUN
Peace – Work – Fatherland
****
UNIVERSITY OF YAOUNDE I
FACULTY OF SCIENCE
DEPARTMENT OF EARTH SCIENCES
****

Postgraduate School for Science, Technology and Geosciences
LABORATORY OF GEOSCIENCES OF SUPERFICIAL FORMATIONS

Geology and geodynamic interpretation of the lithospheric structure of Cameroon and its surroundings from joint analysis of gravity and passive seismic data

Presented in Fulfillment of the Requirements for the Degree Doctor of Philosophy in Earth Sciences

Par : **Goussi Ngalamo Jeannot François**
M.Sc in Earth Sciences

Sous la direction de
Ekodeck Georges Emmanuel
Professor, University of Yaoundé I-Cameroon
Estella Atekwana
Pr. Oklahoma State University - United States of America

Année Académique : 2019 - 2020

UNIVERSITE DE YAOUNDE I

FACULTE DES SCIENCES

The University of Yaoundé I

Faculty of Science

DEPARTEMENT DES SCIENCES DE LA TERRE

DEPARTMENT OF EARTH SCIENCES

ATTESTATION DE CORRECTION

Nous, membres du jury de soutenance de Thèse de Doctorat / PhDde l'étudiant GOUSSI NGALAMO Jeannot François, matricule 02Q147, intitulé : « **Geology and geodynamic interpretation of the lithospheric structure of Cameroon and itssurroundings from joint analysis of gravity and passsive seismic data** » certifions que le candidat a effectué les corrections conformément aux remarques et recommandations formulées lors de la soutenance de la dite Thèse.

En foi de quoi, nous lui délivrons cette Attestation de Correction, pour servir et valoir ce que de droit.

Fait à Yaoundé, le **1 5 MAI 2019**

Le Président du Jury

Ndjigui Paul Désiré
Professeur

Les Membres

J. AVONGO ONANA
MC

YENE ATANGANA J.Q.
M.C.

G. E. EKODECK,
Professeur.

i

DEDICATION

To

My family

ACKNOWLEDGEMENTS

SUMMARY/CONTENTS

LIST OF FIGURES

LIST OF TABLES

LIST OF ABBREVIATIONS

WGM2012   : World Gravity Model 2012

2D   : Two-dimensional

LAB   : Lithosphere-Asthenosphere Boundary

SCLM   : Sub-Continental Lithospheric Mantel

CVL   : Cameroon Volcanic Line

DLA   : Discontinuité Lithosphère – Asthénosphère

K   : Potassium

CHAMP   : Challenging Mini-satellite Payload

GRACE   : Gravity Recovery and Climate Experiment

GOCE   : Gravity field and steady state Ocean Circulation Explorer

BGI   : Bureau Gravimetric International

IFGS   : International Gravity Field Services

ILP   : International Lithosphere Program

CCSZ   : Central Cameroon shear zone

TBF   : Tcholliré-Banyo fault

SF   : Sanaga fault

Pa   : Patos shear zone

Pe   : Pernambuco shear zone

HREE   : Heavy Rare Earth Element

CEC   : The Cameroon Eburnean complex

CAR   : Central Africa Republic

EuCRUST   : European crust

EIGEN-6c   : European Improved Gravity model of the Earth by New techniques

LVZ   : Low Velocity Zone

PEM   : Parametric Earth Models

PREM   : Preliminary reference Earth Model

RGS   : Recherche de Géodésie Spatiale ()

DTU   : Danish Technical University

UNESCO   : United Nations Educational Scientific and Cultural Organization

CASZ   : Central African Shear Zone;

CVL   : Cameroon volcanic line;

SSZ   : Sanaga shear zone;

CCSZ   : Central Cameroon shear zone;

CBSE   : Cameroon broadband Seismic Experiment

TBSZ   : Tchollire-Banyo shear zone

ABSTRACT

The World Gravity Model 2012 (WGM2012) and the regional seismic model of Africa were analyzed to investigate the lithospheric structure of the Archean Congo craton and the Oubanguides orogenic belt in Cameroon. The Oubanguides orogenic belt constitutes, from northwest to southeast, the Neoproterozoic West Cameroon domain, the Paleoproterozoic-Neoproterozoic Adamawa-Yade domain, and the dominantly Neoproterozoic Yaoundé domain (the crustal expression of the suture zone between the Congo craton and the orogenic terranes).

The WGM 2012 data was analyzed to identify different gravity anomalies. The two-dimensional (2D) radially-averaged power spectral analysis was also applied to the WGM 2012 data to estimate the Moho depth and the lithosphere thickness. The termal inversion of passive seismic data was additionally apply to estimate lithosphere thickness and to constrain the spectral analysis result. Finally, 2D forward gravity models along a N-S profile and an ~ NW-SE profile was developed to image the lithospheric structure of the Precambrian entities.

The results show: 1) low gravity anomaly within the Congo craton, the Yaoundé domain, the southeastern part of the West Cameroon domain, and the northern part of the Adamawa-Yade domain; (2) a pronounced E-W trending high gravity anomaly within the southern part of the Adamawa-Yade domain; (3) a thicker crust beneath the Congo craton reaching 51 km; (4) a deeper discontinuity at ~ 139 –199 km was also found beneath the craton and interpreted to be the LAB; (5) a thinner crust beneath the Precambrian orogenic belt (centered beneath the Adamawa plateau) reaching 32 km; (6) Also, was mapped a deeper discontinuity, interpreted to represent the LAB, at ~ 72 km beneath the Precambrian orogenic belt.

The denser material beneath the southern part of the Adamawa-Yade domain is interpreted as possibly due to the densification of an under-thrust portion of the Congo craton through metacratonization processes that accompanied collision between the craton and the Oubanguides orogenic terranes. This is interpreted as possibly due to slab detachment during the Neoproterozoic Pan-African orogenic event allowing for ascendance of asthenospheric material. Ascendance of the asthenosphere provided enough heat to partially melt the lower crust and upper SCLM producing felsic magma that was intruded in the form of high-K granitoids.

The deeper Moho and LAB beneath the Congo craton and the Yaounde domain reaching ~51 km and ~200 km, respectively and the shallow Moho and LAB beneath the CASZ, the

Adamawa plateau, and the Benue trough reaching ~ 25 km and ~70 km, respectively was interpreted as due to modification of the lithosphere by a number of tectonic events that started in the Precambrian. The shallower LAB zone beneath the Oubanguides belt called in the current study the Central Africa magmatic corridor was interpreted as due to zonal sub-continental lithospheric mantle (SCLM) delaminantion along the northern edge of the Congo craton that occurred in association with collisional assembly of greater Gondwana. This allowed for mantle flow channelization during the Cenozoic within the Central Africa magmatic corridor resulting in the formation of the Cameroon Volcanic Line (CVL) and the uplift of the Adamawa plateau.

Finaly, the northwestern limit of thick lithosphere and LAB depth following partly the Central African shear zone was interpreted as the northwestern edge of the Congo craton in Cameroon and that the Yaoundé domain is an allochthon that was thrust atop the Congo craton.

RESUMÉ

Le modèle 2012 de la carte gravimétrique du monde et le modèle sismique régional de ûl'Afrique ont été analysés pour étudier la structure de la lithosphère au niveau de la partie Nord-Ouest du Craton du Congo et de la chaine des Oubanguides. La chaine des Oubanguides se compose du Nord-Ouest au Sud-Est, du domaine Neoproterozoique de l'Ouest Cameroun, le domaine Paléoprotérozoique - Néoprotérozoique de l'Adamaoua-Yade et le domaine à prédominance Néoprotérozoique de Yaoundé.

Les données extraites du modèle 2012 de la carte gravimétrique du monde ont été analysées pour identifier différentes anomalies gravimétriques. L'analyse spectrale a été appliquée aux données gravimétriques pour estimer la profondeur de la discontinuité à la base de la croûte (Moho) et la Discontinuité Lithosphère - Asthénosphère (DLA) situées à la base de la lithosphère. En outre, des modèles de profil gravimétrique en deux dimensions (2D), le premier ~ N-S et le second ~ NW-SE ont été développés pour représenter la structure des entités précambriennes.

Les résultats montrent : (1) une faible anomalie gravimétrique au niveau du craton du Congo, du domaine de Yaoundé, de la partie Sud-Est du domaine Ouest Cameroun et la partie Nord du domaine Adamaoua-Yade ; (2) une forte anomalie gravimétrique positive E-W dans la partie Sud du domaine Adamaoua –Yade ; (3) une croûte plus épaisse sous la zone cratonique atteignant 51 km ; (4) une discontinuité plus profonde à ~ 139-199 km sous le craton interprétée comme la limite entre la lithosphère et l'asthénosphère ou la Discontinuité Lithosphère - Asthénosphère (DLA) ; (5) une croûte plus fine sous la ceinture orogénique postcambrienne (centrée sous le plateau de l'Adamaoua) atteignant 32 km ; (6) une discontinuité plus profonde, associée à la DLA à ~ 104 km sous la ceinture orogénique Panafricaine coïncidant étroitement avec la direction ENE des Cisaillements Centre Africain (CCA).

Le matériau dense sous la partie Sud du domaine de l'Adamaoua-Yade a été interprété comme probablement formé à la suite de la densification d'une portion du craton à travers les processus de métacratonisation qui ont accompagné la collision entre le craton et la chaine des Oubanguides. Cette densification est interprétée comme pouvant être due au processus de délamination pendant l'évènement de l'orogenèse Panafricaine au Néoprotérozoïque, permettant la remonté de l'asthénosphère. C'est cette remontée qui a produit assez de chaleur pour fondre partiellement le manteau supérieur et la base de la croute, produisant un magma felsique injecté sous forme de granitoïdes riche en potassium (K). L'amincissement de la lithosphère au niveau de la zone des CCA serait du au processus de délamination pendant les orogenèses Precambrienne le long de la marge nord du craton du Congo. Cette structure

lithosphérique a ensuite été modifiée pendant le Cénozoïque par canalisation du flux du manteau ; ce qui a entraîné la formation de la Ligne Volcanique du Cameroun (LVC) et l'élévation du plateau de l'Adamaoua. La limite nord-ouest du craton serait superposée à la limite nord-ouest de la zone à forte épaisseur lithosphérique. Elle est associée à la bordure Sud du domaine Ouest Cameroun, cela implique que le domaine de Yaoundé serait allochtone.

Mots clés :

- Métacratonisation
- Analyse spectrale
- Vitesse de l'onde S
- Gravimétrie
- Structure lithosphérique
- Craton du Congo

CHAPTER I:

GENERAL INTRODUCTION

I.1.   BACKGROUND

To learn more about the Earth's structure, geophysicists and geologists use two main sources of information: direct evidence from rock samples and indirect evidence from geophysical data. Geophysical data are the main source of information about the deep interior of the Earth. With geophysical data, the researchers have analysed the Earth's lithosphere and mantle, and their composition, structure and dynamics. Geophysical data are divided into two categories: those received through artificial sources, and those retrieved from the natural sources. In case of artificial sources, the researchers drill holes in the Earth's surface and blast rocks and make inference about the deep conditions of the Earth's surface. While the natural sources include the data generated by earthquakes. Active sources are a time-consuming, expensive, and difficult method, because it is difficult to drill a deep hole due to the high temperature and pressure. Therefore, natural sources are the most common type of geophysical used for those purpose. However, such data cannot provide a global coverage for studying the earth's crust and upper mantle.

An alternative source of information about the Earth's interior is the gravity field and passive seismic. Gravity measurements sense density distribution inside the Earth. They play a vital role in modelling the Earth's interior especially in global and regional studies. Application of gravimetry in studying the global or regional structure of the Earth is facilitated by the advent of modern satellite gravimetry mission as well as by the rapid increase in computational power. Several satellite missions, such as Challenging Mini-satellite Payload (CHAMP) (Reigber *et al.*, 1996, 2002), Gravity Recovery and Climate Experiment (GRACE) (Tapley *et al.*, 2004) and Gravity field and steady state Ocean Circulation Explorer (GOCE) (Drinkwater *et al.*, 2003, Floberghagen *et al.*, 2011) are delivering data that allow the accuracy and spatial resolution of global gravity models to be improved drastically. The latest models based on the data from missions' have spatial resolution of about 80 km in terms of half wavelengths. These models have global and homogeneous coverage and well-known stochastic properties. Further improvement of the spatial resolution can be achieved by combining satellite gravity data with airborne and ground-based gravity data and radar altimetry data over the continents and oceans. We used in this study satellite gravity data from the world gravity model 2012 (WGM 2012) developed from the Earth Spherical Model (Balmino *et al.*, 2012; Bonvalot *et al.*, 2012) with a special resolution of ~9 km. the WGM 2012 data were compiled from land, airborne and marine surveys and satellite gravimetry from the Gravity Recovery and Climate Experiment (GRACE) mission (Bonvalot *et al.*, 2012). These data were compiled

by the "Bureau Gravimetric International" (BGI) with the support of the United Nations in association with the International Gravity Field Services (IFGS). The Bouguer gravity anomaly was computed using the spherical correction instead of the flat or regular slab correction and 2.7 g/cm^3 was used as the reduction density (Balmino *et al.*, 2012). We used the WGM 2012 for radial averaged power spectrum analysis offering a better resolution for high and short wavelength.

One of the primary interfaces of the Earth interior is the boundary between crust and mantle, with is called the Mohorovicic discontinuity, or Moho. Geophysicists widely use seismic and gravity data to investigate the depth to the Moho discontinuity. Regional and global models of the Moho are produced this way. In 1980, the establishment of International Lithosphere Program (ILP) emphasized the importance of investigation the Moho depth variation. The ILP seeks to explain the nature, dynamics, origin and evolution of the lithosphere trough international, multidisciplinary geoscience research projects and coordination. The research provides information for improved resource exploration, environmental protection, and satisfying scientific curiosity. Lithosphere in Latin means stony layer. The crust and upper portion of the mantle are the lithosphere. It is a layer where most important geological processes occur, such as mountain-Building, earthquakes and the source of volcanoes. The movements of the Earth's tectonic plates are due to the slow turning and overturning of the mantle. Edged forces are also thought to have a major role in plate tectonic.

In gravimetric, the gravity data are used to study the deep Earth structure. Generally, the gravity field functional that are computed from the global gravity field models are free air gravity anomalies or gravity disturbances. These gravity fields functional also contain the signal from terrain over continents, bathymetry variation overs oceans, ice, sediments, and different density heterogeneity inside the crust and mantle. To use gravity data for the Moho and the Lithosphere –Asthenosphere Boundarie (LAB), the aforementioned signals contributors have to be removed from the gravity data. The relation between anomalous density distribution and gravitational attraction / potential is provided by the Newton volume integral. Various numerical methods are applied to evaluate the Newton's volume integral when studying the local gravity field. A simple form of the integration is used, such as splitting the integration volume into right rectangular parallelepipeds (prisms) with constant density within each individual prism. For better accuracy of gravity field generated by a body having homogeneous /inhomogeneous density formations, the approximation of geological structures by more general geometrical forms than rectangular prisms have been adopted.

Due to the fact that few works was made to estimate the LAB depth beneath the focus study area, we used the seismic tomography model of Africa Fishwick and Bastow (2011) calculated using the waveform inversion scheme of Cara and Lévêque (1987) to map the S-wave velocity beneath the focus area and we also converted the velocities of the S-waves to temperature following the parameterization of Priestley and Mckenzie (2006) to estimate the LAB.

I.2.   NATURE AND SIGNIFICANCE OF THE PROBLEM

The tectonic setting of Cameroon and surrounding is characterised by; (i) the convergence and collision between the Congo craton and the Neoproterozoic mobile belt (Toteu *et al.* 2001) or between the Sao Francisco-Congo Craton and the West African Craton-Saharan Metacraton (Castaing *et al.*,1994 ; Abdelsalam *et al.*, 2002; Liégeois *et al.*, 2003; Oliveira *et al.*, 2006; Ngako *et al.*, 2008); (ii) an extension process with the result of an alkaline magmatism represent by anorogenic complexes and volcanic magmatism (Deruelle *et al.* 1991; Nkono *et al.* 2014); (iii) major lithospheric scale structures (such as the central Africa shear zone constitutes by the Tchollire-Banyo shear zone and the central Cameroon shear zone, and the Sanaga shear zone) (Fig.1; Toteu *et al.* 2004 Penaye *et al.*, 2006; Dawai *et al.*, 2017). Therefore, Cameroon is a key area to understand the geological and geodynamic evolution of the Neoprotorozoic mobile belt also called the North Equatorial or Panafrican fold belt (Nzenti *et al.*, 1984; 1988; 1998), the Phanerozoic Evolution (Nkono *et al.*, 2014; Tchouankoue *et al.*, 2014) and the northwestern margin of the Congo craton (Poudjom Djomani, 1994, Tadjou et al., 2009) within the African plate. The North Equatorial belt present several main challenges; (1) the origin of the Cameroon Volcanic Line (CVL) which is either associated to plume or non-plume model (e.g. Dorbath *et al.*, 1986; Fairhead & Binks 1991; Lee *et al.*, 1994; Ebinger & Sleep 1998; King & Ritsema 2000; Ritsema & Allen 2003; Deruelle *et al.*, 2007; Nkono *et al.*, 2014; Tchouankoue *et al.*, 2014), (2) the shear zones that are still poorly integrated in a regional or global tectonic model (Njonfang *et al.*, 2008), (3) similarly the northwestern margin of the Congo craton in Cameroon previously delineated on its well exposed part in southern Cameroon (Maurizot *et al.*, 1986) is still not well defined, recently evidence of Archean inheritance was found in Makenene (2.98 Ga; Tchakounte *et al.* 2017), and in Meiganga (2.55-2.72 Ga; Ganwa *et al.*, 2016). Tchakounte *et al.* (2017) suggest that the Adamawa-Yade domain might be a piece of crust detached from the Congo craton and that the limit of the Congo craton was up to the Central Cameroon shear zone (see Fig. 12 in Tchakounte *et al.* 2017),(4) geochemical evidence of magmatic arc setting of Andean-type had be found on the Sinassi

batholith within the West Cameroon domain and associated to a subduction environment (Bouyo *et al.* 2015; 2016). (5) the high horizontal gravity anomaly at lattitude 4°N has been interpreted as the result of the melting at the base of the crust (Toteu *et al.*, 2004; Boukeke *et al.* 1994). Therefore, the limit and extension of the Congo craton in Cameroon, the link between the Central Africa Shear zone, the Congo craton and the Cameroon volcanic line is not well known, and the study of the lithosphere structure can possibly contribute to better the understanding between those different geological features.
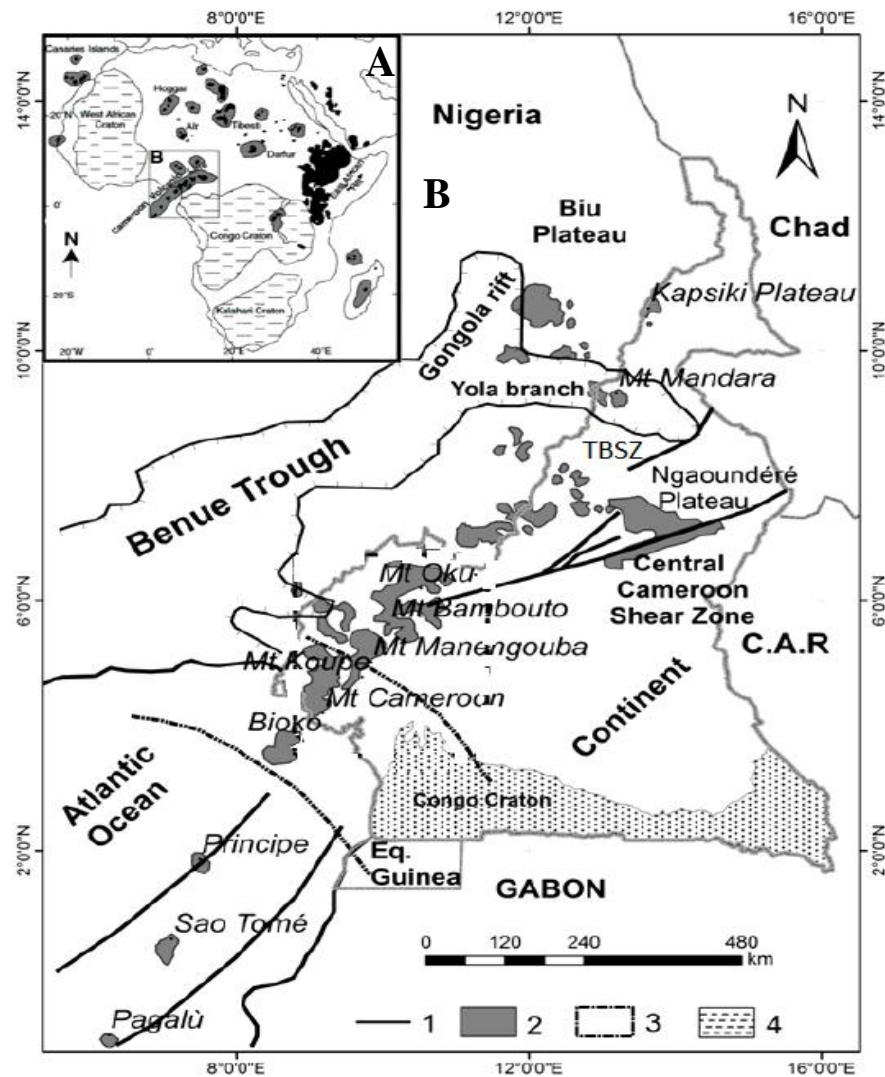
Figure 1: (A) Location map of Cameroon. (B) Simplify geological map of Cameroon and its surrounding (modify from Ngako *et al.* 2006). (1) Faults; (2) Cameroon volcanic line; (3) Oubanguides orogenic belt; (4) Congo Craton. TBSZ, Tchollire-Banyo shear zone.

I.3.   OBJECTIVES

The main goal of this study is to examine the lithospheric structure of Cameroon and its surroundings (Fig. 1A) using satellite gravity and passive seismic data. It is aim to develop new insights on the crustal and lithospheric features and evolution of Cameroon and surrounding countries, and also to contribute towards understanding how deeper lithospheric processes have influenced the main geological formations and shears zones. The basic procedure use in this work for lithospheric modelling consists of two numerical steps; (1) gravity and seismological inverse modelling and (2). gravity forward modelling.

I.4.   OUTLINE OF THE THESIS

Beside the general introduction and the conclusion, the remainder of the thesis is organized as follows:

Chapter two is a synthetic overview of the geological and geodynamic framework followed by the presentation of a study area and a synthesis of the previous work. It explains the geologic/tectonic problem and the objectives of the dissertation.

Chapter three is a brief literature overview of the Earth's structure and a detailed history of the Moho and lithosphere-asthenosphere boundaries interface studies, the isotactic crust models based on different hypotheses, and the existing crustal models from seismic studies. Furthermore, this chapter includes a discussion on geopotential theory, Earth global geopotential models, and definitions of different gravity fields such as geoid, gravity disturbance, gravity anomaly etc. Moreover, this chapter also discusses the computation of global gravity field functional from the Stokes coefficients and the transformation between spherical harmonic coefficients of various gravity field functions. Finally, in this chapter is also illustrate the methodology for Moho and lithosphere-asthenosphere boundary (LAB) depths estimation using 2D radial average power spectral analysis and the inversion of S-wave velocity.

Chapter four consists of results and discussions of gravity anomalies maps and the lithosphere structure, deduced from the gravity and passive seismic data.

CHAPTER II:
GEOLOGICAL AND GEODYNAMIC SETTING

II.1.   REGIONAL GEOLOGICAL CORRELATIONS

The end of the Precambrian period is marked in Africa and South America by the Panafrican/Bresiliano orogeny which integrates globally in the assembly process of the Gondwana supercontinent (Trompette, 1994, Arthaud *et al.*, 2008). The geological reconstruction between Africa and South America before the opening of the Atlantic Ocean to the Mesozoic reveals many lithological and structural similarities between the Panafrican belt of Central Africa and the Braziliano belt of Brazil (Fig.2; Caby *et al.*, 1991; Castaing *et al.*, 1994; Abdelsalam J., 2002; De Witt *et al.*, 2008, Van Schmus *et al.*, 2008; Archanjo *et al.*, 2009;Neves *et al.*, 2012; Ganade *et al.*, 2016). They correspond to the internal zone of the same belt because they are made up of Archean and Paleoproterozoic ages affected by the thermo-tectonic event and the magmatic activity of the Neoproterozoic (Caby, 1989 ; Castaing *et al.*, 1993 ; Trompette, 1994 ; Neves *et al.*, 2003 ;Dada, 2008 ; Dos Santos *et al.*, 2008 ; Arthaud *et al.*, 2008 ; De Wit *et al.*, 2008 ; Kalsbeek *et al.*, 2012 ; Da Silva Amaral *et al.*, 2012). Transcontinental scale shear zones affect this inner zone of the Neoproterozoic belt (Fig. 2; Castaing *et al.,* 1994; Adelsalam *et al.*, 2002). The shear zones and the Transbrezilian lineament are also observed on the African part. They represent different segments of a single, mechanically coherent large shear zone that is more than 4000 km long and associated with the end of the Panafrican/Braziliano orogeny (Caby, 1989, Trompette 1994, Dos Santos *et al.*, 2008; Arthaud *et al.*, 2008; Dawai *et al.*, 2013, 2016).

II.2.   PRECAMBRIAN OF CENTRAL AFRICA

The PCA includes geological formations whose age spread from the PaleoArchean to the late Neoproterozoic (Pin et Poidevin, 1987; Toteu *et al.* 1994; 2001; Ekwueme et Kröner, 2006; Isseini *et al.*, 2012; Penaye *et al.*, 2006; Talla takam *et al.* 2009). The Archean crustal and Paleoproterozoic evolution (Penaye *et al.* 2004) is followed in the Neoproterozoic by the Orogeny that gave birth to the Oubanguides belt (Fig. 5A; Pin and Poidevin, 1987) which is also referred to as the North Equatorial or Central African fold belt (Nzenti *et al.*, 1984; 1988; 1998; Njonfang *et al.*, 2008; Ngako *et al.*, 2006, Nkoumbou *et al.*, 2014). Within the Central African fold belt, is found several shear zones with the Central Africa shear zone the major one. We present below a history of geological studies conducted in this central part of the African continent, and the major sets of Cameroonian basements. The evolution of the Central African shear zone (CASZ) will be also addressed in more detail below.
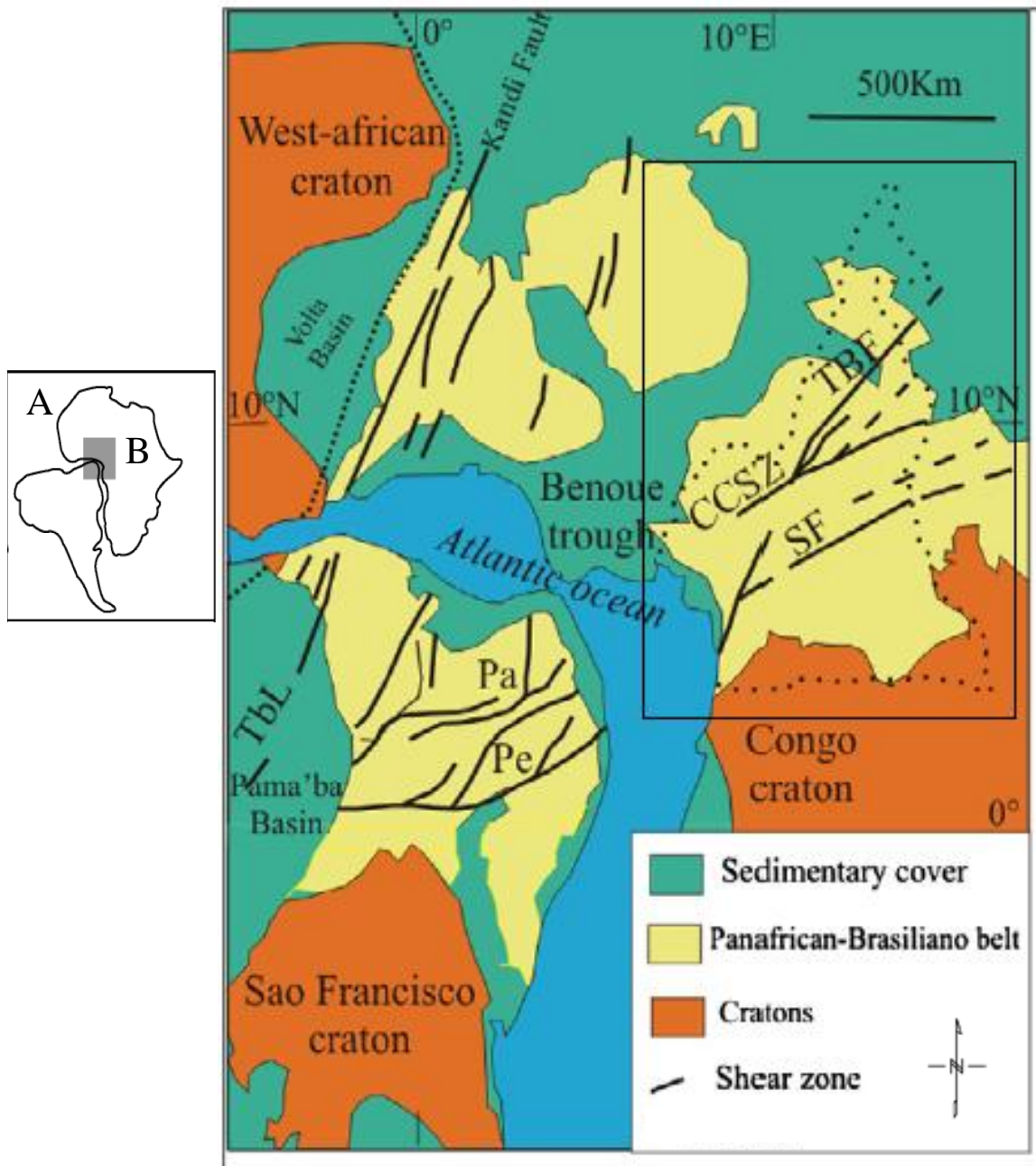
Figure 2 : (A) Location of Fig. 2B ;(B) Geological sketch map of west-central Africa and northern Brazil with cratonic masses and the Pan-African-Brasiliano provinces of the Pan-Gondwana belt in a Pangea reconstruction (modified from Castaing *et al.* (1994) and Abdelsalam *et al.,* (2002)). (C) Location of the study area. TBF: Tcholliré-Banyo fault, CCSZ: Central Cameroon shear zone, SF: Sanaga fault, Pa: Patos shear zone, Pe: Pernambuco shear zone. Dashed outline roughly marks the political boundary of Cameroon.

I1.2.1. Archean complex

In Cameroon the Archean complex is represented by the Ntem complex (Fig. 3; Pouclet *et al.*, 2007; Owona *et al.*, 2011; Boniface *et al.*, 2012; Ntomba *et al.,* 2016) also known as Ntem unit (Maurizot *et al.*, 1986; Nédélec *et al.*, 1990; Toteu *et al.*, 1994; Tchameni *et al.*, 2000, 2001; Shang *et al.*, 2007). The Ntem complex is bounded by major trusts that separate it from the Nyong unit (Fig. 3; Pouclet *et al.*, 2007; Boniface *et al.*, 2012; Ntomba *et al.* 2016) in the northwest and the Yaoundé domain (Fig.3; Nzenti *et al.*, 1988; Mvondo *et al.*, 2007; Owona *et al.* 2011) and extend into north Gabon and Equatorial Guinea (Vicat *et al.* 2001). The Ntem complex is composed of charnockites and TTG suites (Fig. 3: Pouclet *et al.*, 2007). These rocks are deformed and present locally some characteristic of shears with N-S, NE-SW to WNW-ESE sinistral or dextral trend (Tchameni *et al.*, 2010). Some of chanockites and TTG suites formations were previously dated at ca. 2.9 Ga (Delhal and Ledent, 1975; Lasserre and Soba, 1976; Toteu *et al.*, 1994). Recently some studies show evidence of early Paleoarchean (3266 Ma, by shrimp zircon U-Pb technic), magmatic activity, including charnockitic plutonism (Talla Takam *et al.*, 2009). Li *et al.* (2016) shows that the cratonic crust of Cameroon has been differentiated at 3.8 Ga attesting Paleoarchean ages (HFisotopic model). Magmatic bodies were intruded by late K-rich granitoids (2.7-2.5 Ga; Tchameni *et al.*, 2000). Geochemical and mineralogical studies show that the Ntem complex evolves in a subduction environment and are depleted of Heavy Rare Earth Element (HREE) (Nedelec *et al.*, 1989; Shang *et al.*, 2004; Ntomba *et al.*, 2016).
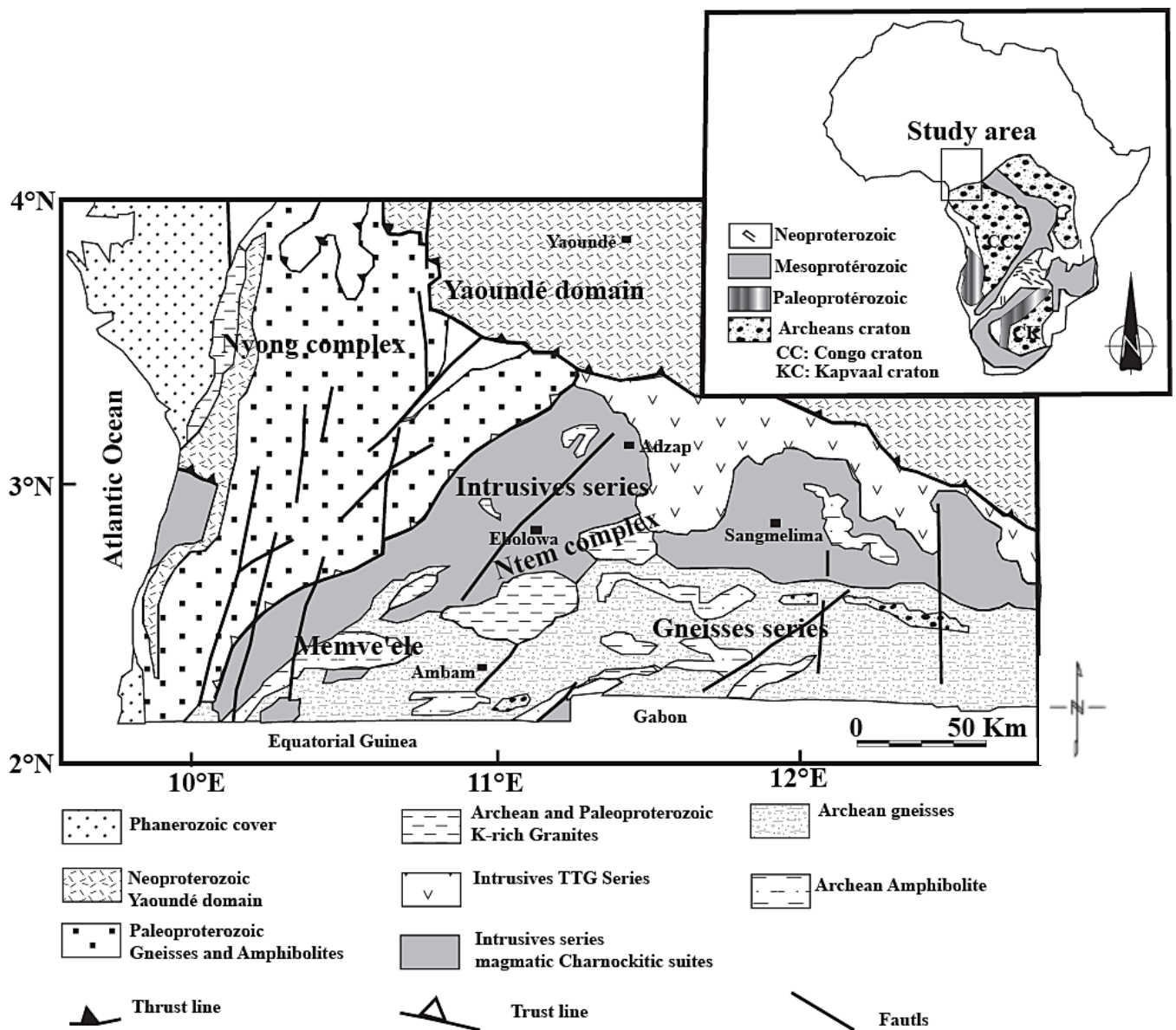
Figure 3: Simplify geolgogy map of the Ntem complex, southern Cameroon (modified after Pouclet *et al.* 2007)

II.2.2. Eburnean complex in Cameroon

The Cameroon Eburnean complex (CEC) is represented by the Nyong unit (Vicat *et al.*, 2001; Tchameni *et al.*, 2001) also call Nyong complex (Owona *et al.*, 2011; Boniface *et al.*, 2012) and the Ayna unit (Fig. 3; Maurizot *et al.*, 1986; Nédélec *et al.*, 1990; Toteu *et al.*, 1994; Tchameni *et al.*, 2000, 2001; Vicat *et al.*, 2001; Shang *et al.*, 2007). The CEC extend to the Paleoproterozoic remnant cropping out withing the Bafia serie, and the Adamawa-yade domain which are the late Neoproterozoic Panafrican fold belt (Ganwa *et al.*, 2016, Tchakounté *et al.*, 2007; 2017). The Bafia serie and the Adamawa-Yade domain would be discuss later below.

II.2.2.1. Nyong complex

The Nyong complex constitutes mafic gneisses and TTG suite, quartzites and granitoids (Fig. 3; Lerouge *et al.*, 2006; Pouclet *et al.*, 2007; Owona *et al.*, 2011; Boniface *et al.*, 2012) and the unit itself represent a SE-verging nappe atop the Ntem complex (Fig. 3; Toteu *et al.*, 1994: Pouclet *et al.* 2007). Toteu *et al.* (1994) dated a high-grade metamorphic event that led to the formation of charnockites in the Nyong unit at ~2.05 Ga and suggested that the unit might have formed as a result of Paleoproterozoic reworking of the northwestern continuation of the Ntem complex. Lerouge *et al.* (2006) documented from geochronological studies of the meta-sedimentary and plutonic rocks of the unit the presence of a major Paleoproterozoic (~2.42 Ga) sedimentation event that preceded the high-grade metamorphic event. Further, Lerouge *et al.* (2006) have shown that the complex witnessed syn-tectonic pluton intrusion event at ~2.05 Ga.

II.2.2.2. Ayna unit

The Ayna unit is located in the southeastern part of the Ntem complex in Cameroon and extends into Gabon and Congo (Fig. 4; Vicat *et al.*, 2001). It consists of rocks similar to those of the Ntem unit, but these rocks overlie discordantly those of the Ntem complex (Vicat *et al.*, 1996; 2007). The complex is also intruded by late Mesoproterozoic granitoids localized at the base of the cover rocks and thought to represent lower crustal melt (Fig. 4, Vicat *et al.*, 1996; 2007).
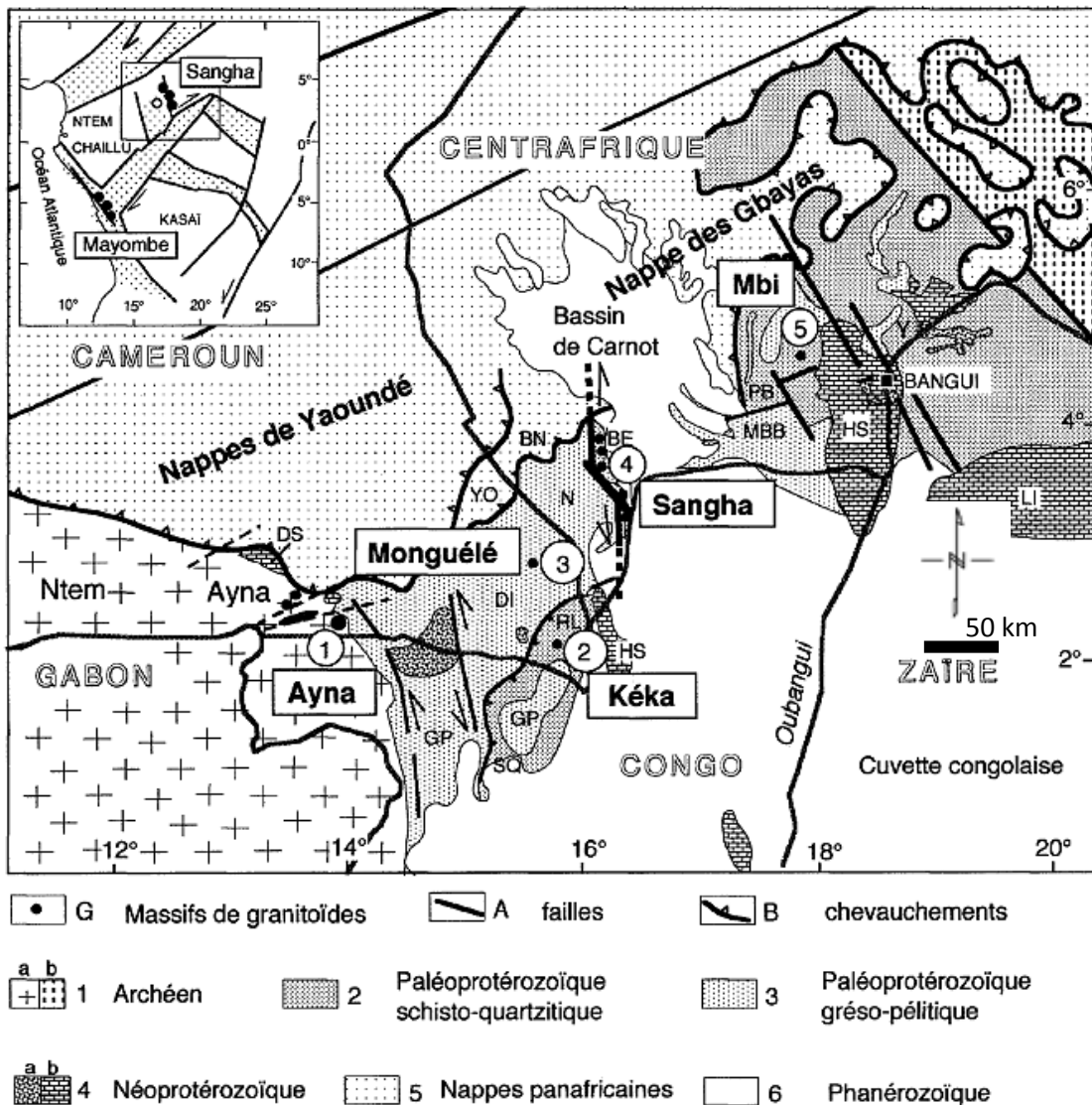
Figure 4: Geological sketch of Cameroon, Congo and CAR borders. G, granitoid and syenite bodies (1, Ayna granites; 2, Keka granodiorite; 3, Monguele syenite; 4, Sangha granites; 5, Bi granodiorite). A, main strike slip faults. B, main Pan-African thrusts. 1, Archean; a, Ntem basement; b, CAR basement reworked by the Pan-African event. 2, Paleoproterozoic sericitoshists, micaschist and quartzites (SQ, schisto-quartzitic series of Ouesso; RL, ride de la Lobeke series; BE, Bole-Est; PB, Pama-Soda series; MBB, M'Baiki-Bangui-Boali series). 4, Neoproterozoic cover; a, Cryogenian tillites and fluvio-lacustrine sandstones; b, Neoproterozoic III limestones (DS, upper Dja series; HS, Haute Sangha carbonated series; LI, Lindian). 5, Pan-African nappes (BN, Bole-Nord series; YO, Yokadouma series). 6, Phanerozoic deposits of the Cuvette du Congo and the Canot Basin (Vicat *et al.,* 2001).

II.3. OUBANGUIDES OROGENIC BELT

The Oubanguides orogenic belt also called North Equatorial or Panafrican Equatorial fold belt (Nzenti *et al.*, 1988) or Central African fold belt (Ngako *et al.*, 2008; Nkoumbou *et al.*, 2014; Bouyo *et al.*, 2016) covers several central African countries (Nigeria, Cameroon, Chad, and Central African Republic) and continues toward the East Sudan, Uganda and Tanzania (Fig. 5A. Theunissen *et al.*, 1992; Abdelsalam *et al.* 2002). The Oubanguides belt call in Central Afriac the Central Africa fold belt (Bouyo *et al.*, 2016) was formed during the convergence of the West African craton, the Congo and Sao Francisco cratons, and the Latea and Saharan metacratons (Castaing *et al.*, 1994; Abdelsalam *et al.*, 2002; Liegeois *et al.*, 2003).Toteu *et al.* (2004) suggest that the general evolution of the Central African fold belt between those cratons was controlled by their relative movements. The Central African fold belt in Cameroun and surrounding will be addressed in detail below.

II.3.1. Central African fold belt

The majority of recent works highlight three major domains in the Central African fold belt in Cameroon also called the North Equatorial or central African fold belt (Nzenti *et al.* 1988: 1998; Toteu *et al.* 2004; Bouyo *et al.*, 2015; 2016) and some of these domains extend into Equatorial Guinea, Gabon, Congo, Central African Republic, Chad and Nigeria, but we will focus mainly on the Central Africa fold belt in Cameroon.

II.3.1.1. West Cameroon domain

The western Cameroon domain crops out to the northwest of the Tchollire-Banyo shear zone which separates it from the Adamawa-Yade domain (Fig. 5; Toteu *et al.*, 2004; van Schmus *et al.*, 2008; Kwekam *et al.*, 2010; Isseini *et al.* 2012). This western domain croup out partly in the Estern part of Nigeria (Fig.5B). A major difference between this domain and the Adamawa-Yade domain is the absence of pre-Neoproterozoic rocks (Fig. 5B; Toteu *et al.*, 2004; van Schmus *et al.*, 2008; Bouyo *et al.* 2015; 2016). Rb-Sr and U-Pb zircon ages, and Sm-Nd model ages indicate that most of the rocks of the western Cameroon domain are Neoproterozoic in age with minor contamination by Paleoproterozoic crustal material (Ferre *et al.*, 1998; Toteu *et al.*, 2001; Bouyo *et al.* 2015; 2016). Different from the Paleoproterozoic crust of the Adamawa-Yade domain which was re-mobilized during the Neoproterozoic Pan-African orogenic event, the Western Cameroon domain is entirely made-up of Neoproterozoic medium-grade to high-grade metamorphic and volcano-sedimentary rock forming extensive gneissic exposures (Fig. 5) referred to as the Poli group (Toteu, 1990). Toteu *et al.* (2006b)

obtained U-Pb zircon ages ranging between 730 Ma and 920 Ma and Sm-Nd model ages ranging between 0.8 and 1.1 Ga from some of the gneisses of the Poli group. These are intruded by pre-tectonic and syn-tectonic calk-alkaline granitoid plutons (Toteu *et al.*, 1987; 2001; Penaye *et al.*, 2006: Tchameni *et al.*, 2016) as well as post-tectonic mafic and felsic dikes and granitic and rhyolitic plugs (van Schmus *et al.*, 2008). The crystalline rocks of the Western Cameroon domain are overlain by Neoproterozoic low-grade meta-sedimentary and meta-volcanic rocks interpreted as Neoproterozoic Pan-African molasses basins (Montes-Lauar *et al.*, 1997).

The dominance of Neoproterozoic ages from the rocks of the western Cameroon domain has been taken as an indication of its formation as a juvenile terrane, possibly magmatic arc that was formed within the Oubanguides orogenic belt (Penaye *et al.*, 2006; Toteu *et al.*, 2006b; Isseini *et al.* 2012). Geochemical evidence of magmatic arc setting of Andean-type had be found on the Sinassi batholith within the West Cameroon domain and associated to a subduction environment (Bouyo *et al.* 2015; 2016). As shown by the passive seismic study that there is a sharp difference in the thickness of the lithosphere across a faults just north of the Tchollire-Banyo shear zone (thicker lithosphere beneath the Adamawa-Yade domain and relatively thinner lithosphere beneath the Western Cameroon domain) (Plomerova *et al.*, 1993), the age difference between the two domains is a further indication that the shear zone is a major lithospheric suture zone.

II.3.1.2. Adamawa-Yade domain

The Adamawa-Yade domain extends between the Western Cameroon domain in the northwest and the Yaoundé domain to the south, cross cutting the center part of Cameroon and the western part of the Central African Republic (Fig. 5). The domain is characterized by the presence of Archean-Paleoproterozoic inheritance (Toteu *et al.*, 2004; 2006a; Van Schmus *et al.*, 2008; Ganwa *et al.*, 2016; Negue *et al.*, 2017). For instance, in the eastern part of the Adamawa-Yade domain, Ganwa *et al.* (2016) found the ages of metasediments of the Meiganga area to span from Archaen (2.93, 2.72 and 2.55 Ga), to Paleoproterozoic (2.12Ga) and Neoproterozoic (0.82 Ga). Toteu *et al.* (2001) also found the ages of metaquartzite of the Lom series to be 0.82 Ga in the western part, in the Foumban area, Nd isotopic data obtained on a calc-alkaline orthogneiss demonstrated that it included and inherited Archean/Paleoproterozoic component. The Paleoproterozoic inheritance was also found in the Banyo and Tchollire area in the northern part of the Adamawa-Yade domain (Toteu *et al.*, 2001; Bouyo Houketchang *et al.*, 2009)
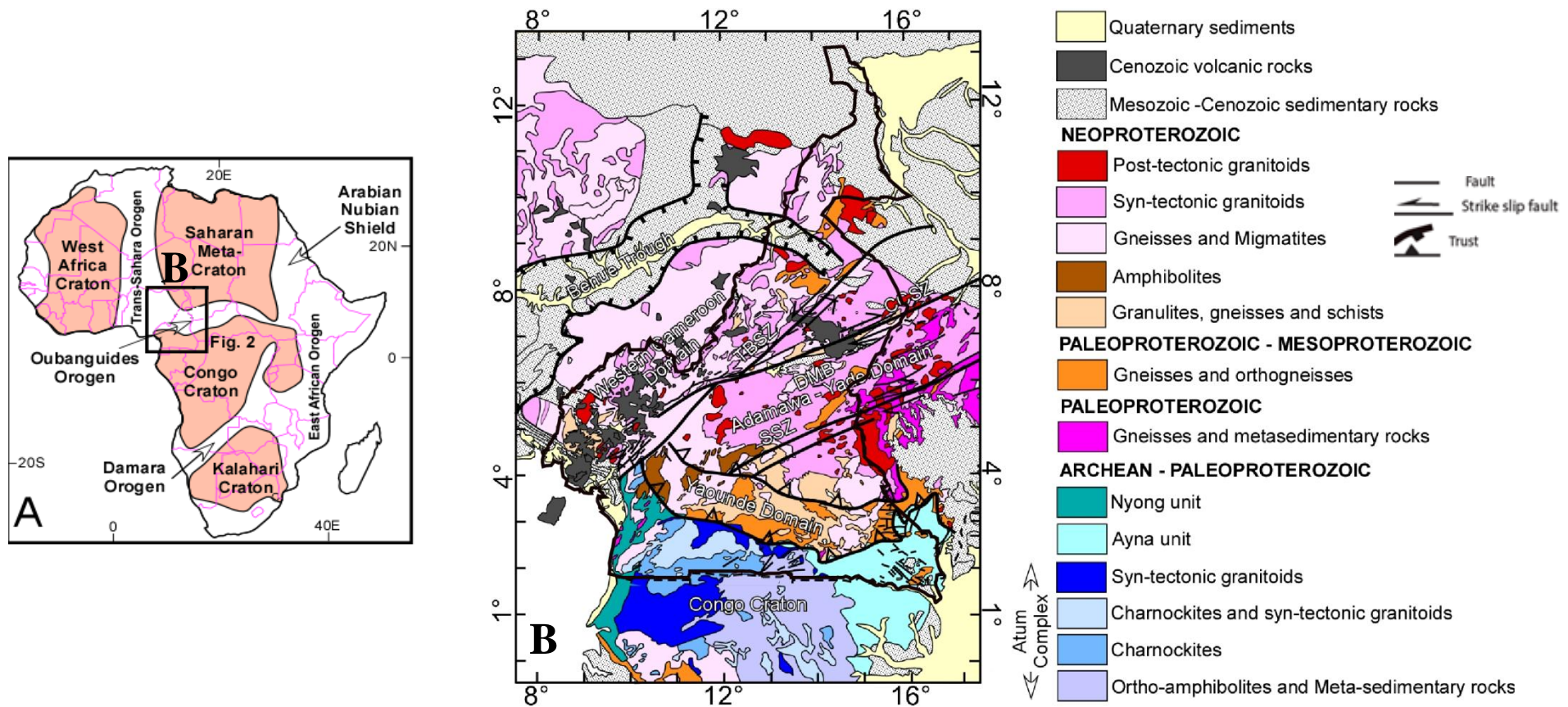
Figure 5: (A) A map showing the cratons, metacraton, and orogenic belts of Africa (After Abdelsalam *et al.* 2011); (B) Geological map of Cameroon and environs showing Central African Shear Zone and major tectonic elements of the Precambrian and Phanerozoic basement. Surface geology is modified from the International Geological Map of Africa 1:5 000 000 scale. Third Edition 1985-1990; a co-publication of GMW/UNESCO with financial support from PRGM. TBSZ = Tchollire-Banyo shear zone. DMB= Djerem-Mbere basin. CASZ = Central African shear zone. SSN = Sanaga shear zone.

One of the striking features of the Adamawa-Yade domain is the presence of widespread exposures of syn-tectonic to post-tectonic granitoids (Fig.5; e.g.; Kwékam *et al.*, 2010; 2013; Tchameni *et al*., 2006; Dawai *et al.*, 2017). Two plutonic bodies from this suite of granitoids gave U-Pb zircon ages of 620 +/- 3 Ma and 613 +/- 2 Ma (Kwekam *et al.*, 2010). The Adamawa-Yade domain is also intruded by post-tectonic gabbro-norite suite that gave a U-Pb zircon age of 576 +/- 4 Ma (Kwekam *et al.*, 2013). Kwekam *et al.* (2010, 2013) concluded that the source of magma of these bodies came from a mixture of juvenile mantle source and melting of an Archean to Paleoproterozoic lower crust. Similar conclusion was reached for the magmatic sources of other syn-tectonic to post-tectonic granitoids of the Adamawa-Yade domain (e.g. Toteu *et al.*, 1994, 2001).

Toteu *et al.* (2001; 2004) proposed, regardless of the presence of minor Paleoproterozoic juvenile mantle contribution, that the Adamawa-Yade domain is a Paleoproterozoic crust that was recycled from an Archean crust through weathering and sedimentation as well as melting and intrusion of plutonic rocks. Further, Toteu *et al.* (2001; 2004) proposed that this Paleoproterozoic crust was highly re-mobilized during the Neoproterozoic Pan-African orogenic event. Toteu *et al.* (2001; 2004) compared the evolution of the Adamawa-Yade domain to that of the Nyong complex in the northwestern edge of the Congo craton (Fig. 5). Penaye et al. (2004) also considered the Nyong complex to be the continuation of the Adamawa-Yade domain. Further, Toteu *et al.* (2001; 2004) suggested that the two tectonic entities might have shared the same geological evolution as part of the Congo craton but only that the Nyong unit remained attached to the craton while the Adamawa-Yade domain was rifted and drifted away from the craton during its early Neoproterozoic fragmentation.

The Adamawa-Yade domain is separated from the western Cameroon domain by the Tchollire-Banyo shear zone (labeled TBSZ in Fig. 5) which is suggested to be a lithospheric-scale ENE-trending sinistral strike slip shear zone (Toteu *et al.*, 2004; Njonfang *et al.*, 2008; Negue et al., 2017). This shear zone is part of the Neoproterozoic Central Africa shear zone that extends eastward across Chad and western Sudan and westward into Brazil before Gondwana fragmentation (e.g. van Schmus *et al.*, 2008). It is suggested that the Central Cameroon shear zone has been reactivated during the Cretaceous in association with the opening of the South Atlantic Ocean and this reactivation resulted in the formation of pull apart basins along the shear zone as exemplified by the Djerem-Mbere basin (Labeled DMB in Fig. 5). Plomerova *et al.* (1993) have

shown from passive seismic study that the lithosphere beneath the Tchollire-Banyo shear zone (they referred to as the Central African shear zone) is thinner where the asthenosphere is found at 120 km depth beneath the shear zone compared to 190 km depth away from the shear zone. Further, Plomerova *et al.* (1993) observed an abrupt change in the lithospheric thickness across a fault just to the north of the Tchollire-Banyo shear zone and suggested that it may represent a suture zone between different tectonic terranes. Kwekam *et al.* (2010) proposed that the Tchollire-Banyo shear zone might be the northern lithospheric boundary of the Congo craton.

II.3.1.3. Yaoundé domain

The Yaoundé domain is exposed in the northern edge of the Congo craton (Fig. 5) and extends to the Central African Republic (Fig.5B; Pin and Poidevin, 1987; Nzenti *et al.* 1988; Ngnotue *et al.*, 2012). It consists of a mixture of low-grade to high-grade metamorphic rocks of both sedimentary and igneous origin (Fig. 5B; Nzenti *et al.*, 1988; Toteu *et al.*, 1994; Tchakounte *et al.*, 2007; Mvondo *et al.* 2007; van Schmus *et al.*, 2008). These metasedimentary and meta-igneous rocks are divided into the Mbalmayo, Yaoundé, Bafia and neoproterozoic estern nappes groups (which consist of the upper Dja, the Lower Dja and the dolorite complex) (summarized in van Schmus *et al.*, 2008 and Nkoumbou *et al.* 2014). The Mbalmayo, Yaoundé and thus the eastern nappes groups correspond to the Neoproterozoic rocks within the Yaoundé domain whereas the Bafia group corresponds to the Paleoproterozoic – Mesoproterozoic rocks within the domain (Fig. 5; Nzenti *et al.,* 2008; Tchakounte *et al.,* 2007; Yonta *et al.,* 2010; Nkoumbou *et al.*, 2014). These groups are interpreted as constituting an allochthon which was emplaced during the Neoproterozoic orogenic event from north to south onto the northern edge of the Congo Craton (Toteu *et al.*, 2004). The rocks of the Mbalmayo and Yaoundé groups are of Neoproterozoic age and are made-up of metapelites, meta-sandstones, amphibolites and talc schist together with meta-plutonic rocks ranging in composition from gabbro to granite (Nzenti *et al.*, 1988; Toteu *et al.*, 2004; Yonta *et al.*, 2010; Owona *et al.*, 2011). Toteu *et al.* (2006a) documented that all rock units of the Mbalmayo and Yaoundé groups are deformed by the structures associated with the nappe emplacement. Toteu *et al.* (2004) pointed to the almost complete absence of post-tectonic granitoids within the Yaoundé domain and consider this to be a major difference between it and the Adamawa-Yade domain (Fig. 5).

The depositional age of the metasedimentary rocks of the Mbalmayo and Yaoundé groups is suggested to be post ~620 Ma given that detrital zircons from these rocks gave an age of ~620 Ma (Toteu *et al.*, 2006a). Nzenti *et al.* (1988) suggested that the sedimentary rocks of the Yaoundé group were deposited in a passive margin environment predicting that the sediment source of these rocks was the Congo craton. However, Penaye *et al.* (1993) and Toteu *et al.* (1994; 2001) used Sm-Nd isotopic data to argue for insignificant contribution from the Congo craton. Rather, Penaye *et al.* (1993) and Toteu *et al.* (1994; 2001) suggested that both the meta-sedimentary and meta-igneous rocks of the Yaoundé group were formed through mixing of juvenile Neoproterozoic and old Paleoproterozoic sources. Further, Toteu *et al.* (2006a) suggested that the source of the sedimentary rocks lies further north in the form of Neoproterozoic continental arc developed atop the Paleoproterozoic crust of the Adamawa-Yade domain. Recently Nkoumbou *et al.* (2014) used whole-rock major and trace element compositions and isotopic data within the Yaounde domain (Boumnyebel area) on metasediments and meta-igneous rocks and found that the Yaounde domain was filled with siliciclastic sediments derived from both reworked older continental crust (Paleoproterozoic to Archean in age) and Neoproterozoic juvenile volcanogenic material. Nkoumbou *et al.* (2014) also show that the Yaounde goup present the composition of island-arc basalt and considered it to be the expression of an incipient oceanisation. They interpreted these results as the expression of extensional processes to the north of the Congo craton, which led to rifting, fragmentation and limited oceanisation.

The Bafia group is made-up of meta-sandstone, biotite and amphibolite gneiss, and amphibolites (van Schmus *et al.*, 2008; Mvondo, 2009; Tchakounte *et al.* 2007; 2017). It shares common geological characteristics with the Yaoundé group in that its rock units are deformed by the nappe-related structures and that it is intruded by pre-tectonic and syn-tectonic granitoids (Toteu *et al.*, 2001; 2006a). However, the overwhelming Paleoproterozoic ages obtained from Sm-Nd model ages led to the suggestion that a major portion of the Bafia group was part of the Adamawa-Yade domain (Toteu *et al.*, 2001; 2006a; Tchakounte *et al.*, 2017). Hence, Toteu *et al.*, (2001; 2006a) suggested that the Bafia group constitutes interleaved thrust sheets made-up of Neoproterozoic, Mesoproterozoic and Paleoproterozoic rocks. Furthermore, recent study identifies three main ages goups in the Bafia area showing that the Bafia group and more broadly the Adamawa Yade domain are polycyclic, resulting from Archean, Paleoproterozoic and Neoproterozoic magmatic and tectono-metamorphic orogenic event. For instance, the protoliths of

the Nomale and Makenene migmatitic are emplaced at ca. 2.98 Ga and 2.55 Ga during Paleoproterozoic partial melting event coeval to emplacement of plutonic rocks at ca 2.07 Ga (Tchakounte *et al.* 2017). Those observations led them to suggest that, the part of Bafia group and broadly the Adamawa-Yade group was a piece of Archean/Paleoproterozoic crust detached from the Congo craton in the early neoproterozoic time as result of an extended north Congo craton margin. They also suggest that the Adamawa-Yade domain represents an Archean-Paleoproterozoic microcontinent detached from the northern margin of the Congo craton before being re-accreted with the Mayo Kebbi (magmatic) arc during the Pan-African orogeny.

The boundary between the Yaoundé domain and the Congo craton is considered to represent the crustal expression of the suture zone between the craton and the orogenic terranes to the north and that the low-grade metamorphic rocks of the Yaoundé group that show dominant sub-horizontal planar fabric represent the sole thrust of the allochthon (Nédélec *et al.*, 1990). However, it is also suggested that the northern lithospheric boundary of the Congo craton might be found further north along the Central Cameroon shear zone (TChakounte *et al.*, 2017) or along the Tchollire-Banyo shear zone (Kwekam *et al.*, 2010, Goussi Ngalamo *et al.*, 2018). Additionally, the geometry and kinematics of the structures of the Yaoundé domain are interpreted as developed from two-phase N-S contraction with the younger phase resulted in the southward emplacement of the Yaoundé allochthon onto the northern edge of the Congo craton (Toteu *et al.*, 2004; 2006a). However, Mvondo *et al.* (2003) argued that the sub-horizontal planner fabric developed during the late deformation phase within the Yaoundé domain might be in the form of pure shear extension triggered by rapid exhumation of the domain.

II.4. CENOZOIC FORMATIONS

II.4.1. Cameroon volcanic line

The Cameroon Volcanic Line (CVL) is divided into two parts; the southern part, which extends from the coast to the southern edge of the Adamawa-Plateau, and the northern part, which consists of two branches; one passing through the Adamawa Plateau and the other stretching towards the Biu Plateau in north-eastern Nigeria (Fig. 5). The CVL is underlain by Pan African basement rocks consisting mainly of shists and gneisses intruded by granite and diorites (Fitton 1987; Deruelle *et al.*, 2007, 1991; Nkono *et al.*, 2014; Nzolang *et al.*, 2005; Kamgang *et al.*, 2010 Tchouankoue *et al.*, 2012; 2014). Cretaceous sediments, mostly sandstones and small amounts of

limestone and shales, are found in the coastal plain. The volcanic rocks that comprise the CVL range in composition from Basalt to trachyte (Nzolang *et al.*, 2005; Kamgang *et al.*, 2010; 2013; Nkono *et al.*, 2014; Tchouankoue *et al.*, 2012; 2014). The geochemical and isotopic similarities between the continental and the oceanic part of the CVL attest that the continental crust did not play any role in the magma genesis and that the sources is not of lithospheric origin (Derouelle *et al.*, 2007). In spite of the similarities in geochemical composition of volcanic lavas, no evidence has been found for a consistent migration of volcanic activity with time beneath the CVL. Along the CVL, mantle derived (ultramafic) xenoliths have been found in several locations in basaltic lavas (Fig. 5: Derouelle *et al.*, 1991; Princivalle *et al.*, 2000). The xenoliths provide evidence for metasomatism within the upper mantle beneath the CVL (Derouelle *et al.*, 2007). Several mode of formation of the CVL have been suggested; the plume model (Morgan *et al.*, 1983) or multiple plumes (Ngako *et al.*, 2006), but these models present some weekness due to the no age progression along the line (Derouelle *et al.*, 2007) and the non plume models (Tchouankoue *et al.* 2014; Ebinger and sleep, 1998; Fairhead and bink 1991; Reusch *et al.*, 2010; Elsheikh *et al.*, 2014. Nkono *et al.*, 2014). The non plume models span from decompressional melting beneath re-activated structures (Ebinger and sleep, 1998), Edge driving convection (King and Ritsema, 2000), Convection cell model (Meyers *et al.*, 1998); edge convection model with lateral flow of warm material from beneath the Congo craton (King and Anderson, 1995), Corner flow Eddy model (King and Anderson, 1998; King and Ritsema, 2000) and lithospheric instability along continental margin (Mileni *et al.*, 2012).

II.4.2.   Benue trough

The Benue trough is a NE-SW trending basin that extends from the Niger delta basin (Gulf of Guinea) to Lake Chad (Fig. 5). Its origin is linked to the opening of the South Atlantic Ocean in the Cretaceous (Guiraud and Maurin 1992). The Yola trough also known as the Garoua rift and the Mamfe basin are eastward extensions of the Benue trough into Cameroon (Figs 4 and 5B). The similar Y-shape of the Benue trough and the CVL, together with the similarity in the Composition of the Alkalin basalt in both the Benue trough and CVL (Coulon *et al.* 1996; Tchouankoue *et al.*, 2014), suggest common geodynamic controls on their formation (Fitton 1987; Tchouankoue *et al.*, 2014). For example, Guiraud and Mauring (1992) have argued that the orientation of the trough and the CVL may be controlled by the northeast-trending Pan African dextral shear zones.

II.4.3. Chad basin

The Chad basin consists of several sub-basins spread around Niger, Cameroon, Chad and Nigeria (Fig. 5; Genik, 1992). It occupies a vast area at an altitude of between 200 and 500 m above the sea level, and most of it is quaternary formations masking older rocks. The origin of the Chad basin has been generally attributed to the rift system that developed in the early Cretaceous when the African and South American lithospheric plates separated and the Atlantic opened. Pre-Santonian Cretaceous sediments were deposited within the rift system. The Nigerian sector of the Chad basin constitutes only about 6.5% of the entire basin and extends in Bono, Bauchi, Plateau and Kano State territory. The Basin has developed at the intersection of many rifts, mainly in an extension of the Benue trough. Major graben then developed, and sedimentation started. Sedimentary sequence span from the Paleozoic to Recent accompanied by several stratigraphic gaps. Sediments are mainly continental, sparsely fossiliferous, poorly sorted, and medium to coarse-grained, feldpathic sandstone called the Bima sandstone. A transitional calcerous deposit Gongila formation that accompanied the onset of marine incursions into the basin overlies the Bima sandstones. These are overlain by graptolitic shale. Various formations (sandstone, shale and siltstone) are encountered. Three major sediment packages Bima formations, Gongila-Fika Shale and the Chad formations have been identified. Also, the Fika formation is suspected to be associated with intrusive rocks (Nwankwo *et al.*, 2009).

II.5. TECTONIC SETTING OF THE CENTRAL AFRICAN SHEAR ZONE IN CAMEROON

II.5.1. Precambrian evolution.

The CASZ is a ~4000 km long, ENE-trending strike-slip fault system in central Africa that extends from Cameroon and Chad into Sudan (Fig. 6A). To the west-southwest, it was suggested to be linked to the Pernambuco fault in Brazil before Gondwana fragmentation (Dorbath *et al.*, 1986; van Schmus *et al.*, 2008). In Cameroon, the CASZ is considered as constituting the sinistral Tchollire-Banyo shear zone, the dextral Central Cameroon shear zone and the Sanaga shear zone (Fig. 6B; Toteu *et al.*, 2004). It crops out within the Precambrian Oubanguides orogenic belt which constitutes from northwest to southeast, the Neoprotorozoic western Cameroon domain, the Paleoproterozic-Neoproterozoic Adamawa-Yade domain, and the Paleoproterozoic – Neoproterozoic Yaounde domain (Fig. 6B). These domains are exposed on the northern edge of

the Congo craton (Fig. 4; Ngalamo *et al.*, 2017). In Cameroon, the CASZ is defined by mylonite fabric that variably developed within gneisses and migmatites, granitic intrusions (Njonfang *et al.*, 2008: Negue *et al*., 2017). It was suggested that the shear zone was part of the contractional structures that were formed as a result of collision between the Congo craton and the terranes Oubanguides orogenic belt during the Neoproterozoic Pan-African orogeny. However, a number of subsequent workers considered the shear zone to be superimposed on the structures that were formed during the Neoproterozoic Pan-African collision event (Toteu *et al.*, 2004; Njonfang *et al.*, 2008). From the presence of high-K plutonic complex that gave U-Pb ages of ~620 and ~613 Ma, Kwekam *et al.* (2010) concluded that the northern margin of the Adamawa-Yade domain has been metacratonized. Abdelsalam *et al.* (2002) defined metacraton as 'a craton that has been remobilized during an orogenic event, but that is still recognizable predominantly through its rheological, geochronological, and isotopic characteristics'. Further, Kwekam *et al.* (2010) proposed that the metacratonization was the result of zonal removal of the sub-continental lithospheric mantle (SCLM) from beneath the Central Cameroon shear zone which defines the northern margin of the Adamawa – Yade domain (Fig. 6B).
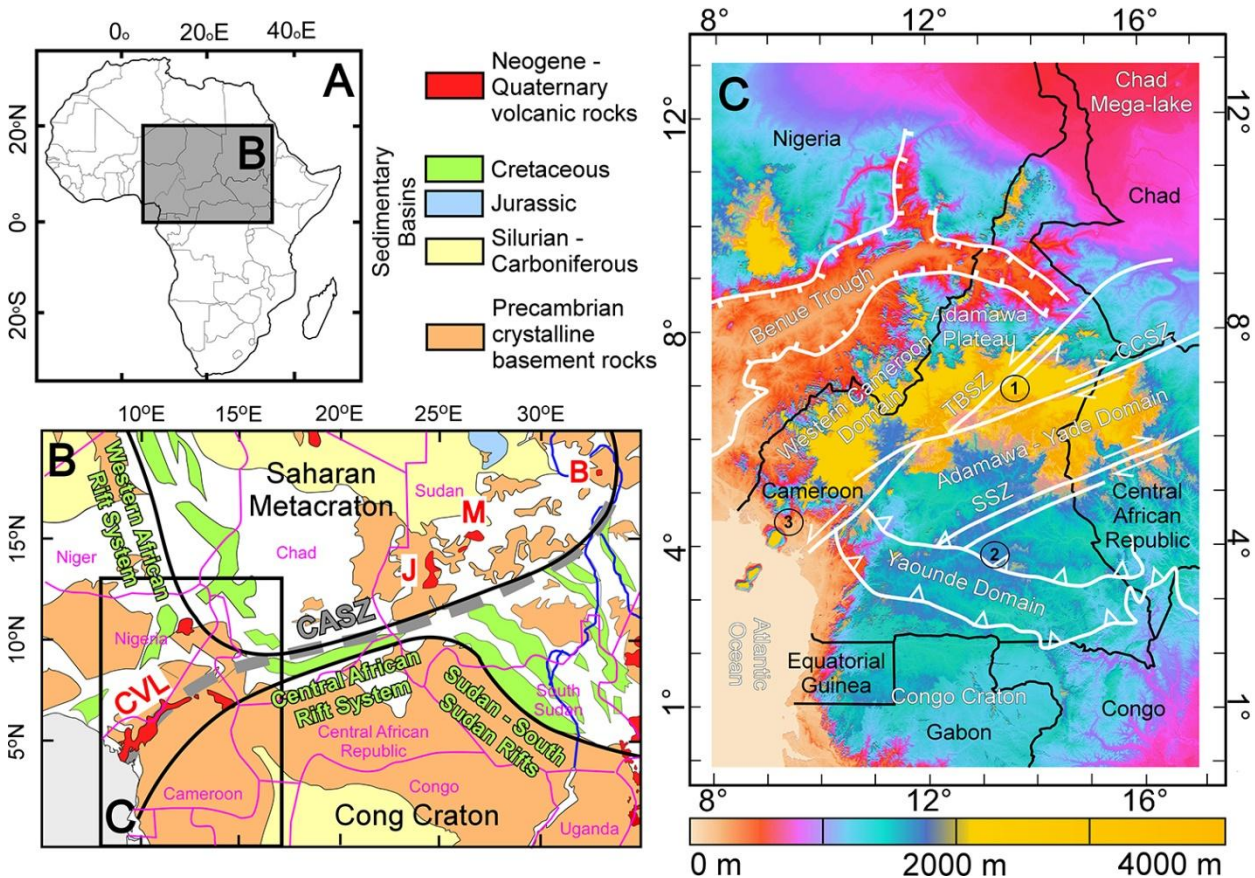
Figure 6: (A) Localisation of B within the Africa continent. (B) Tectonic map of the Central African Shear Zone (CASZ) and the surrounding tectonic elements. Modified from the Tectonic Map of Africa 1:10,000,000 scale. Commission for the Geological Map of the World (CGMW) – United Nations Educational, Scientific and Cultural Organization (UNESCO) 2010 publication with financial support from Bureau de Recherches Géologiques et Minières (BRGM). CVL = Cameroon Volcanic Line. J = Jebel Marra. M = Meidob Hills. B = Bayuda Desert. (C) Shuttle Radar Topography Mission (SRTM) Digital Elevation Model (DEM) of Cameroon and surroundings showing major physiographic features. TBSZ = Tchollire-Banyo shear zone. CCSZ = Central Cameroon Shear Zone. SSZ = Sanaga shear zone.

Earlier, Toteu *et al.* (2001, 2004) showed from geochronological data that the Adamawa – Yade domain is dominatly made-up of Paleoproterozoic crust of possible Archean origin and that this crust has been highly injected by Neoproterozoic high-K granitoids that led to significant remobilization of the domain. Toteu *et al.* (2004) attributed this remobilization as due to SCLM delamination that accompanied the collision between the Adamawa-Yade domain and the Congo craton after the consumption of an oceanic basin between them during the Neoproterozoic Pan-African orogeny. This implied that the Yaounde domain represent the crustal manifestation of the suture zone between the Adamawa-Yade domain and the Congo craton (Fig. 6B). However, Kwekam *et al.* (2010) argued that the Adamawa-Yade domain is the north continuation of the Congo craton and that it was evolved as an integral part of the craton throughout its history. Hence,

24

Kwekam *et al.* (2010) proposed that the northern boundary of the Congo craton be assigned to the Central Cameroon shear zone system which represents a Neoproterozoic suture zone that separates the craton from the Western Cameroon domain which is dominated by Neoproterozoic Pan-African juvenile material.

II.5.2. Mesozoic evolution

The Mesozoic evolution of the CASZ is marked by two events. First, it has long been observed that some of the ENE-trending Cretaceous basins of the Central African rift system (CARS) are aligned along the CASZ (Fig. 6A). The largest of these basins is the Doba – Doseo – Salamat basin that follows the border between Chad and the Central African Republic (Fig. 6A). The onset of the basin has been linked to reactivation of the CASZ during the Cretaceous following the opening of the Southern Atlantic Ocean (Genik, 1992, 1993). Reactivation of the shear zone through dextral strike-slip movement resulted in the development of this basin as major transtensional basin in central Africa. A tectonic setting similar to that of the Doba – Doseo – Salamat basin can be adopted for the smaller Djerem-Mbere basin which is found within the Adamawa Plateau in central Cameroon (Figs. 6A). For example, Stuart *et al.* (1985) summarized that the CASZ in the Adamawa plateau has been reactivated during the opening of the South Atlantic Ocean and this has resulted in the formations of a series of grabens aligned along the shear zone including the Djerem-Mbere basin.

Second it has also been suggested that the CASZ represented an important tectonic boundary in the Cretaceous during the evolution of the NW-trending Sudan – South Sudan rifts. It has long been observed that these rifts do not extent northwest-ward beyond the CASZ (Fig. 1A; Brink and Fairhead, 1992). Brink and Fairhead (1992) explained the absence of the interior rifts of Sudan – South Sudan as that the "northern plate" (now the Saharan Metacraton of Abdelsalam *et al.*, 2002; Fig. 6A) had enough rigidity not to be rifted during this Cretaceous rifting event. Hence, the CASZ acted as an important lithospheric structure that separated a less rigid southern plate that was rifted during the Cretaceous rifting event (Arabian-Nubian Shield) from a rigid northern plate that was not rifted (Saharan Metacraton). Also, Fairhead (1988) suggested that the CASZ was active as a dextral strike-slip fault system during the onset of the Sudan – South Sudan interior rifts and that, because of preferred angular relation between the two, most of the dextral strike-slip movement along the shear zone was accommodated as ENE-WSW directed extension on the rifts.

II.5.3. Cenozoic evolution

It is long been observed that the CASZ in Cameroon is spotted by the outcrops of the CVL (Fig. 6A). This spatial association has been explained by Fairhead (1988) that the CVL was formed due to decompressional melting of the asthenosphere that ascended through the CASZ. Further east-northeast, in Sudan there are a number of Cenozoic volcanic rocks exposed in Jebel Marra, Meidob Hills, and Bayuda Desert (Fig. 6A). Vail (1972) suggested that these volcanic rocks are aligned with the CVL. Also, although the CASZ is not specified, Vail (1972) suggested that the Cenozoic volcanic rocks in Sudan are possibly controlled by post-Mesozoic ENE-trending fractures.

II.6. PREVIOUS GEOPHYSICS STUDIES

Previous studies that focused in estimating the Moho and the lithosphere – asthenosphere boundary (LAB) depth beneath Cameroon and surrounding using active seismic studies, passive seismic data and ground gravity surveying data are summarized in Ngalamo *et al.* (2017). From active seismic study using 40 receivers, Stuart *et al.* (1985) found that the Moho depth in the central part of the Adamawa plateau between the Tchollire – Banyo shear zone and the Central Cameroon shear zone to be ~33 km (Labelled 1 in Fig. 5B). Tokam *et al.* (2010) and Gallacher and Bastow (2012) used a passive seismic receiver function studies for the 32 seismic stations from the Cameroon Broadband Seismic Experiment (CBSE) to estimate the Moho depth in Cameroon. Both studies found a deeper Moho beneath the Congo craton and the Yaoundé domain reaching 48 km in the northern edge of the latter (Labeled 2 in Fig. 5B). These studies also found relatively shallower Moho beneath the Adamawa – Yade domain and the Western Cameroon domain reaching ~28 km in the southwestern part of the latter (Labeled 3 in Fig. 6B)

Poudjom Djomani *et al.* (1995) used spectral analysis for ~32000 ground gravity measurements in Cameroon to suggest that the thickness of the continental crust decreases from ~50 km in the south to ~ 18 km to the north. Poudjom Djomani *et al.* (1995) suggested progressive northward thinning of the crust from ~50 to 22 km beneath the Congo craton, the Yaoundé domain and the Adamawa-Yade domain, to 22-18 km beneath the West Cameroon domain. Additionally, Nnange *et al.* (2000) used spectral analysis for ~ 38,000 new and existing ground gravity measurements in Cameroon to find out that the Moho depth in southern Cameroon (Congo craton and Yaoundé domain) is 35 ± 3 km deep, in northern Cameroon (Adamawa-Yade domain) is 37 ±

2 km deep, and in western Cameroon (Western Cameroon domain) is 30 ± 2 km deep. Tugume *et al.* (2013) used three-dimensional (3D) inversion of the global gravity model EIGEN-6c to image the Moho depth and to estimate crustal thickness of the Africa continent. Results from the 3D inversion of the global gravity model were calibrated with result obtained from 377 passive seismic stations that were used to calculate crustal thickness using receiver function approach. For our focus area, Tugume *et al.* (2013) presented an average crustal thickness of 45 ± 2 km for the Congo craton and 39 ± 3 km for the Oubanguides orogenic belt. Eyike and Ebbing (2015) used 3D gravity inversion of the Earth Gravity Model 2008 (EGM 2008) to produce crustal thickness map that covers the northeastern part of our study area and show a relatively uniform crustal thickness, with the Moho depth ranging between 28 and 37 km.

Limited number of studies had been focusing on estimating the lithospheric thickness and LAB depth beneath Cameroon. Plemerova *et al.* (1993) used data from the 40 stations of the active seismic experiment to show that the LAB is shallower (~100 km) beneath the CASZ and it reaches up to ~190 km depth away for it. Poudjom Djomani *et al.* (1997) estimate the lithosphere thickness of 80 km beneath the Adamawa plateau from forward modelling of a N-S profil. Poudjom Djomani *et al.* (1997; 2000).

Fichwick and Bastow (2011) used passive seismic tomography data (discussed below) to report a thinner lithosphere (~60 to ~80 km) beneath the Adamawa-Yade domain and the West Cameroon domain, and a thicker lithosphere beneath the Congo craton and the Yaoundé domain reaching a thickness of ~120 to ~200 km. Eyike and Ebbing (2015) used 3D gravity inversion of the earth gramvity model 2008 (EGM 2008) to image the lithospheric thickness of the northeastern part of our study area and sound it to be ranging between ~70 km and ~110 km.

CHAPTER III:

EARTH STRUCTURE AND GRAVIMETRIC METHODS FOR RECOVERY OF THE MOHO AND LAB GEOMETRY

III.1. COMPOSITION OF THE EARTH

Geophysical studies reveal that the Earth consists of several distinct layers with different physical properties and chemical Compositions. The three main layers are the crust, the mantle and the core. The crust is the outermost and thinnest layer. The next layer is the mantle, which extends to a depth of 2900 km. This is further subdivided into two parts: the upper mantle and the lower mantle. The innermost layer is the core. This is also further divided into the outer core and the inner core. The boundaries of these layers form discontinuities that may refract and reflect seismic waves or can be sensible to potential field methods with gravity exploring deeper than magnetic. Global density models for different layers assume a spherically symmetric density distribution, which is a function of radial distance from the center of the Earth (Dziewonski and Anderson, 1981, Bullen, 1975).

The crust consists of silica-rich rocks which developed due to the melting of underlying mantle material, and subsequent metamorphic or erosional processes. Crustal rocks are broadly classified as igneous, metamorphic, or sedimentary, according to their individual characteristics. The crust is mainly divided into oceanic and continental crust. The thickness of the Oceanic crust ranges from 6 to 12 km, while the continental crust is thicker; its thickness is more than 70 km. the oceanic crust is formed due to the decompression melting in the mantle at shallow depths beneath the mid-ocean ridges. The upper part of the crust consists of the exposed rocks and thin sedimentary layers having sharp variations in density and thickness. In the continental area, the upper crust below the sedimentary layer consists of granitic rocks with a mean density of 2.7 g/cm^3 (Torge. 1991). The granitic zone does not exist in the Oceanic area. The lower crust is located beneath the upper crust, with the mean density of 2.9 g/cm^3. The lower crust consists of basic rocks such as Gabbro (Basalt). Below the lower crust, an abrupt increase in the velocity of seismic body waves and density is observed. For instance, the P-wave velocity increases from 7.1 km/s to 8.1 km/s. The lower boundary of the crust is called Mohorovičić discontinuity, or in short Moho. The Moho separates the crust from the underlying Mantle.

The mantle consists of magnesium-iron oxide and relative silica rich solid rock layer between the crust and the core. Since the top of the mantle lies at a depth of 7-70 km depending on location, while its base lies at a depth of 2900 km beneath the surface, the mantle contains most of the Earth's mass. In general, the mantle consists of very hot, but solid rock. However, at depths

of about 100-200 km beneath the oceanic crust, the mantle has undergone a slight amount of partial melting. Here, about 2-4 % of rock has transformed into magma and this magma occurs in very thin films along grain boundaries or in small pores between grains. Although the chemical composition of the mantel is roughly uniform throughout, the mantle can be subdivided into three distinct layers, delineated by seismic-velocity discontinuities. These discontinuities probably mark depths to which minerals making up mantle peridotite undergo abrupt phase changes. At shallow depths, mantle peridotite contains olivine, but at greater depths, where pressures are greater, the olivine lattice becomes unstable, and atoms rearrange to form a different, more compact lattice. The three layers of the mantle from, top to bottom are: the upper mantle (Moho-400 km), the Transition zone (400 km-670 km) and the lower mantle (670 km-2900 km). Within the upper mantle lie another major discontinuity called the lithosphere-asthenosphere discontinuity also called "Lithosphere-Asthenosphere Boundaries" (LAB) which is a brittle-ductile transition defined by a significant change in rock physical properties (viscosity) in contrast with the compositional change observed between the crust and the mantle (Moho discontinuity).

III.2. MOHO DISCONTINUITY

Andrija Mohorovicic (1857-1936) discovered the Moho discontinuity in 1910, while he was studying the seismogram of the 8 October 1909 earthquake in the Kulpa Valley, together with other earthquakes in this region (Mohorovicic, 1910, 1992). He observed two distinct pairs of compressional and shear waves. He wrote: "When I was sure based on data, that two kinds of first preliminary waves exist, both kinds reaching all locations from 300 km to 700 km distance, and that from the epicenter to approximately 300 km distance only the first kind arrives, whereas from 700 km distance onward only the second kind arrives, I tried to explain this until now the unknown fact". This observation led Mohorovicic to the conclusion that the Earth is not homogeneous, and at a specific depth there has to be a boundary surface, which separates two media with different elastic properties, and through which the waves must propagate with different velocities. He suggested that the first kind of arrival is from crystalline crust while the second kinds of arrival correspond to the mantle. The interpretation of two sets of arrival times led Mohorovicic to the discovery of a velocity discontinuity. In the past 100 years, seismologist studied different seismic profiles generated by earthquakes at different locations and proved that this discontinuity is present throughout the globe.

The discontinuity discovered by Mohorovicis provides the primary definition of the boundary between the crystalline crust and the upper mantle in terms of seismic waves velocities. Generally, the velocity of P-waves in the upper mantle is about 7.9 km/s or more, and consequently, shows a velocity contrast of more than 1.0 km/s. This large velocity contrast indicates that there is a significant difference between the crust and the mantle in terms of elastic parameters, which can be explained by a difference in composition. Another definition for the Moho is in term of the density contrast between the Earth crust and the mantle. The commonly used mean density of the crust is 2670 kg/m^3, while for the mantle it is about 3300 kg/m^3 providing a density contrast of about 630 kg/m^3 at the Moho interface (Heiskanen, 1967).

Many researches about the Moho geometry have been published (e.g. Mooney *et al.*, 1998, Kaban *et al.*, 1999, Braitenberg *et al.*, 2000) computed a global crustal model using fully non-linear inversion of fundamental mode surface waves. Moho in Australia was studied by Aitken *et al.* (2013) using gravity data. The Moho model for the European plate has been produced by Grad *et al.* (2009) using seismic as well as gravity maps. A new reference model for the European crust (EuCRUST-07) was presented by Magdala *et al.* (2008). Recently Van der Meijde *et al.* (2013) have produced gravity drive Moho for South America. Mariani *et al.* (2013) have identified a thick crust in Parana basin, Brazil, with GOCE gravity data. Tugume *et al.* (2013) used three-dimensional (3D) inversion of the global gravity model EIGEN-6c to image the Moho depth and to estimate crustal thickness of the Africa continent, and locally Poudjom Djomani *et al.* (1995) used spectral analysis to image the Moho geometry of Cameroon and surroundings.

III.3. REFERENCE DENSITY OF CRUST AND MOHO DENSITY CONTRAST

The numerical value of the mean density of the crust used in the gravity reduction (Bouguer anomaly) is 2.67 kg/m^3 (Woolard, 1971). The average density of the upper continental crust 2.670 g/cm^3 is often adopted for defining the topographic and reference crust densities. This density better corresponds to the average density of the upper continental crust (cf. Hinze, 2003).

In global studies, most authors use a constant value of the Moho density contrast and compute the stripping corrections relative to the reference crustal density. The constant value of the Moho density contrast is again computed relative to the constant reference density of crust. Tenzer *et al.* (2012) used the consolidated crust-stripped gravity data to estimate the average Moho density contrast with respect to a homogenous crust layer of reference density of 2.670 g/cm^3.

III.4. LITHOSPHERE AND LITHOSPHERE-ASTHENOSPHERE DISCONTINUITY

The lithosphere is the long-term rigid outer layer of the Earth, which comprises the crust and a portion of the uppermost upper mantle. It is a chemical, mechanical, and thermal boundary layer composed of a number of plates that translate coherently over a hotter and much less viscous material, active in the convection process. In detail, although the concept of a lithosphere is straightforward, it can be defined in different ways depending on what particular property is under study. This gives rise to a debate over which definition is best, and whether different definitions are consistent among themselves.

In a seismological sense, the seismic lithosphere has been classically defined as the high-velocity material that overlies the upper mantle Low Velocity Zone (LVZ) (e.g. Anderson, 1989). In ocean basins the LVZ is marked by a strong decrease in S-wave velocities, typically at depths 100 km.

From a mantle convection point of view, the thermal lithosphere is defined as the thermal boundary layer within which heat is transferred primarily by conduction. Its base is typically taken as the depth at which the conductive geotherm intersects a particular adiabat (usually the 1300 - 1315 ^{0}C adiabat).

Since the strength of silicate rocks is strongly dependent on temperature, a mechanical lithosphere can be defined as the material above a certain isotherm that is effectively isolated (mechanically) from the underlying convective mantle over geological time scales. This isotherm is typically around 800 - 900 ^{0}C, since olivine-rich rocks at temperatures lower than this value cannot be deformed by more than 1 % in time scales of 100 Ma (Schubert *et al.*, 2001). The above definition implies then that the thermal lithosphere includes the mechanical lithosphere. In this way, a geochemical lithosphere can be defined. Griffing *et al.* (1999b), for example, have shown that the lithosphere-asthenosphere boundary (LAB) in continental regions can be defined as the maximum depth from which low-Y (< 10 ppm) garnets, characteristic of depleted lithosphere, are derived. Using thermobarometric techniques, these authors have estimated that the geochemical LAB coincides with temperatures of 1250 - 1300 ^{0}C, establishing then a close correlation with the thermal definition of the lithosphere.

When a certain minimum volatile content (mainly C + H + O) is introduced into the upper mantle composition, a petrological lithosphere is defined as the uppermost portion of the upper

mantle where amphibole (magnesian pargasite) is stable (Green *et al.*, 2001). Below the pargasite stability field, the mantle begins to experience partial melting. The total amount of melt generated in this region depends strongly on the total volatile content. For a geotherm representative of mature oceanic lithosphere (age > 80 Ma), the base of the petrological lithosphere should be at depths of ~ 80 – 95 km, according to the dehydration solidus of Green and Falloon (1998). This definition provides a petrological basis for the LVZ in oceanic lithosphere, as well as a correlation with the thermal definition in the same domain. On the other hand, besides being strongly dependent on the local volatile content, this definition is highly ambiguous for continental domains. For instance, in continental areas with thermal thickness > 200 km, the petrological lithosphere does not have a lower boundary at all, while in continental domains with thermal thickness ranges from 120 - 150 km, the petrological lithosphere is not thicker than ~100 km (Green & Falloon, 1998).

In this study, the thermal lithosphere definition would be the one used to estimate the lithosphere asthenosphere boundary depth. This definition is preferred over others for the following reasons: (a) there is a close correlation between the geochemical and thermal definition, (b) there is a simple functional relationship between the thermal and the mechanical definition, and (c) the thermal definition eliminates ambiguities between different lithospheric domains, since it must exist everywhere (i.e. there is always an intermediate isotherm between the convective interior and the surface temperatures).

III.5. REFERENCE DENSITY OF LITHOSPHERE AND LAB DENSITY CONTRAST

The vertical variation of density in the upper mantle is a key for studying the lithosphere-asthenosphere dynamics. Unfortunately, large uncertainties remain in density-depth models, from the Moho to several hundred kilometer-depths. Reason for such uncertainties lies in the complexity of the upper mantle structures: lateral heterogeneities, anisotropy, low velocity zone. Seismological data have been extensively used in the past to infer density-depth variations Kaban *et al.* (2014). Accurate surface wave data have recently provided great results for direct estimation of the density-depth variations in the upper most 500 km of the earth. Furthermore, density contrast at the lithosphere-asthenosphere boundary has been estimated using gravity data. The composition

of the asthenosphere mantle body was assumed to be an average of the values expected for a fertile lherzolite and harzburgite. In this study the asthenosphere density was choose ~ 3.2 g/cm^3

III.6. EARTH STRUCTURE MODELS

Several models of the Earth's structure have been developed based on the analysis of seismic data. Dziewonski *et al.* (1975) introduced the Parametric Earth Models (PEM) consisting of piece-wise continuous analytical functions of the radial density and velocity variations defined individually for the oceanic (PEM-O) and continental (PEM-C) lithosphere down to a depth of 450 km, below this depth these models are identical. They also provide an averaged function for the whole lithosphere (PEM-A). Dziewonski and Anderson (1981) presented the Preliminary reference Earth Model (PREM), which provides information on the seismic velocities and density structure within the whole Earth's interior by means of spherically homogenous stratigraphic layers. Van der Lee and Nolet (1997) prepared the 1-D average model MC35 based of the PEM-C, while replacing the high and low velocity zones of the PEM-C by a constant S-wave velocity of 4.5 km/s within the upper mantle down to a depth of 210 km. Kustowski *et al.* (2008) derived the transversely isotropic reference Earth model STW105. In addition to their Earth's synthetic models, several other global and regional seismic velocity models were developed. A summary of these models can be found in Trabant *et al.* (2012).

The PEM and PREM models provide 1-D density information. Models based on a stratigraphic layering with a variable depth, thickness and laterally varying density distribution obviously represent the Earth's interior more realistically. Currently available global models provide information on a 3-D density structure only within the crust and upper mantle. The recently developed model by Simmons *et al.* (2010) contains the 3-D density structure of the whole mantle.

Nataf (1996) derived a global model of the crust and upper mantle density structure based on the analysis of seismic data and additional constraints such as heat flow and chemical composition. Mooney *et al.* (1998) compiled the global crustal model CRUST 5.1 with a 5^0x5^0 spatial resolution. More recently, the global crustal model CRUST 2.0 was compiled with a 2^0x2^0 spatial resolution (Bassin *et al.*, 2000). This model has been prepared and administered by the U.S. Geological Survey and the Institute for Geophysics and Planetary Physics at the University of California. Both models were compiled based on seismic data published until 1995 and a detailed compilation of the ice and sediment thickness.

Meier *et al.* (2007) produced a global crustal model CRUST07, using fully non-linear inversion of fundamental mode surface wave. The resolution of CRUST07 model is 2^0x2^0. They use neural networks for finding 1-D marginal probability density functions (pdfs) of global crustal parameters. They have inverted the fundamental mode Love and Rayleigh wave phase and group velocity for the pdfs of crustal thickness. The constructed model provides the mean Moho depths and its standard deviations.

Most recently, Crust 1.0 has been released, which has a 1^0x1^0 spatial resolution (Laske *et al.*, 2013). Crust 1.0 is the result of a comprehensive effort to compile a global model of the Earth's crust and lithosphere, LITHO 1.0 (Pasyanos *et al.*, 2012, Laske *et al.*, 2013). LITHO1.0 is a 1^0x1^0 model of the curst and uppermost mantle of the Earth. It is created by constructing an appropriate starting model and perturbing it to fit high-resolution surface wave dispersion maps. The CRUST 1.0 consists of the topography, ice, water layers and crustal layers. In addition, lateral varying density structure of the upper mantle is incorporated into CRUST1.0. The globally averaged data from active seismic methods and deep drilling profiles were used to predict the sediment and crustal structure. In regions where no seismic measurements were available (most of Africa, South America, Greenland and large parts of the oceanic lithosphere) the crustal structure assigned by a generalization to similar geological and tectonic settings. For cells with no local seismic or gravity constraints, statistical averages of crustal properties, including crustal thickness, were extrapolated. The Moho depth in CRUST1.0 is based on 1^0x1^0 averages of a recently updated database of crustal thickness data from active source seismic studies as well as from receiver function studies. This model incorporates an updated version of the global sediment thickness.

The compilation of Crust 1.0 initially followed the philosophy of the crustal model CRUST 2.0 by assigning elastic properties in the crystalline crust according to the basement age or tectonic setting. This reduces the possibilities of errors in both models. The sediment model (Laske, 2013) is an independent part of the CRUST1.0 model. The sediments layers in CRUST 5.1 and CRUST 2.0 are divided into two layers of soft and hard sediments, while CRUST 1.0 consist of three sediment layers namely, upper, middle and lower sediments. Each 1^0x1^0 cell of CRUST 1.0 provides thickness, compressional and shear wave velocity and density for eight layers: water, ice, three sediment layers and three crustal layers. Topography, bathymetry and ice cover are taken from the 1'x1' ETOPO1 model (Amante and Eakins, 2009). Chen and Tenzer (2014) compiled the

Earth's Spectral Crustal Model (ESCM80) by incorporating more detailed information's on the topography, bathymetry, polar ice sheets and geoid surface into the CRUST 1.0 model.

Beside the global models, there are some regional models of the crust available in the literature (e.g. Magdala *et al.*, 2008, Grad *et al.*, 2009 Van der Meijde *et al.*, 2013 and Mariani *et al.*, 2013; Tugume *et al.* (2013); Poudjom djomani *et al.* (1995)). The model developed by Magdala et al, (2008) is termed as Eucrust-07. The model is 15'x15' point spacing for download and it is based on the results of seismic reflection, refraction and receiver functions studies. The Moho model of the European plate developed by Grad *et al.* (2009) has a point spacing of 0.1 degree and is compiled using more than 250 data sets of seismic profiles, 3-D models obtained by body and surface waves, receiver function results and maps of seismic and gravity data. Recently a regional model of the Moho for South America has been published by Van der Meijde *et al.* (2013). This model is based upon the European Improved Gravity model of the Earth by New techniques (EIGEN-6C; Förste *et al.* (2011) model derived from GOCE satellite and other gravity data. The authors inverted the gravity data by assuming a two-layer model with constant density contrast over the interface. The point spacing of the model is 15'x15'. The regional model developed for the crustal thickness of Africa is derived from global gravity field data using Euler deconvolution (Tedla *et al.* (2011). The model has a point spacing of 3'x2.5'. The model is based on EIGEN-GL04C (Foerste *et al.*, 2008) free air gravity anomalies which contain 30 months of GRACE Level 1B data covering the period from February 2003 to July 2005 together with surface gravity data from seven different sources. More recently, Tugume *et al.* (2013) developed a regional crustal model for Precambrian Crustal Structure in Africa and Arabia (PCSAA). The Model of crust thickness for Africa and Arabia is based on the gravity data from EIGEN-6C gravity field model. Poudjom Djomani *et al.* (1995) developed a local crustal model for Precambrian structure in Cameroon and surrounding based on ground gravity data.

III.7. GRAVITATIONAL POTENTIAL OF A SOLID BODY

According to Newton's law of gravitation, the gravitational potential ***Wa*** of an attracting body with density ρ is given by the Newton integral (Mader, 1951)

$$\text{Wa}\,(x.y.z) = \text{G}\iiint_v \quad \frac{\rho(x.y.z)}{\sqrt{(x-x\prime)^2+(y-y')^2+(z-z')^2}}\, dx'dy'd^z \ (2.1)$$

Over the volume v of the body, where G is the Newtonian gravitational constant, dv= dx'dy'dz' is the volume element, and $l = \sqrt{(x - x')^2 + (y - y')^2 + (z - z')^2}$ is the Euclidean distance between the computation point *(x.y.z) and* integration point (x'.y'.z')

The potential $W\alpha$ is continuous throughout the space and for$l \to \infty$ it behaves like the potential generated by a point mass located at the body's centre of mass. The "first derivative* of the potential are also continuous throughout the space but the second derivatives are not continuous at density discontinuities (Kellogg, 1929).

It can be shown that

ΔW_α = - 4πGρ (2.2)

Where $\Delta = \dfrac{\delta^2}{\delta x^2} + \dfrac{\delta^2}{\delta y^2} + \dfrac{\delta^2}{\delta z^2}$ is the Laplacian operator. Outside the surface of the body the density ρ is zero, so Eq. (2.2) turns into

$\Delta W a = 0$. (2.3)

Eq. (2.3) is called the Laplace equation and its solutions are called harmonic functions.

III.8. EARTH GRAVITY AND GEOID

The total force acting on an object located at the surface of the Earth is the sum of gravitational force *and* centrifugal force. The centrifugal potential is

$\Phi(xyz) = \dfrac{1}{2}\omega^2(x^2 + y^2)$

Where ω is the angular velocity of Earth's rotation and *x. y, z* are the coordinates defined in an Earth-Fixed reference frame. The gravity potential *W is* the sum of the Earth gravitational potential *Wa* and the centrifugal potential Φ:

$W(x, y, z) = Wa\ (x, y, z) + \Phi(x, y, z)$. (2.4)

The gravity vector g is the gradient of the gravity potential (Moritz, 2006).

$g = \nabla W$, (2.5)

With components

$$gx = \frac{\partial W}{\partial X} = -G \iiint \frac{x-x'}{\iota 3} dx' \, dy' \, dz' + \omega 2x.$$

$$gy = \frac{\partial W}{\partial y} = -G \iiint \frac{y-y'}{\iota 3} dx' \, dx' \, dy' + \omega 2y.$$

$$gz = \frac{\partial W}{\partial X} = -G \iiint \frac{z-z'}{\iota 3} dx' \, dx' \, dy' \, dz'$$

where $\nabla = \frac{\delta^2}{\delta x^2}\vec{\iota} + \frac{\delta^2}{\delta y^2}\vec{\jmath} + \frac{\delta^2}{\delta z^2}\vec{k}$ and $\vec{\iota}.\vec{\jmath}$ and $\vec{k}$ are the unit vectors in the terrestrial reference frame along the *x.* y and z direction, respectively. The magnitude of the gravity vector

g = ∇W   (2.6)

is called gravity.

   Surface W = constant is called the geops, and one particular geops $W = W_O$ is the geoid. It is the geops which best approximates mean sea level.

   The force of gravity at the geoid surface is always normal to it. The gravity potential *W* can be split into the normal potential *U* usually generated by a level ellipsoid and the disturbance potential *T:*

W = U + T

Thus, the disturbance potential is defined as the difference between the actual gravity potential and the normal gravity potential. In geodetic coordinates, it can be written as

T($h. \lambda. \Phi$) = W (h.λ. Φ) − U (h.Φ). (2.7)

where *h* is the ellipsoidal height. *X* is the longitude and Φ is the latitude. The gradient of the normal potential is called the normal gravity vector

$\vec{n} = \overrightarrow{\nabla U}$

and its magnitude is called the normal gravity

n = $\overrightarrow{\nabla U}$

III.9. GRAVITY DISTURBANCE AND GRAVITY ANOMALY

The gradient of the disturbance potential is called the gravity disturbance vector and is denoted by δg (Moritz. 2006):

$\delta g = \vec{\nabla}(W\text{-}U) = \vec{\nabla}T.$

and the difference in magnitude is the gravity disturbance (Moritz, 2006)

$\delta g = \left|\overrightarrow{\nabla W}\right| - \left|\overrightarrow{\nabla U}\right| = gp - Yp.$ (2.8)

The classical gravity anomaly vector Δg is defined as the difference between the gravity vector *gp* at a point *P* on the geoid and the normal gravity vector YQ at the corresponding point on the reference ellipsoid (see Fig. 2.1):

$\Delta g = gp - YQ$

and the difference in magnitude is the gravity anomaly

Now consider the geometrical representation of geoid and reference ellipsoid as given in Fig. 7 where *n* is the local normal at *P* while *n'* is the normal to the reference ellipsoid at *Q* passing through point *P* on the geoid. Omitting subscript *P* for brevity, the gravity disturbance can be written as

$\delta g = -\left(\dfrac{\partial W}{\partial n} - \dfrac{\partial U}{\partial n\prime}\right)$
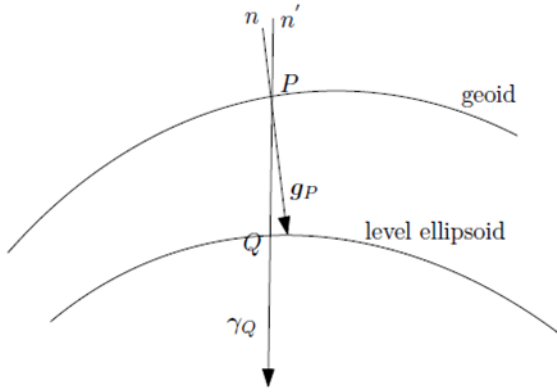
Figure 7: Geometrical representation of geoid and reference ellipsoid

The direction of the normal vectors *n* and *n'* almost coincide, moreover the normal *n is* directed along the elevation *h* therefore, gravity disturbance can be approximately written as

$$\delta g \sim -\frac{\partial T}{\partial h}$$

In spherical approximation, the gravity disturbance is the negative radial derivative of the disturbance potential (Heiskanen. 1967)

$$\delta g \sim -\frac{\partial T}{\partial r} \; (2.9)$$

and similarly, the expression for the gravity anomaly reads.

$$\Delta g = -\frac{\partial T}{\partial r} - \frac{2}{r} T. \; (2.10)$$

Eqs. (2.9) and (2.10) relate gravity disturbances and gravity anomalies to the disturbance potential.

III.10. HARMONIC EXPANSION OF THE GRAVITY FIELD

The total potential W of the Earth can be represented outside a sphere comprising all masses (Brouillon sphere) in term of spherical harmonic (Moritz, 2006)

$$W(r.\theta.\lambda) = \frac{GM}{R} \sum_{l=0}^{\infty} (\frac{R}{r})^{l+1} \sum_{m=0}^{l} (\overline{C_{lm}} \cos m\lambda + \overline{S_{lm}} \sin m\lambda) \, \overline{P_{lm}} (\cos\theta) + \frac{1}{2}\omega r^2 \sin 2\theta.$$

(2.11)

where G = 6.674x 10^{-11} m^3 kg^{-1}s^{-2} is Newton's gravitational constant, and *M* is the mass of the Earth. The numerical value of the scaling terms *(GM,R)* are: *GM*=3986004.415 x 10^8 m^3 s^{-2} and *R* = 6378136.3 m , θ is co-latitude. λ is longitude, $\overrightarrow{Clm}$ and $\overrightarrow{Slm}$ are the fully normalized spherical

harmonic coefficients (Stokes coefficients). l is the degree and m is the order. $\overrightarrow{Plm}$ are normalized associated Legendre's functions of degree l and order m; they are defined by (Moritz. 2006).

$$\overline{Plm} = \begin{cases} \sqrt{2l + 1}Plm & If \ m = 0 \\ \sqrt{2(2l + 1)\frac{(l-ml)}{(l-ml)}} \ Plm & \\ & If \ m \neq 0 \end{cases}$$

Similarly, the normal potential can be written as

$$\cup (r.\theta.\lambda) = \frac{GM}{R} \sum_{l=0(2)}^{\infty}(\frac{R}{r})^{l-1} \ \overline{C}_{10}^{U} \ \overline{P_{10}} \ (\cos\theta)+\frac{1}{2} \ \omega r2 \ \sin2\theta \ (2.12)$$

The summation over l has a step size of 2. Using Eq. (2.11) and Eq. (2.12). one can express the disturbance potential as.

$$T (r.\theta.\lambda) = \frac{GM}{R} \sum_{l=2}^{\infty} \left(\frac{R}{r}\right)^{l-1} \sum_{m=0}^{1} (\overrightarrow{\Delta C_{lm}}\cos m \ \lambda + \overrightarrow{\Delta C_{lm}} \ \sin m\lambda) \ \overline{Plm \ (\cos\theta)} \ (2.13)$$

Where

$$\begin{vmatrix} |\Delta \overline{C}_{lm}| \\ |\Delta \overline{S}_{lm}| \end{vmatrix} = \begin{vmatrix} |\overline{C}_{lm} - C_{lm}^{U}| \\ |\overline{S}_{lm} - S_{lm}^{U}| \end{vmatrix}$$

Assuming that the total mass of the level ellipsoid is the same as the mass of the Earth, the zero-degree term vanishes (i.e; $\Delta \overline{C_{00}} = \overline{S}_{00} = 0$). Furthermore, assuming that the centre of mass of the Earth and the level ellipsoid coincide with the origin of coordinate system, the disturbance potential vanishing degree t terms (i.e., $\overline{C}11 = \overline{C}10 = \overline{S}11 = 0$).

Eq. (2.13) can be written for a point at the mean sphere, which approximates the Earth's surface of radius r = R:

$$T(R.\theta.\lambda) = \sum_{l-2}^{\infty} \sum_{m=0}^{l} \quad (\Delta \overline{C}_{lm}^{T}\cos m \ \lambda + \Delta \overline{CS}_{lm}^{T}lm \ \sin m\lambda) \ \overline{P}_{lm^-}(\cos \infty).$$

Where

$$\begin{vmatrix} |\Delta \overline{C}_{lm}^{T}| \\ |\Delta \overline{S}_{lm}^{T}| \end{vmatrix} = \frac{GM}{R} \begin{vmatrix} |\Delta \overline{C}_{lm}| \\ |\Delta \overline{S}_{lm}| \end{vmatrix} (2.14)$$

are the Stokes coefficients associated with the disturbance potential of the earth from Eq. (2.9) and Eq. (2.10) it follows that the expressions for gravity disturbances and gravity anomalies on the sphere with radius r = R are

$$\delta g(R.\theta.\lambda°) = \frac{GM}{R^2} \sum_{l=2}^{\infty}(l+1) \sum_{m=0}^{l} \quad (\Delta\overline{C}_{lm}\cos m\lambda + \Delta\overline{S}_{lm} \sin m\lambda) \, Plm \, (\cos\theta) \quad (2.15)$$

and

$$\Delta g(R.0.\lambda) = \frac{GM}{R^2} \sum_{l=2}^{\infty}(l-1) \sum_{m=0}^{l} \quad (\overline{\Delta Clm}\cos m\lambda + \overline{\Delta Slm} \sin m\lambda) \, Plm \, (\cos\theta) \quad (2.16)$$

Respectively, from Eq. (2.15) and (2.16) it follows that the expression for the corresponding Stokes coefficient of the gravity disturbances and gravity anomalies are respectively.

$$\begin{vmatrix} \left|\Delta\overline{C}_{lm}^{\delta g}\right| \\ \left|\Delta\overline{S}_{lm}^{\delta g}\right| \end{vmatrix} = \frac{GM}{R} (l+1) \begin{vmatrix} \left|\Delta\overline{C}_{lm}\right| \\ \left|\Delta\overline{S}_{lm}\right| \end{vmatrix} \quad (2.17)$$

And

$$\begin{vmatrix} \left|\Delta\overline{C}_{lm}^{\delta g}\right| \\ \left|\Delta\overline{S}_{lm}^{\delta g}\right| \end{vmatrix} = \frac{GM}{R} (l-1) \begin{vmatrix} \left|\Delta\overline{C}_{lm}\right| \\ \left|\Delta\overline{S}_{lm}\right| \end{vmatrix} \quad (2.18)$$

III.11. GLOBAL GRAVITY FIELD MODEL

In April 2008, the National Geospatial-Intelligence Agency (NGA) released "the Earth Gravitational Model 2008" (EGM2008) (Pavlis *et al.*, 2008). The model is complete to spherical harmonic degree and order 2159. It is a combined model based on information from CHAMP. GRACE satellite gravity missions as well as a global gravity anomaly database. In April 2011, a new combined global gravity field model EIGEN-6C »Foerste *et al.*, 2011) had been developed by GeoForschungs Zentrum Potsdam and Croupe the Recherche de Geodesie Spatiale (GRGS) Toulouse. The EIGEN-6C gravity model is complete to the spherical harmonic degree and order 1420 and it is based on the data from CHAMP. GRACE. GOCE satellite gravity missions and terrestrial global gravity anomaly data provided by the Danish Technical University (DTU10 gravity model) (Anderson *et al.* 2009. Anderson 2010). Recently, EIGEN-6C2, a new combined global gravity field model complete to degree and order 1949 (10 km spatial resolution) is released

by GFZ Potsdam and GRGS Toulouse (Forste *et al.*, 2013). The EIGEN-6C2 model is based on data from GOCE together with data from previous satellite gravity missions, and surface gravity data from DTU10. Another combined model used in the current work is the World Gravity Model 2012 (WGM 2012). The WGM 2012 was developed from the Earth Spherical Model (Balmino *et al.*, 2012; Bonvalot *et al.*, 2012) with spatial resolution of ~9 km.

The WGM 2012 data were compiled from land, airbone and marine surveys and satellite gravimetry from the Gravity Recovery and Climate Experiment (GRACE) mission (Bonvalot *et al.*, 2012). These data were compiled by the Bureau Gravimetrique International (BGI) with the support of the United Nations Educational Scientific and Cultural Organization (UNESCO) in association with the International Gravity Field Services (IFGS). These high-resolution, high-accuracy, and combined modern gravity models offer new opportunities to study different interfaces and the dynamics of various processes which occur inside the Earth.

The improved resolution and accuracy of available gravity field models enhance the interest of researchers to studies the interior of the Earth structure in detail especially in regions where limited or inhomogeneous seismic data is available. These models provide an opportunity for improving our knowledge of basic crustal and lithospheric structure of the Earth.

III.12. ISOSTASY AND CRUST MODELS

The term Isostasy is used to describe the state of equilibrium to which the Earth lithosphere and asthenosphere tend, in the absence of external disturbance forces.

The alternative view of isostasy is the Archimedes principle of hydrostatic equilibrium. According to this principle, a lighter solid body always floats on the denser underlying fluid. From the hydrostatic equilibrium, the pressure generated by the column of the Earth crust at a given depth of compensation at the underlying mantle is constant, otherwise a lateral pressure gradient occurs, which causes the mantle material to move until a constant pressure condition is reached. The theory of isostasy states that a distribution of hydrostatic pressure exists below the surface of compensation (Torge. 1991).

The theory of isostasy is in line with the observation that the global Bouguer anomalies (free air gravity anomaly corrected for the effect of the topography above the geoid) have a systematic pattern over the globe. It is generally positive in the oceanic regions, mostly negative in the

continental regions and shows strong correlation with the topographic heights. This means that the mass excess and deficiency are at least partially compensated by the corresponding mass distribution inside the Earth. According to the isostasy principle, the mass of mountains must be compensated by a mass deficit below it. While the mass deficit at an ocean basin must be compensated by an extra mass at depth. In the mid of the nineteen centuries, two compensation mechanisms were proposed by Airy and Pratt.

1. The Airy model is based on constant density, where different topographic heights are compensated by changes in the lithospheric thickness (Airy. 1855, Heiskanen and Meinez. 1958).

2. The Pratt model, where different topographic heights are compensated by lateral changes in the lithospheric density (Pratt, 1855; Hayford, 1909a; Hayford and Bowie, 1912).

III.12.1. Airy isostatic model

Fig. 8(a) illustrates the Airy isostatic model. The Airy model is based on a constant density ρ_o and varying thickness of crust columns (Torge. 1991). T_0 is the thickness of normal column of crust which has the height H = 0 above sea level. The continental column of mountain height H forms mountain roots of thickness d_{cont} beneath the normal column of crust, and the oceanic column of depth t forms anti-roots with thickness d_{ocean} beneath the oceanic column.
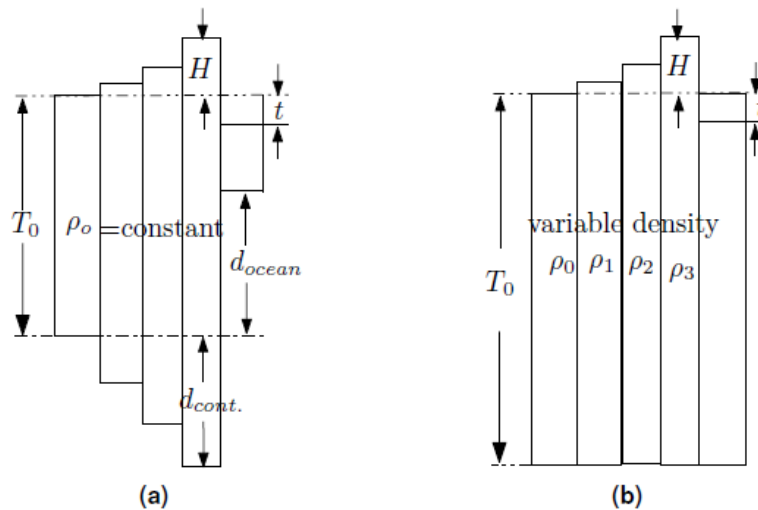
Figure 8: (a) Isostatic model of Airy; (b) Isostatic model of Pratt

According to the isostatic condition, the pressure p produced by a column of homogeneous density is given by

$$P = \frac{weight}{area} = \frac{\rho o g V}{\Delta S} = \rho_o g h = \text{constant}$$

where g is gravity. V is the volume of the column. ΔS is the column area, ρ_o is the column density and h is the total column thickness. If pm and px represent the density of mantle and sea water, respectively, then the pressure exerted by the normal column having height H = 0 is given by

$$P = \rho Q g T_0 + \rho m g d cont \quad (2.19)$$

and pressure exerted by the continental column of mountain height H is given as

$$p = \rho o g H + \rho o g T_0 + \rho o g d cont. \quad (2.20)$$

Similarly, for the oceanic column we have.

$$P = \rho o g t + \rho m g (d_{ocean} + d cont) + \rho_0 g (T_0 - t - d_{ocean}) \quad (2.21)$$

According to the condition of hydrostatic equilibrium, from Eqs. (2 19) and (2.20) we get

$$(\rho_m - \rho_o) d_{con} ; = \rho_o H \quad (2.22)$$

for the continent's equilibrium. Using Eqs. (2.19) and (2.21) we get

$$(\rho_m - \rho_o) d_{ocean} = (\rho_o - \rho_\omega) t \qquad (2.23)$$

for oceanic equilibrium. Using the conventional values for the homogeneous density $\rho o = 2670$ kg/m^3. Mantle density pm = 3270 kg/m^3, and density of water $\rho_\omega = 1030$ kg/m^3 the relation for the thickness of the roots and anti-roots are given by,

$$d_{cont} = 4.45H,$$

$$d_{ocean} = 3.72t$$

respectively.

The isostatic phenomena have a direct link with the observed gravity field of the Earth. The thickness to of the normal column of crust can be estimated using isostatic gravity anomalies obtained for different depths of compensation. Generally, for the depth of compensation equal to $T_0 = 30$ to 40 km the gravity anomalies are independent of topographic height. This result is in line with the result from seismic studies, which show that the isostatic surface of compensation can be approximated by the Mohorovicic discontinuity.

III.12.2. Pratt isostatic model

The Pratt model is based on the layer of constant thickness T_0 with lateral variations in crust density ρ (Torge. 1991). The isostatic model of Pratt is illustrated in Fig. 7.b. The normal column of height H= 0 has a density ρo, continental columns have smaller densities, while oceanic columns have higher densities. According to the Pratt model the equilibrium condition can be written as

$$\rho_0 T_0 = \rho cont(T_0 + H), \text{ for continents}$$

and

$$\rho_0 T_0 = \rho\omega t + \rho_{ocean}(T_0 - t), \text{ for oceans.}$$

Using the values $\rho cont = 2670$ kg/m^3, $\rho u = 1030$ kg/m^3 for the normal crust density and sea water density, respectively, the relation for the densities of the continental column and oceanic column can be written as;

$$\rho cont = 2670 \frac{T_0}{T_0 + H}$$

And $\rho ocean = \dfrac{2670To - 1030t}{T_0 - t}$

respectively.

Both Airy and Pratt isostatic models are based on local compensation. They assume that the compensation takes place along the vertical columns. In 1931 Vening Meinesz modified the Airy isostasy theory and introduced a regional instead of a local compensation. In this model the topography is considered as a load on unbreakable but yielding elastic crust. Moritz (2006) summarized the two models: as, *"standing on the thin ice sheet. Airy will break through, but under Vening Meinesz ice is stronger and will bend but not break"*.

III.13. MOHO AND LAB DEPTH ESTIMATION USING 2D RADIALLY AVERAGED SPECTRUM ANALYSIS

Moho depth in southern Cameroon and its surroundings was estimated using the two-dimensional (2D) radially-averaged power spectrum analysis (Tselentis *et al.*, 1988) for the WGM 2012 satellite gravity data. This method has been widely used for the Moho depth estimation from gravity data (Maden, 2010; Hussein *et al.*, 2013; Leseane *et al.*, 2015, Ngalamo *et al.*, 2017) and the lithospheric thickness (Green *et al.*1911; Makris *et al.*, 1991, Fairhead and Girdler, 1972; Stein and Cohran, 1985). The WGM 2012 satellite gravity data were upward continued to 2 km (Fig.

8A) to remove the effects of shallow sources, and then divided into 1°x1° (110x110 km) sub-regions with an overlap of 50% in all direction. Subsequently, the crustal thicknesses of 425 sub-regions with 1°x1° dimensions were calculated. By calculating the 2D radially-averaged power spectrum of the gravity data and plotting "ln (Power Spectrum)" against the "wavenumber (k)", Tselentis *et al.* (1988) showed that the depth to different gravity anomaly sources represent significant density change boundaries and can be estimated by fitting straight lines through the linear segments of the curve. Examples of the 3 mains types of the 2D radially-averaged power spectral curves observed is shown in (Figs. 9 B, C, D). This 2D radially-average power spectrum curve is for a sub-region of 1°x1° shown in Fig. (9A). Three linear segments of the radially-averaged power spectral curves were identified mainly out of the Benue trough and 4 linear segments were observed within the Benue trough (Fig. 9.B, C, D). These segments represent different density discontinuities (Fairhead and Okereke, 1987; Tselentis *et al.*, 1988; Gómez-Ortiz *et al.*, 2005). The segment of the curve that corresponds to the lowest wavenumbers (between 0.00 and 0.005) is taken to represent the regional or deep density boundary possibly the lithosphere-asthenosphere boundary. Differently, the portion of the curve that corresponds to the highest wavenumbers (between 0.25 and 0.55) represents possible shallow density boundaries within the crust or random noise contained in the data. For the three linear segments of the radially-averaged power spectral curves, the intermediate slopes corresponding to the intermediate wavenumbers segment (between 0.05 and 0.25) represent the Moho depth (Tselentis *et al.*, 1988; Sanchez-Rojas and Palma, 2014). For the four linear segments of the radially-averaged power spectral curves (Fig. 8B), there is two intermediate slopes the deepest one was associated to the mid-lithosphere-asthenosphere boundaries discontinuity which is not the focus in this study, and the second one to the Moho depth. The segment of the curve that corresponds to the highest wavenumbers is taken to represent the regional or deep density boundary possibly the lithosphere-asthenosphere boundary and the portion of the curve that corresponds to the lowest wavenumbers represents possible shallow density boundaries within the crust or random noise contained in the data. The error in the Moho depths estimates was calculated as the standard deviation of the linear fit of the intermediate segment. The error estimate range between 0.7 and 2.9 km.
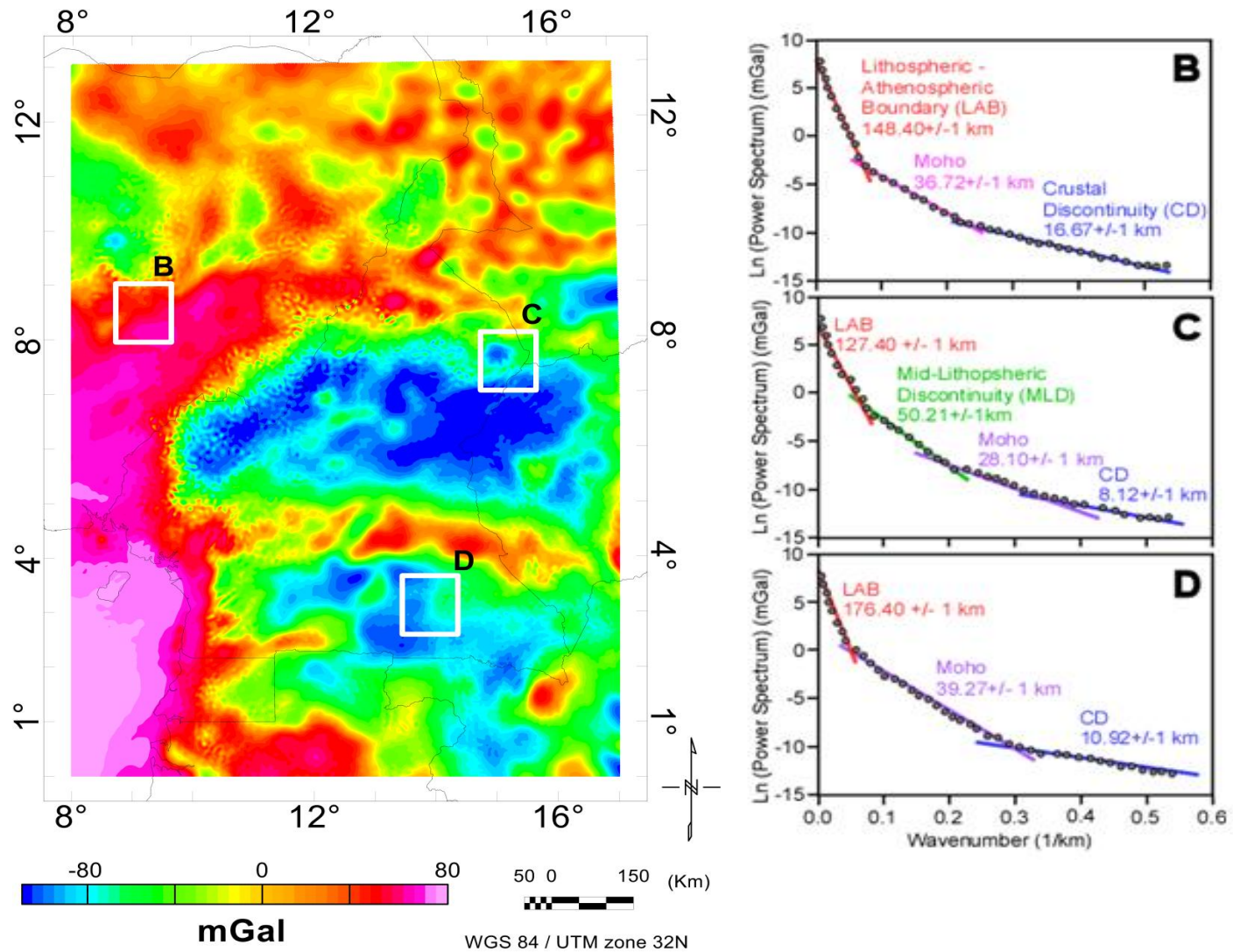
Figure 9: (A) Bouguer anomaly map from the World Gravity Map 2012 (WGM 2012). (B) Examples of the average radial spectral curve extracted from 1x1 degree sub-windows form World Gravity Map 2012 (WGM 2012) within the Benue trough; (C) Average radial spectral curve within the Benue trough. (D) Average radial spectral within the Congo craton.

III.14. LAB ESTIMATION USING THE INVERSION OF PASSIVE SEISMIC DATA

Fishwick and Bastow (2011) seismic tomography model of Africa was used in this study. The model has been calculated using the waveform inversion scheme of Cara and Lévêque (1987) based on S-wave dataset with nearly 12,000 paths in the African plate. The data for the S- wave tomography model come from a mixture of permanent seismic stations located on the African continent in addition to the data from Africa Array project (Nyblade *et al.*, 2008) and data from a number of temporary stations. The model is mainly for the uppermost mantle with a resolution of $0.5^{\circ} \times 0.5^{\circ}$ in area and 25 km in depth interval. The depth to LAB was obtained by converting the velocities of the S-waves to temperature following the parameterization of Priestley and Mckenzie (2006) where;

$$Vs = Vs\ (P, \Theta, a)\ (1)$$

P representing the pressure, Θ the temperature in ^{0}C and a is a variable describing the activation process

$$a = A' \exp -(E + PVa)/\ RT\ (2)$$

where A' is a frequency factor, E the activation energy, Va the activation volume and T is the temperature in Kelvin. The activation process responsible for the rapid decrease in Vs as the melting point is approached is presumably the same as that responsible for the corresponding decrase in Q (attenuation). it is convenient to remove the nonactivated part of the pressure dependence of Vs by writing

$$Vs^* = Vs/(1 + bv\ (z\text{-}50))\ (3)$$

Where z is the depth in km and bv is an empirical constant. Since the variation of Vs in the upper mantle is small, we expend $Vs^*(a)$ using a Taylor series

$$Vs^*(a) = Vs^*\ (0) + (\frac{\partial Vs*}{\partial a})_0\ a\ (4)$$

And write

$$Vs^* = m\Theta + c + A \exp\text{-}(E+PVa)/RT.\ (5)$$

Vs (z, Θ) can be obtained from Eqs. (3) and (5). To invert Eq. (5) to obtain Θ (z, vs), Vs was first converted to Vs*.

So to estimate the depth to the LAB (z), we used a GMT script to track the coordinates from 25 km till 250 km depths regarding the velocity to temperature conversion (Vs (z, Θ)). The GMT tool was also used to plot S-wave velocities at different depth.

CHAPTER IV:
RESULTS AND DISCUSSION

IV.1. RESULTS

IV.1.1. Gravity anomaly characteristic of Cameroon and surrounding

Fig. 10A shows the gravity anomaly characteristics of Cameroon and the surrounding regions through a 2 km upward continuation of the Bouguer gravity anomaly, vertical derivative tilt map from the 20 km upward continuation of the Bouguer gravity anomaly data (Fig. 10B), and positive (Fig. 11A) and negative (Fig. 11B) tilt derivative maps.

These images show different gravity anomalies that can be broadly associated with the Precambrian tectonic entities and more recent Phanerozoic tectonic features. The gravity anomalies associated with the Phanerozoic tectonic features was describe before focusing on describing the gravity anomalies associated with the Precambrian tectonic entities.

The post-Precambrian geological features are represented by the Benue trough, the Cameroon volcanic line, The Chad basin and the coastal zone of the Atlantic Ocean. The Benue trough (Fig.10A) is characterized by the presence of a NE-SW elongated high gravity anomaly (Figs. 10A, 10B and 11A). This anomaly is likely due to a combination of an elevated asthenosphere and mafic bodies underplating beneath the trough (Poudjom Djomani *et al.*, 1997). Differently, the Cameroon volcanic line (Labeled CVL in Fig. 10A) is marked by a NE-SW elongated low gravity anomaly that is especially apparent in the vertical tilt derivative of the 2 km upward continuation of the Bouguer anamaly map (Figs. 10B and 11B). This low gravity anomaly might be due to the presence of melt beneath the Cameroon volcanic line. The Chad basin (Figs. 10A; 10B and 11A) is characterized by the presence of a large band of high Bouguer anomaly covering one part of Chad, North Cameroon and North Nigeria. This large band of high gravity anomaly associated with either the sedimentary basins and grabens formed during the Cretaceous (Genik, 1992; Poudjom Djomani *et al.*, 1997) or a basic intrusion into the basement beneath shallow sedimentary cover (Poudjom Djomani *et al.*, 1997). For the large part, the coastal zone of the Atlantic Ocean is characterized by the presence of a high gravity anomaly (Fig. 10A). It is possible that the source of this anomaly is the presence of the high-density oceanic crust of the Atlantic Ocean.

The presence of low gravity anomaly characterizing the Cameroon volcanic line that we considered to be associated with melt is consistent with results from passive seismic studies from the "Cameroon Seismic Experiment'. Reusch *et al.* (2010) found a low-velocity anomaly beneath

the Cameroon volcanic line that is defined by (-1%) to (-2%) relative reduction in the velocity of the P-wave and (-2%) to (-3%) relative reduction of the velocity of the S-wave. Reusch *et al.* (2010) attributed this low-velocity anomaly to thermal perturbation of the mantle beneath the Cameroon volcanic line and that this thermal perturbation extends to a depth of at least 300 km.

Similarly, Adams *et al.* (2015) used the same Cameroon Seismic Experiment data to show that Rayleigh wave phase velocities decreases by (-2%) from the regional average beneath the Cameroon volcanic line. Adams *et al.* (2015) proposed that this might be due to infiltration or thermal erosion of the SCLM underneath the Cameroon volcanic line possible due to small-scale convection due to the edge effect of the thicker SCLM root of the Congo craton.

The gravity anomalies associated with the Precambrian tectonic entities was divided into those associated with the Congo craton and the Yaoundé domain, the northern Adamawa-Yade domain, and the southern Adamawa-Yade domain (Fig. 10A and 10 B). The source of the gravity anomalies associated with the West Cameroon domain might not represent features associated with its Precambrian lithospheric structure. Rather, these gravity anomalies are likely associated with younger tectonic elements such as the Benue trough and the Cameroon volcanic line. Nonetheless, the southeastern part of the Western Cameroon domain is characterized by the presence of NE-SW elongated low gravity anomaly, the southwestern margin of which closely coincides with spotty high gravity anomalies aligned along the NE-trending Tchollire-Banyo shear zone (Labeled TBSZ in Fig. 10A). This anomaly is likely associated with the Cameroon volcanic line. Differently, the northwestern part of the West Cameroon domain, northwest of the Cameroon-Nigeria border is marked by a prominent high gravity anomaly (Fig. 10A). This anomaly is clearly visible in the positive tilt derivative map of the Bouguer gravity data (Fig. 10B). It is likely that this anomaly is directly related to the lithospheric structure of the Benue trough.

For the most part, the Congo craton, the Yaoundé domain and the northern part of the Adamawa-Yade domain are characterized by low gravity anomalies (Fig. 10A, 10B and 11B). For the Congo craton and the Yaoundé domain this low gravity anomaly might be due to the nature of the outcropping crystalline basement rocks which consist of low-density lithology's such as felsic gneisses and metasedimentary rocks, and syn-tectonic granites (Fig. 5).
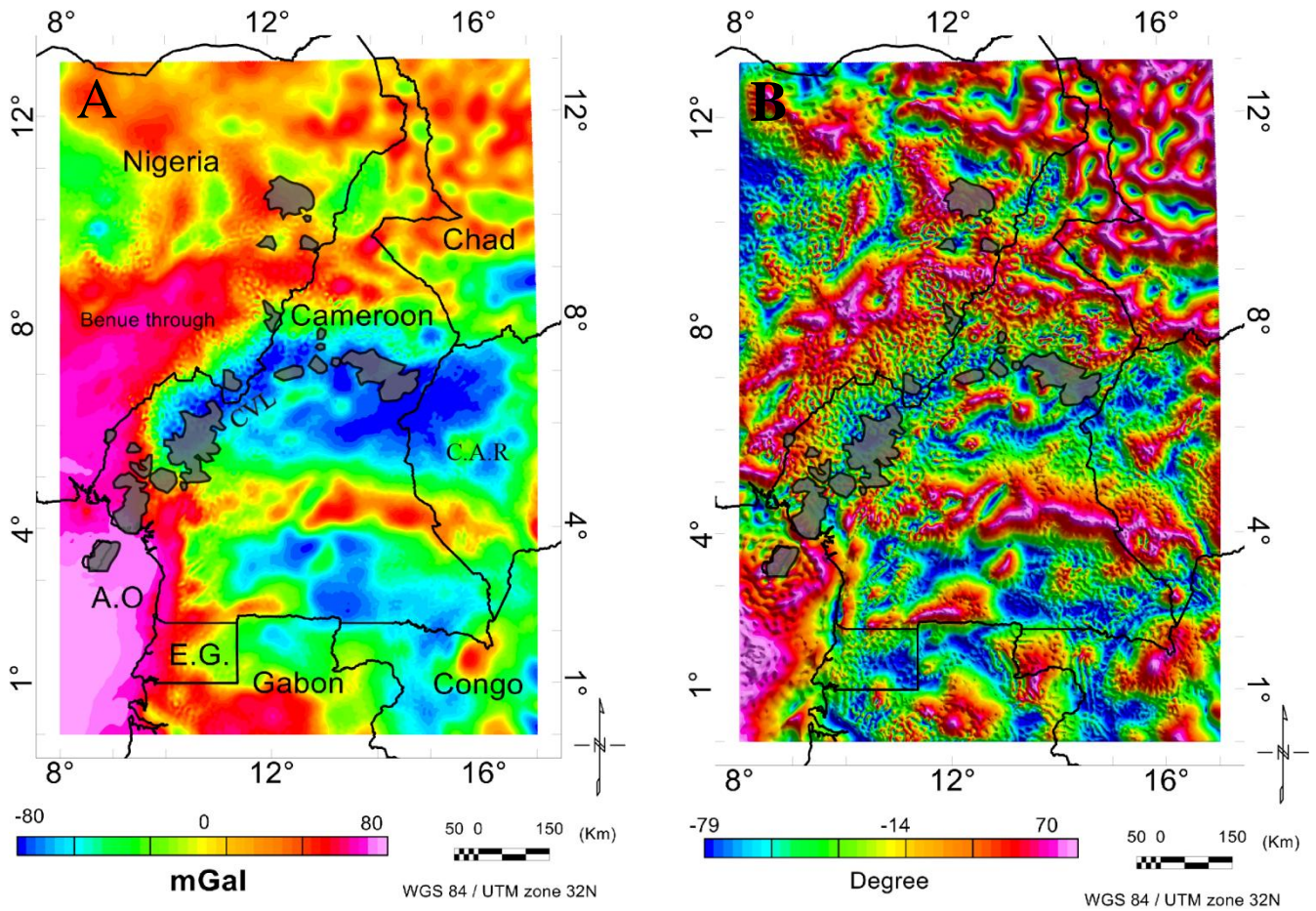
Figure 10: (A) Two km upward continuation of the Bouguer anomaly map extracted from the World Gravity Map 2012 (WGM 2012) data. The WGM 2012 data are used for the estimation of the crustal thickness and lithospheric thickness of southern Cameroon and surrounding regions using two-dimensional (2D) power-density spectrum analysis and the development of lithospheric-scale cross-sectionals view. CVL = Cameroon volcanic line. (B) Vertical tilt derivative of the 2 km upward continuation of the Bouguer anamaly map overlap by the Cameroon volcanic line.
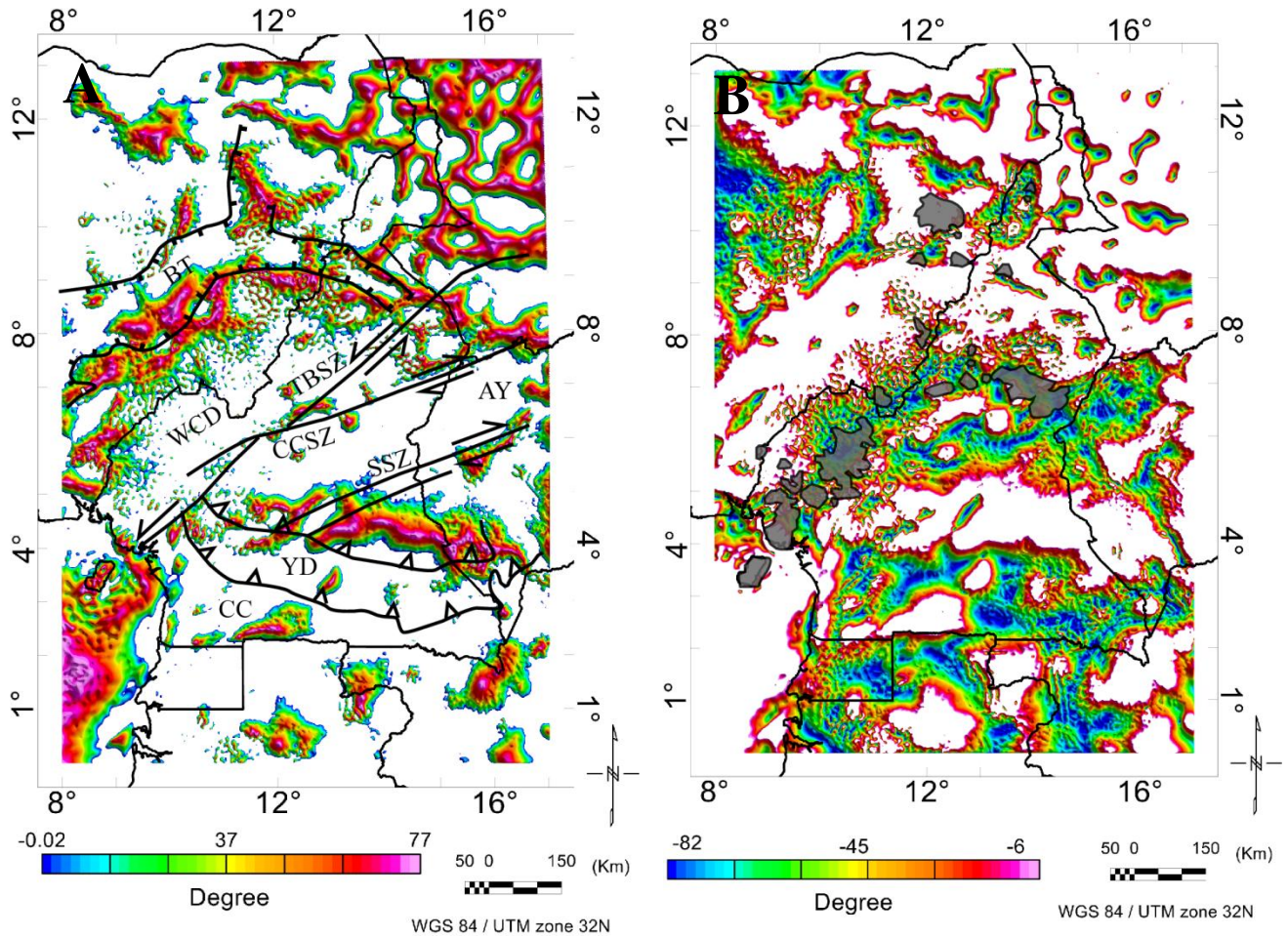
Figure 11: Positive (A) and negative (B) tilt derivative maps of southern Cameroon and surrounding regions extracted from the vertical tilt derivative of the 2 km upward continuation map shown in Fig. 10 A. CC= Congo craton, YD = Yaounde domain, AY = Adamawa-Yade domain, WCD = West Cameroon domain, SSZ = Sanaga shear zone, CCSZ = Central Cameroon shear zone, TBSZ = Tchollire-Banyo shear zone, BT = Benue trough.

The low gravity anomaly of the northern part of the Adamawa-Yade domain can be attributed to the presence of voluminous amount of granitoids within the crust (Fig. 5).

The high gravity anomaly within the Yaounde domain and the Congo craton (Fig. 11A) can be attributed to the nature of volcano-sediment or to the metasomatised lithosphere associated with uplift and erosion at the base of the craton during a Mezozoic tectonic event characterize by uplift, basin formation and wide spread of magmatism within the cratonic area (Poudjom Djomani *et al.* 1997).

The most prominent gravity feature in southern Cameroon is the E-W elongated high gravity anomaly that extends within the southern part of the Adamawa-Yade domain parallel to latitudes

4° and 5° N between longitudes 10° and 17° E (Figs. 10A and 11A). In its central part this high gravity anomaly reaches ~100 mGal and its positive tilt derivative reaches ~55° (Figs. 10B and 11A). This anomaly does not correspond to the presence of denser lithological units in the southern part of the Adamawa-Yade domain. This observation, together with the vast geographic extent of this high gravity anomaly and its persistence in the 20 km upward continuation map strongly suggest that it is associated with a deeper source, possibly at the Moho depth level. Hence, we suggest that this anomaly is associated with a denser region at the Moho beneath the southern margin of the Adamawa-Yade domain. This will be explained further below under the "Results from the Two Dimensional (2D) Forward Modeling" section.

It has long been recognized that Precambrian suture zones are characterized by what is referred to as "paired gravity anomaly". The gravity signature across a Precambrian suture zone is characterized by a low gravity anomaly over the more felsic cratonic domains and a high gravity anomaly over the more mafic juvenile domains. The low and high gravity anomalies are separated by steep gravity gradient that coincides with the suture zone between the two domains (e.g. Gibb and Thomas, 1978). Paired gravity anomalies have been observed in many Precambrian regions including Australia (e.g. Mathur, 1974; Wellmann, 1988), Canada (e.g. Gibb *et al.*, 1983), India (e.g. Subrahmanyam *et al.* 1978; Narain *et al.* 1986), and Africa (e.g. Black *et al.*, 1979; Abdelsalam and Dawoud, 1991). The steep gravity gradient is often explained as due to presence of denser material along the suture zone such as ophiolitic material. For example, Black *et al.* (1979) explained the presence of paired gravity anomaly in Mali as due to presence of an ophiolite-decorated suture zone between the West Africa craton in the west and the Pan-African (Neoproterozoic) terranes to the east. Similarly, Abdelsalam and Dawoud (1991) explained the presence of paired gravity anomaly in Sudan as due to the presence of an ophiolite-decorated suture zone between the Saharan Metacraton in the west and the juvenile terranes of the Arabian-Nubian Shield to the east.

There are differences between the typical paired gravity anomalies their sources on the one hand and the prominent high gravity anomaly of southern Cameroon on the other hand. First, the southern Cameroon high gravity anomaly is much broader (~200 km in width) and higher in magnitude (~100 mGal at its peak) (Fig. 10A) than what is observed in the paired gravity anomalies in other regions around the world. Second, different from the cross-sectional geometry of the paired gravity anomalies (low and high gravity anomalies separated by steep gravity

gradient), the high gravity anomaly of southern Cameroon is surrounded by low gravity anomalies over the northern edge of the Congo craton (Maurizot *et al.*, 1986) and the Yaounde domain in the south and the Adamawa – Yade domain to the north (Fig. 10A). Third, unlike the paired gravity anomalies stemming from the juxtaposition of less dense (cratonic blocks) and denser (juvenile terranes) crustal blocks along suture zones containing even denser material (ophiolitic fragments), there is no significant lithological variation between the Congo craton, Yaounde domain and Adamawa – Yade domain that can explain the presence of such a prominent high gravity anomaly.

IV.1.2   Crustal thickness and Moho depth estimation

IV.1.2.1. The crustal thickness and Moho depth estimation from two dimensional (2D) radially-averaged power spectrum analysis.

Four hundred twenty-five of the 2D radially-averaged power spectral analyses of the Bouguer gravity anomaly from the WGM 2012 data were used to image the Moho depth in southern Cameroon. The rasterized version of this map is shown in Fig. 12A whereas the discrete Moho depth values obtained from the 2D radially-average spectral curves of the individual 1^oX1^o sub-regions are shown in Fig. 12B. The Phanerozoic tectonic features are represented by the Cameroon volcanic line (Labeled CVL in Fig. 12B), and the Benue trough. It is note that the Cameroon volcanic line (Labeled CVL in Fig. 12B) is underlain by heterogeneously thinned crust compared to the crust underlying the Precambrian tectonic entities, where the Moho depth shallows to ~33 km in some places (Figs 12 A and B).

The most notable feature in the Moho depth map is the presence of thicker crust beneath the Congo craton, the Yaoundé domain and the southern part of the Adamawa – Yade domain (Fig. 10B). In the southeastern part of the Adamawa-Yade domain the crust is as thick as 45 km (Figs. 10A and B). This is different from the central and northern part of the Adamawa-Yade domain where thinner crust appears to underlie this part of the domain (Figs. 12 A and B). In parts of the northern part of the Adamawa-Yade domain, the Moho is as shallow as 32 km (Figs. 12 A and B). The thinnest crust was found to be in the southwest beneath the crust of the Atlantic Ocean and in the northwest beneath the Benue trough where the Moho is as shallow as 17 km (Figs. 12A and B).
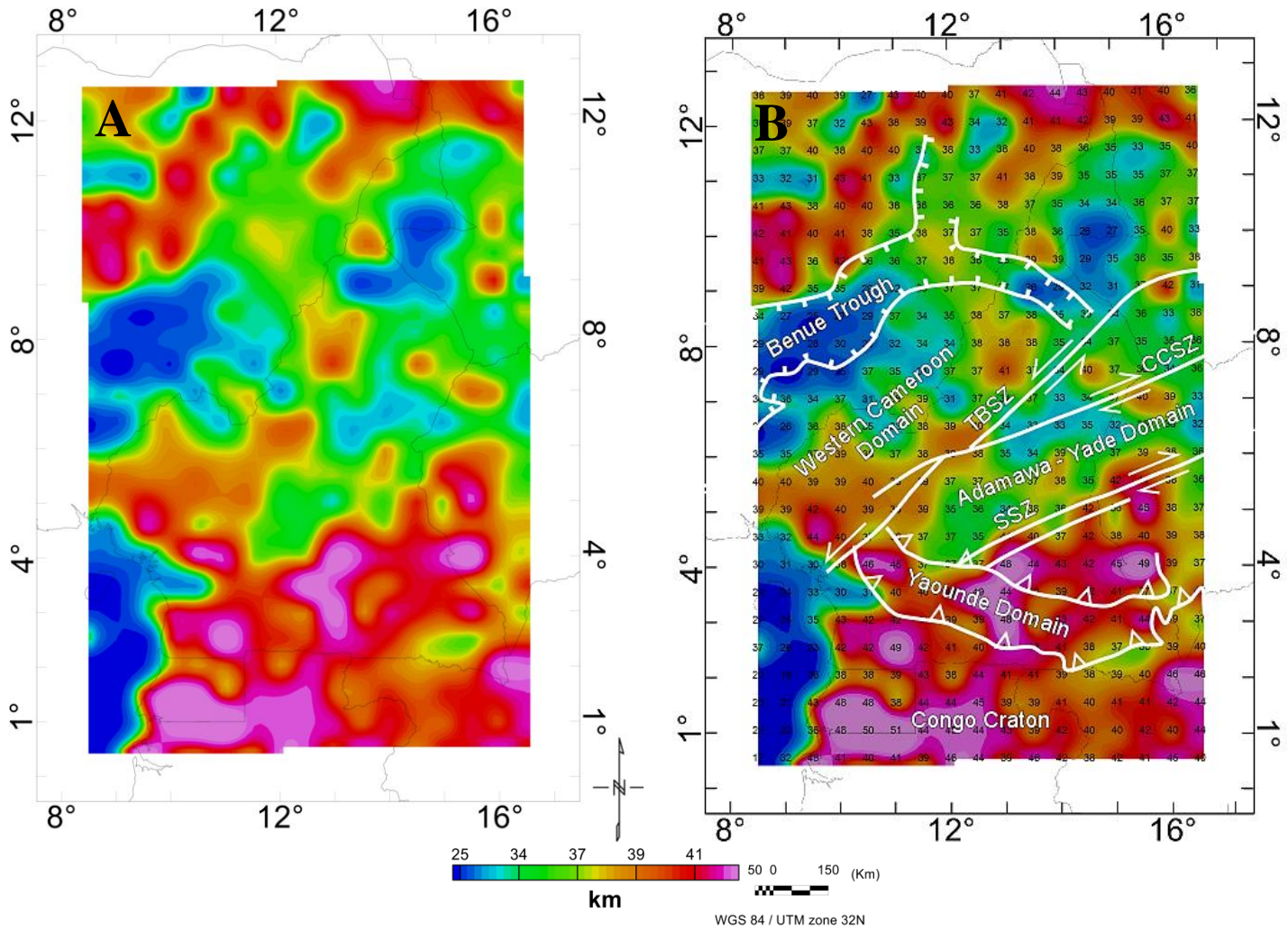
Figure 12: (A) Color-coded map showing crustal thickness (Moho depth) of the CASZ and its surrounding in Cameroon estimated from the World Gravity Map (WGM2012) data using two-dimensional (2D) radially-averaged power-spectrum analysis. (B) a map showing the values (in Km) of crustal thicknesses obtained for individual 1x1 degree sub-regions used in the 2D radially-averaged power spectrum analysis of the WGM2012 data covering southern Cameroon and surrounding regions. CASZ = Central African Shear Zone; CVL= Cameroon volcanic line; SSZ = Sanaga shear zone; CCSZ = Central Cameroon shear zone.

IV.1.2.2. Comparison of gravity Moho result derived from radial averaged power spectrum analysis with previous geophysical studies.

Previous estimates of the thickness of the continent crust and the Moho depth of Cameroon came from seismic studies, passive seismic studies and ground gravity surveying studies. The earliest studies across the Adamawa plateau and the Garoua rift used 40 seismometers deployed from November 1982 to March 1983 (white small circles Fig. 13B) and 30 blasts in four neighboring quarries as energy source (Stuart *et al.*, 1985).Stuart *et al.* (1985) found that the crustal thickness in the central part of the seismometer network (closed to circle number 26 in Fig. 13A) is ~33 km. Moho depths estimate for this region for the 2D radially-averaged power spectrum analysis is 37 km. Tokam *et al.* (2010) used one-dimensional (1D) S-wave velocity model obtained from joint inversion of Rayleigh wave group velocities and P-receiver functions for the 32 seismic stations from the Cameroon broadband Seismic Experiment (CBSE) to estimate the crustal thickness in Cameroon (Table 1; Fig. 13A). Eight stations were deployed between January 2005 and January 2007 while 24 stations were deployed between January 2006 and January 2007. Gallacher and Bastow (2012) used the same data from the CBSE to estimate the Moho depth using teleseismic receiver function. In their studies, Tokam *et al.* (2010) reported Moho estimates for all stations except stations 8 and (Table 1; Fig. 13A). Additionally, Tokam *et al.* (2010) considered Moho depth estimate of station 9 to be questionable (Table1). Gallacher and Bastow (2012) used all the stations except stations, 8, 9, 14, 15, 18, 19, 28 and 31 (Table 1; Fig. 13A). The Moho depth estimates of 23 out of the 27 passive seismic stations reported by Tokam *et al.* (2010) are within ± 6 km of the Moho depth estimates from the 2D radially-averaged power spectrum analysis (Table 1).
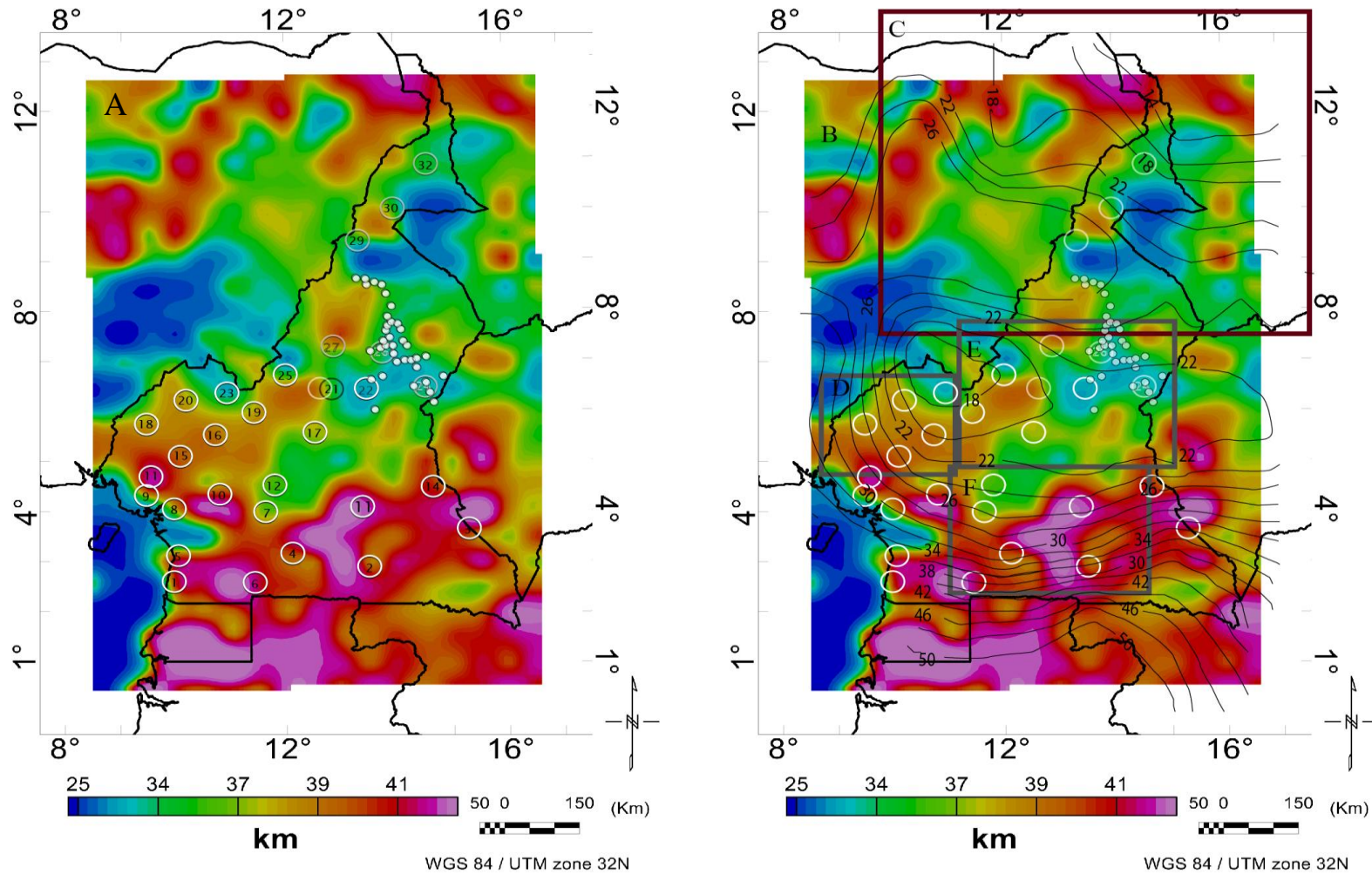
Figure 13: (A) Color code showing the crustal thicknesses or Moho depth of Cameroon and environs estimated from the World Gravity Map (WGM2012) data using two-dimensional (2D) radially-averaged power-spectrum analysis. The white circles with number in Fig.13 A and white circles in Fig. 13B represent the locations of the passive seismic station of Tokam *et al.* (2010) and Gallacher and Bastow (2012). (B) Color code showing the crustal thicknesses or Moho depth of Cameroon and environs estimated from the World Gravity Map (WGM2012) data using two-dimensional (2D) radially-averaged power-spectrum analysis. The box labeled "D", "E" and "F" defines the sub-regions used by Nnange *et al.* (2000) to estimate the Moho depth using spectral analysis of ground gravity data. The solid black line with numbers represents the Moho depth estimates from Poudjom Djomani *et al.* (1995) using spectral analysis of ground gravity data. The red box labeled "B" defines the location of the sub-region used by Eyike and Ebbing (2015) to image the crustal thickness using gravity inversion.

Impressively the Moho depth estimated by Gallacher and Bastow are 22 out of 24 within ± 6 km from the 2D radially-averaged power spectrum derived Moho depth (Table1).

One of the highest difference in the Moho depth estimate between our 2D radially-averaged power spectrum analysis and passive seismic results of Tokam *et al.* (2010) came from stations 1 (14 km) and 5 (15 km) (Table1). These stations are located close to the shore line of the Atlantic Ocean in the Western edge of the Congo craton. It is possible that the Moho depth estimate from passive seismic study reflects the thickness of the thinner crust close to the Atlantic Ocean whereas the Moho depth estimate of the 2D radially-averaged power spectrum analysis measure the average of the crust close to the Atlantic Ocean and the thicker crust of the Congo craton since the $1^0 \times 1^0$ degree sub-region used in the latter method span an area of ~110 x 110 km.

Table 1: Comparison between the Moho depth estimates from the two-dimensional (2D) radially-averaged power spectral analysis and estimates from passive seismic study of Tokam *et al.* (2010) and Gallacher and Bastow (2012)

Station	Gravity	Seismic Moho depth (Tokam *et al.*, 2010)	Seismic Moho Gallacher and Bastow (2012)	Difference (Seismics)	Difference between gravity and seismic (Tokam *et al.*, 2010)	Difference between gravity and seismic (Gallacher and Bastow, 2012)
1	42	28	37.6	9.6	+14	4.4
2	43	43	44.6	1.6	0	-1.6
3	41	43	44.6	1.6	-2	-3.6
4	39	45	47.5	2.5	-6	-8.5
5	43	28	37.4	9.4	+15	5.6
6	42	45	41.8	3.2	-3	0.2
7	37	43	41.8	-1.2	-6	-4.8
8	38					
9	30	25.5?				
10	37	38	35.8	-2.2	-1	1.2
11	44-	48	43.3	-4.7	-4	0.7
12	37	38	37.8	-0.02	-1	-0.8
13	44	28	36.5		16	7.5
14	42					
15	40	33			7	
16	40	35.5	34.1	-1.4	4.5	5.9
17	37	35.5	37.8	2.3	1.5	-0.8
18	39	30.5			8.5	
19	38	35.5			2.5	
20	36	33	33.7	0.7	3	2.3
21	34	35.5	34.1	-1.4	+1.5	-0.1
22	33	35.5	35.8	0.3	-2.5	-2.8
23	37	40.5	38.3	2.5	-3.5	-1.3
24	35	35.5	38.2	2.7	-0.5	-3.2
25	39	38	38.2	0.2	-14	+0.8
26	37-33	33	34.9	1.9	1	2.1
27	34-37	35.5	39.0	3.5	1.5	-2
28	38	30.5			7.5	
29	26-39	25.5	25.3		0.5	0.7
30	29	28	26.5		1	2.5
31	35	30.5			4.5	
32	34	33	33.3	0.3	1	0.7

Other method has been also used to estimate Moho depth beneath Cameroon. Poudjom Djomani *et al.* (1995) with ground gravity data used spectral analysis for ~ 32000 ground gravity measurements in Cameroon to show that the thickness of the continental crust in the focus area decreases from ~ 50 km in the south to ~ 18 km to the north (Fig. 12B). Poudjom Djomani *et al.* (1995) results agree with current result mainly in the southern part of the study area, the Adamawa-Yade and west Cameroon domain area presenting some considerable difference (Fig. 13B). Poudjom Djomani *et al.* (1995) suggest progressive northward thinning of the crust from ~50 to 22 km underneath the Adamawa-Yade domain, to 22-18 km beneath the west Cameroon domain (Fig. 13B). Result from our 2 D radially averaged power spectrum analysis do not support such uniform northward thinning of the crust. This discrepancy with the radial-averaged power spectrum analysis is due to the difference in the sub-regions used in the 2D radially-averaged spectrum analysis by Poudjom Djomani *et al.* (1995) (444 km x 444 km) compared to the current analysis (110 km x 110 km) with 50% overlap in all direction, that allowed for more detailed imaging of the variation in crustal thickness and Moho depth.

Additionally, Nnange *et al.* (2000) used spectral analysis for ~ 38,000 new and existing ground gravity measurements in Cameroon to calculate the average Moho depth in northern, western and southern Cameroon (shown as box labeled "D", "E", "F" in Fig. 13B). Nnange *et al.* (2000) estimated the Moho depth to be 30 ± 2 km in the area "D", 37 ± 2 km in the area "D", and 35 ± 3 km in the Area (F). The shallow Moho depth average reported by Nnange *et al.* (2000) for area "D" is shallower than what was obtained from the 2D radially-averaged power spectrum analysis (Fig. 13B). The Moho depth estimate obtained by Nnange *et al.* (2000) for area "E" generally agrees with results from 2 D radially-averaged power spectrum analysis which show that the center of this region is underlain by a relatively thin continental crust were the Moho can be as shallow as ~34 km (Fig). Also, the Moho depth average obtained by Nnange *et al.* (2000) for area "F" which covers dominantly the Congo craton and the overlying Yaoundé domain is significantly shallower than what have been obtained for this region in the current work (Fig. 13B). These discrepancies might be due to the significantly larger sizes (~450 km x450 km) of the sub-regions used by Nnange *et al.* (2000) for their spectral analysis.

Furthermore, Eyike and Ebbing (2015) used gravity inversion to produce a crustal thickness map. Eyike and Ebbing (2015) study area continues further north of the focus zone (area labelled "C"). The study area covers the southern part of their study area (Fig. 13B). The result of crustal

thickness obtained by Eyike and Ebbing (2015) shows relatively constant crustal thickness, with Moho depth comprise within the range of 28 -37 km. Their shallowest Moho is found beneath the upper branch of the Benue trough while the other parts are relatively constant with Moho depths comprise within the range of 30 to 37 km. Those results differ slightly from our result from radial-averaged power spectrum analysis where crustal thickness in few places reaches 43 km.

Tegume *et al.* (2013) used three-dimensional (3D) inversion of the global gravity model EIGEN-6c to image the Moho depth and to estimate crustal thickness of the Africa continent. Results from the 3 D inversion of the global gravity model were calibrated with result obtained from 377 passive seismic stations that were used to calculate crustal thickness using receiver function approach. Tugume *et al.* (2013) presented an average crustal thickness of 45 ± 2 km for the Congo craton and 39 ± 3 km for the Oubanguides orogenic belt. Further, in the study area Tugume *et al.* (2013) found that the majority (20 out of 27) crustal thickness results obtained from the 3D inversion of the global model are within ± 6 km of the results obtained from passive seismic receiver function analysis. It is not possible to compare our results with those of Tugume *et al.* (2013) because only crustal thickness averages are presented for major Precambrian entities in that study. However, we note that the crustal thickness results we obtained from the 2D radially-Average power spectrum analysis are also within ± 6 km of result obtained from passive seismic receiver function analysis by Gallacher and Bastow (2012) (Fig. 13A, Table 1).

IV.1.3. Seismic velocity underneath Cameroon and its surroundings

Figs. 14A-E shows the S-wave velocity distribution beneath Cameroon and its surroundings obtained from the regional seismic tomography model of Africa (Fishwick and Bastow, 2011) at 100 km, 125 km, 150 km, 175 km, and 200 km depth. We observed two contrasting S-wave velocity structures of the lithosphere beneath Cameroon and surroundings. On the one hand, the Congo craton and the Yaoundé domain are characterized by faster S-wave velocity reaching ~4.8 km/s and this faster S-wave velocity persisted to a depth of ~175 km (Fig. 14A-D). On the other hand, the Western Cameroon domain and the Benue trough are characterized by slower S-wave velocity reaching ~4.1 km/s and this anomaly also persisted to a depth of ~175 km (Fig. 14A-D). These two contrasting S-wave velocity lithospheric domains are separated by a NE-SW elongated zone of intermediate S-wave velocities and this zone stretches along the Adamawa – Yade domain within the Tchollire – Banyo shear zone, the Central Cameroon shear zone, and the Sanaga shear

zone (Fig. 14A-D). These contrasting S-wave velocity structures of the lithosphere beneath Cameroon and surroundings seem to fade out at ~200 km depth (Fig. 14E).

Fig. 14F is a NW-SE trending 2D cross-section of the S-wave seismic tomography below the depth of 75 km. It reinforces the observation that the Congo craton (and the overlying Yaoundé domain) and most of the Adamawa – Yade domain are underlain by a lithosphere that is characterized by faster S-wave velocities reaching ~4.8 km/s and this faster velocity extends to a depth of ~175 km. This is different from the lithosphere beneath the West Cameroon domain and the Benue trough which is characterized by relatively slower S-wave velocities that can be as slow as 4.1 km/s and that it extends to a depth of ~175 km.
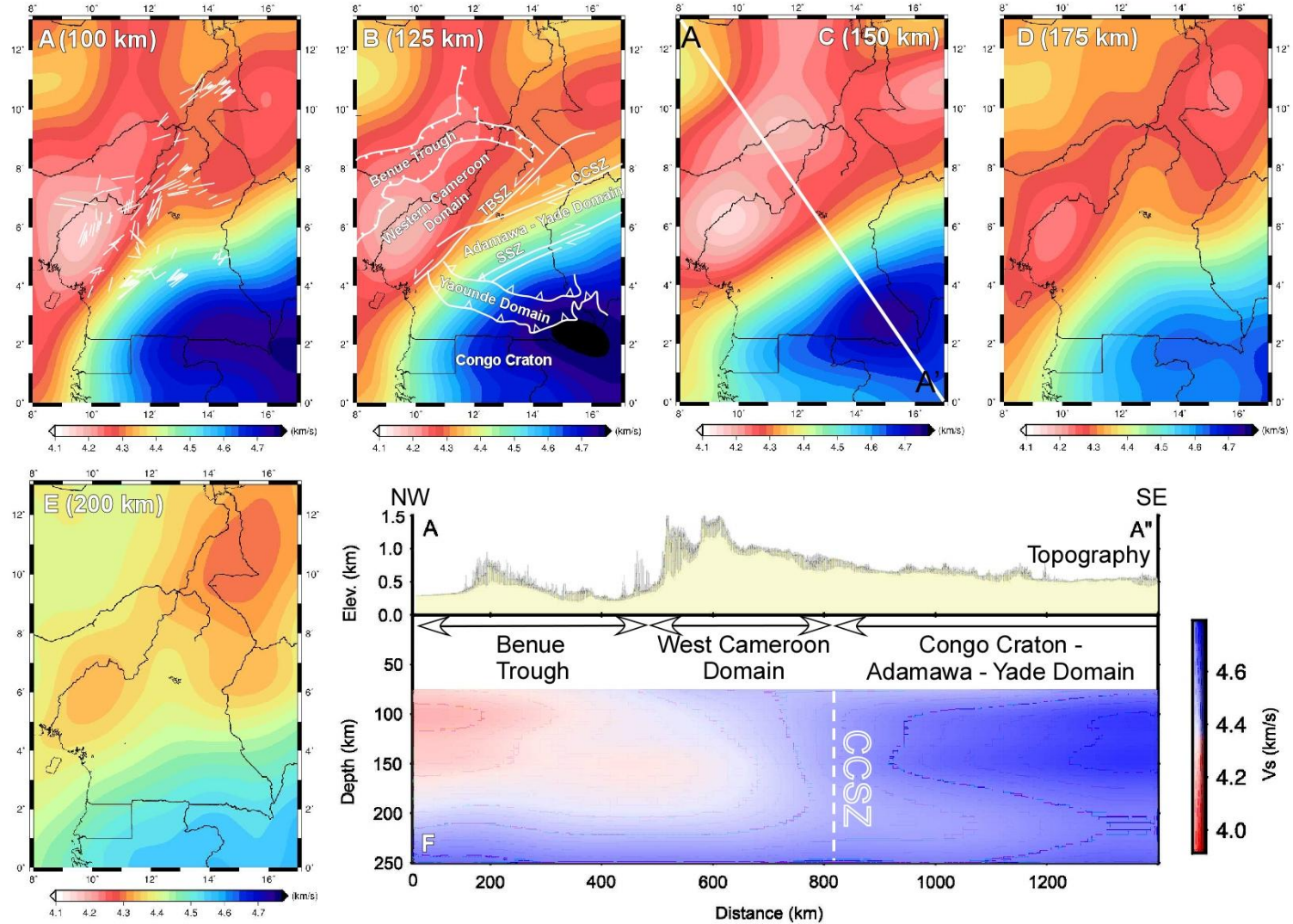
Figure 14: Shear-wave velocity structure of the lithosphere beneath Cameroon and surroundings at: (A) 100 km depth. (B) 125 km depth. (C) 150 km depth. (D) 175 km depth. (E) 200 km depth. (F) NW-SE lithospheric-scale cross-section showing S-wave velocity variation at depth beneath Cameroon and surroundings. See Figure 8C for cross-section location. TBSZ = Tchollire-Banyo shear zone. CCSZ = Central Cameroon Shear Zone. SSZ = Sanaga shear zone.

IV.1.4.   **Lithosphere thickness and LAB depth estimation**

> **IV.1.4.1. Lithosphere thickness and LAB depth estimation from two dimensional (2D) radially-averaged power spectrum analysis**

Fig.15 shows the resulting lithospheric thickness obtained from two-dimensional (2D) radially-averaged power spectrum analysis of the World gravity map 2012 (WGM 2012). Lithosphere thickness map (Fig. 15) shows thick lithosphere from 150 km to 199 km underneath the southern part of the Adamawa domain, the Yaoundé domain and the Congo craton. The border of this thick lithosphere has a general NE-SW trend and seems to follow a similar NE-SW trend of the Sanaga fault (SF) south of the CASZ line. North of the SF, underneath the northern part of the Adamawa-Yade domain, the WCD, The Benue trough, the coastal area and the oceanic area, the lithosphere thickness range from 75 km to 155 km underneath the ocean and from 113 km to 160 km in the hinterland area except at the latitude 10 N where horizontal spotted thick lithosphere (LAB depth ranges from 160 to 181 km) are observed south of the Biu Plateau and North of the Adamawa plateau. It can be noted that the lithosphere within the continental part appears to be thinner underneath the Benue trough, the CVL and the CASZ.

IV.1.4.2. Lithosphere thickness and LAB depth estimation from S-wave velocity inversion

Fig. 16 shows the depth to the LAB beneath Cameroon and surroundings obtained from the thermal inversion of the passive seismic tomography data. It shows that the thickness of the lithosphere beneath Cameroon and surroundings ranges between 72 km and 200 km. This variation in the lithospheric thickness can be diveded into three major ranges of 200 km – 166km, 166 km – 101 km, and 101 – 72 km. The regions where the thickness of the lithosphere is greater than 166 km are found beneath the Congo craton and the Yaounde domain (Fig. 16). The lithosphere with thickness ranging between 101 km and 166 km is found beneath the Adamawa-Yade domain including the Central Cameroon shear zone as well as the region to the northwest of the Benue trough. The thinnest lithosphere with thickness ranging between 72 km and 101 km is found beneath the Western Cameroon domain including the Tchollire – Banyo shear zone as well as the Benue trough (Fig. 16).
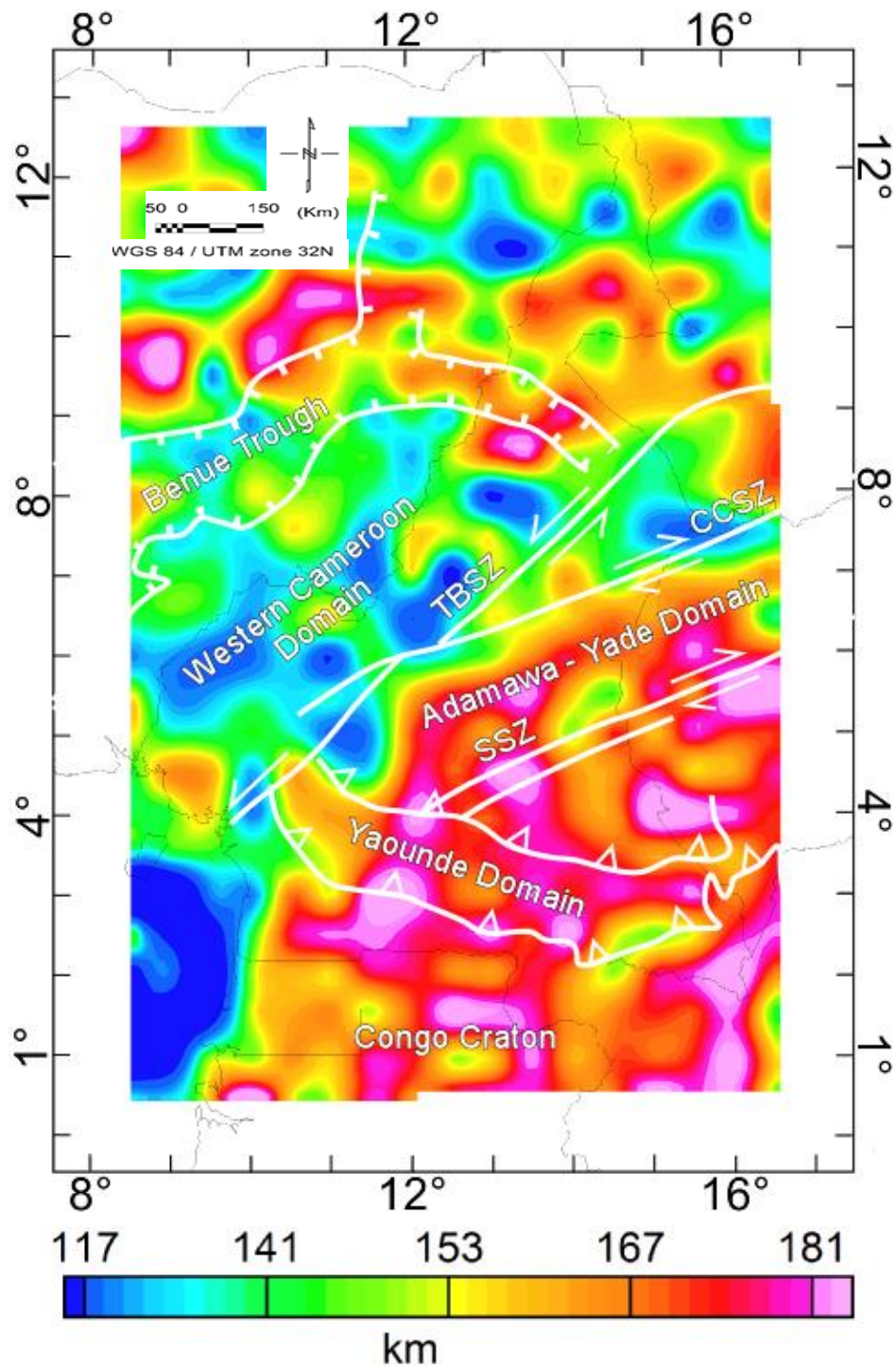
Figure 15: Color-coded map showing lithosphere-asthenosphere (LAB)/Mid-lithosphere discontinuity (MLD) of the CASZ and its surrounding in Cameroon estimated from the World Gravity Map (WGM2012) data using two-dimensional (2D) radially-averaged power-spectrum analysis. CCSZ = Central Cameroon Shear Zone; CVL= Cameroon volcanic line; SSZ = Sanaga Shear Zone. TBSZ = Tchollire-Banyo Shear Zone.
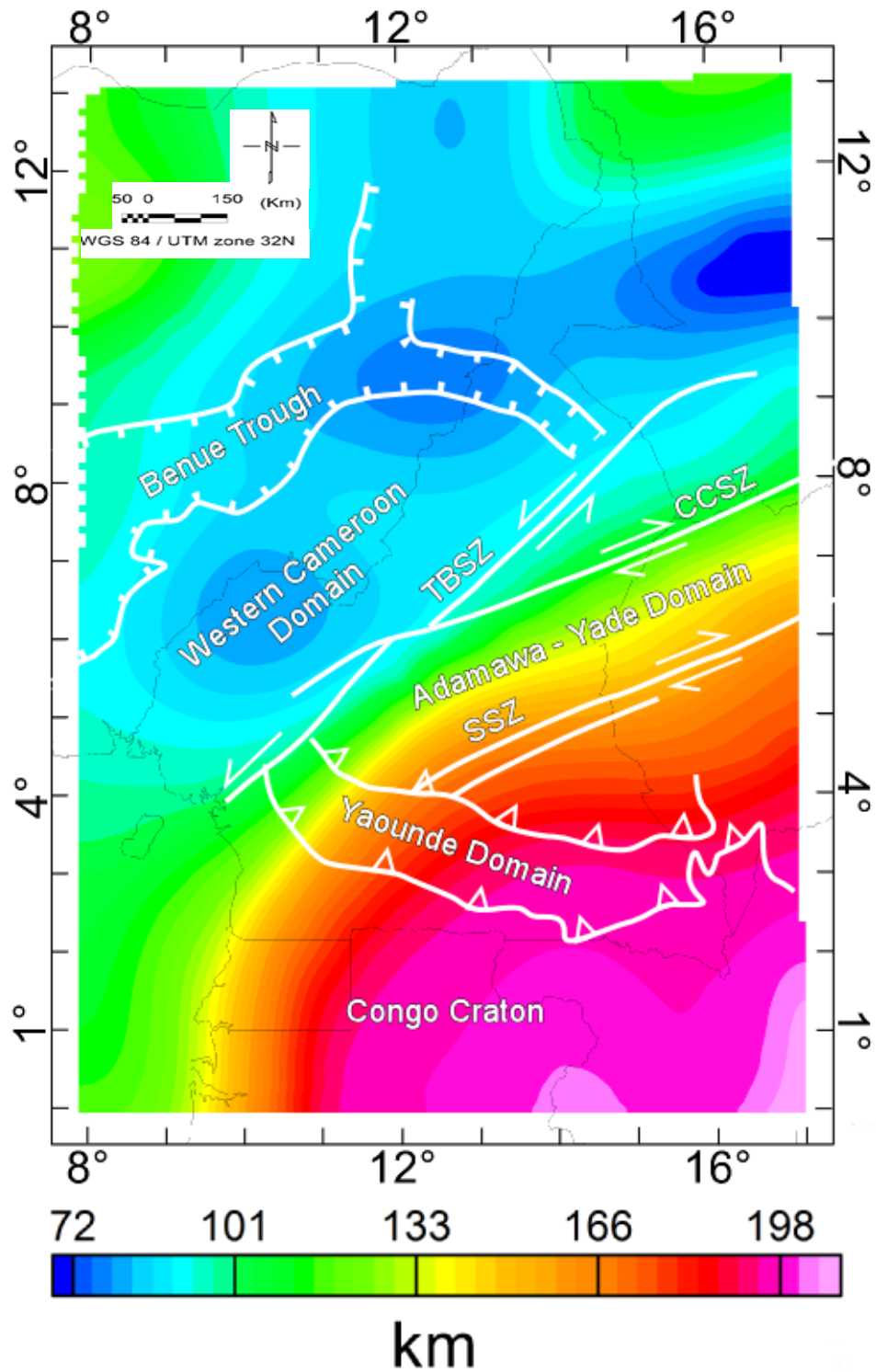
Figure 16: Lithosphere - Asthenosphere Boundary (LAB) depth estimates for Cameroon and its surroundings obtained from the thermal inversion of seismic data. TBSZ = Tchollire-Banyo shear zone. CCSZ = Central Cameroon Shear Zone. SSZ = Sanaga shear zone.

IV.1.4.3. Comparison of gravity LAB results from radial average spectral analysis, inversion of S-wave velocity from the current study with previous geophysical studies.

The depth to the LAB obtained from the 2D radial-averaged power spectrum analysis of the WGM2012 (Fig. 15) and that obtained from the thermal inversion of passive seismic tomography data (Fig. 16) are impressively similar. In both analyses the thickest lithosphere (as thick as ~200 km) is found beneath the Cameroon craton, the Yaounde domain, and the southeastern part of the Adamawa-Yade domain (Figs. 15 and 16). Also, in both analyses thinner lithosphere is imaged beneath the northern part of the Adamawa-Yade domain, the Western Cameroon domain and the Benue trough (Figs.15 and 16). The boundary between these two lithospheric blocks with different thicknesses seems to coincide with the Central Cameroon shear zone (Figs. 15 and 16). However, we found differences between the two analyses regarding the range of LAB depth beneath the northern part of the Adamawa – Yade domain and the West Cameroon domain. The LAB depth from the 2D radial-averaged power spectrum analysis for these two domains ranges between ~113 and ~162 km, whereas the LAB depth estimated from the inversion of the passive seismic tomography data is relatively shallower and ranges between ~72 km and ~133 km (Figs. 15 and 16). Poudjom Djomani *et al.* (1997) used forward modelling along a NS profile cross cutting the Adamawa plateau and found lithosphere thickness of ~80 km. this result is 33 km less than the result from the spectral analysis and 8 km more than the result from the thermal inversion of passive seismic data. This coold be due to the difference of the method used, however both studies highlight a thin lithosphere beneath the northern part part of the Adamawa-Yade domain.

IV.1.5. Result from forward modeling

IV.1.5.1. Results from two-dimensional (2D) forward modeling

Profiles XX' and AA' was used for the two-dimensional (2D) forward modelling (Fig. 17). The N-S X-X' (Fig. 17) trending baseline that we used to construct the 2D forward gravity model (follows longitude 13° E and extends between latitudes 2° N and 8° N) is almost perpendicular to both the trend of the gravity anomalies (Fig. 17). The baseline of the 2D forward gravity model also runs close to the location of 4 passive seismic stations from Tokam *et al.* (2010) and Gallacher and Basto (2012) deployment (circles 2, 11, 22 and 27 in Fig.13A). The Moho depth estimates from these passive seismic stations were used to constraint the initial Moho depth of the 2D forward gravity model. The second profile AA' (Fig. 17) used to construct the 2D forward gravity

model is quasi perpendicular to the strike of the CASZ, the Cameroon volcanic line, the Benue trough and cut indifferently the west Cameroon domain, the Adamawa-Yade domain and the Congo craton. The Moho depth estimates from these passive seismic stations and the LAB boundaries estimate from radially-averaged power spectrum analysis were used to constraint the initial Moho and LAB depth of the 2D forward gravity model.

IV.1.5.1.1. Profile 1 (X-X')

The 2D forward gravity model (Fig. 18B) suggest a number of tectonic features that can help better understand the geodynamic evolution of the northern edge of the Congo craton and its relationship with the Oubanguides orogenic belt to the north: (1) There is a general thinning of the continental crust from the northern part of the craton where it is ~48 km thick to the Western Cameroon domain in the north where the crust thinned to ~ 34 km (Fig. 18B). This crustal thinning might be due to post-Precambrian tectonic events such as the eruption of the Cameroon volcanic line and the uplifting of the Adamawa plateau. (2) The Yaoundé domain is modelled as an allochthon that was thrust onto the northern edge of the Congo craton structurally underlain by a cratonic crust (Fig. 18B). (3) The southern half of the Adamawa-Yade domain is underlain by a dense (2.86 g/cm^3) material that seems to be the northern continuity of the Congo craton. This is modeled as a dense material that might represent an under-thrusted wedge of the Congo craton that was subducted beneath the Oubanguides orogenic terranes during the Pan-African convergence event.
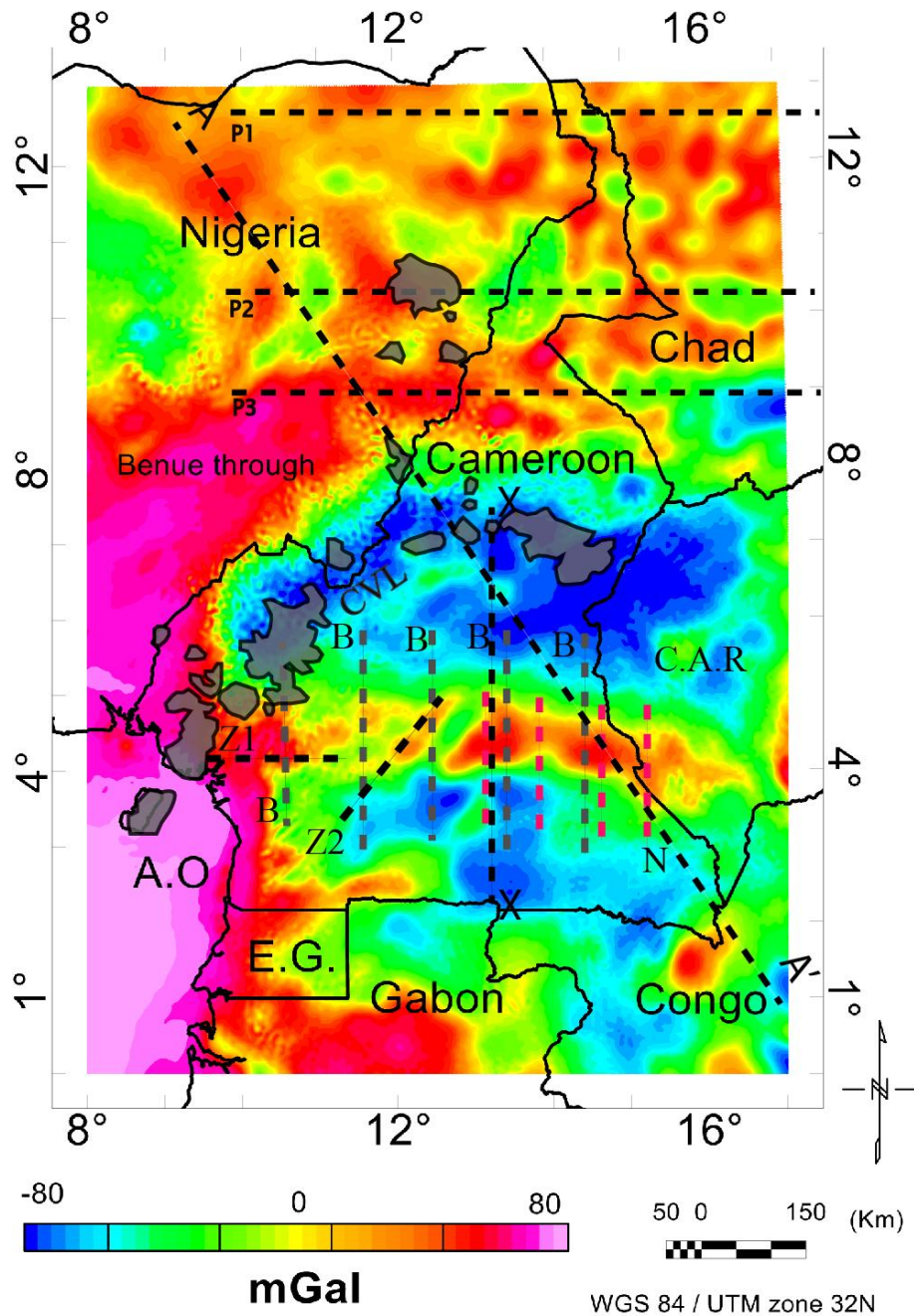
Figure 17: Bouguer gravity anomalies from the World Gravity Model 2012 (WGM2012) covering Cameroon and surrounding, showing the locations of current and previous 2D forward models' profiles. The dash black line labeled "XX" and "AA" shows location of the 2D forward model used in the current study. The black dash lines labeled "P1", "P2" and "P3" show locations of 3D forward models used by Eyike and Ebbing (2015) to image the lithospheric structure using gravity inversion. The black dash lines labeled "B" show locations of two-dimensional (2D) forward gravity model of Boukeke (2014). The dash black lines labeled "Z1" and "Z2" show the locations of the 2D forward model of Tadjou *et al.* (2009).). The red dash line labeled "N" show location of 2D forward model of Zanga-Amougou *et al.* (2013). CVL = Cameroon volcanic line. E.G = Equatorial Gunea. A.O. = Atlantic Ocean. C.A.R = Central Africa Republic.
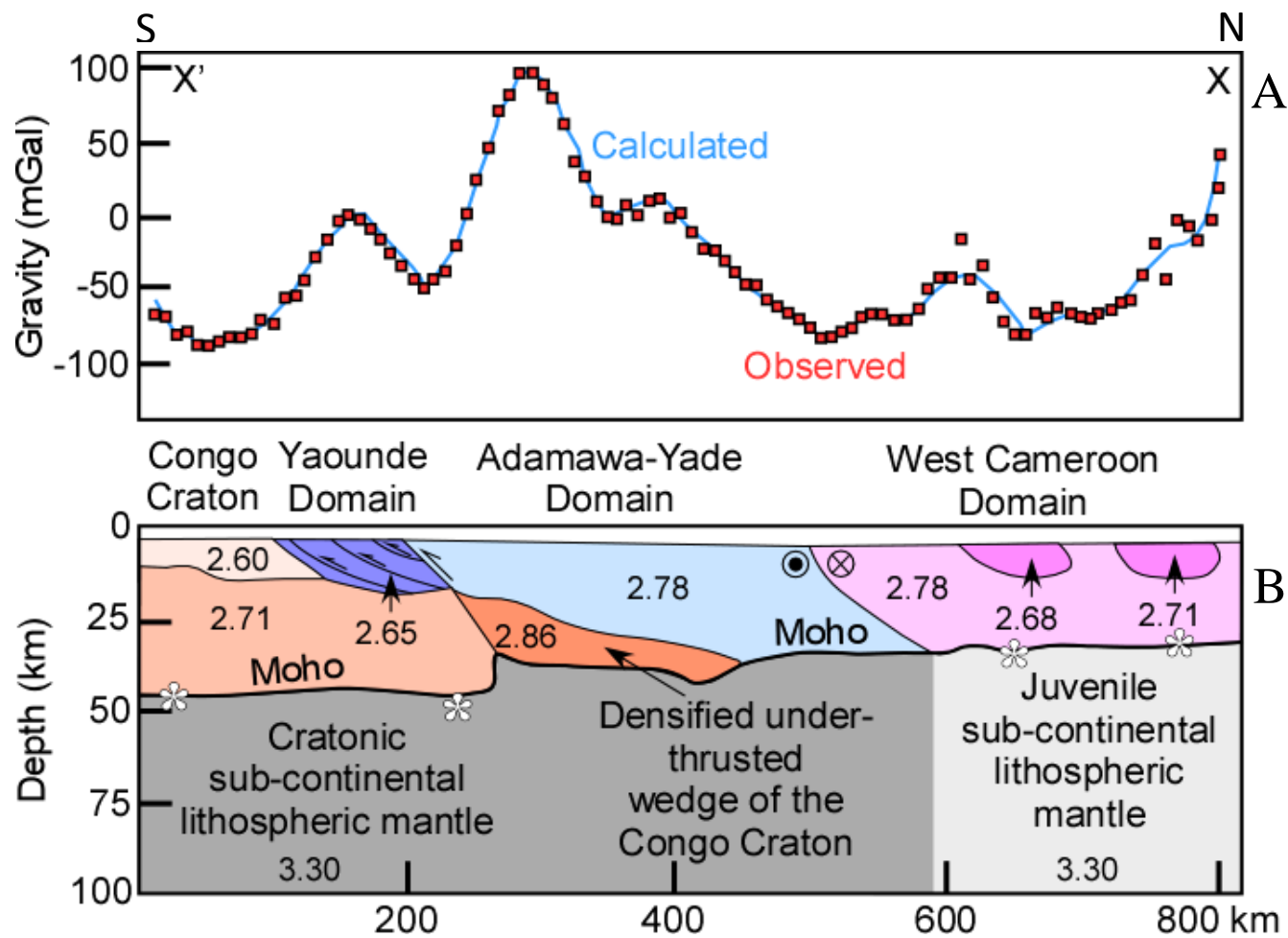
Figure 18: (A) Observed Bouguer gravity anomalies (red squares) extracted along a N-S profile flowing longitude 13ºE from the World Gravity Map (WGM2012) data covering southern Cameroon and surrounding regions. Calculated Bouguer gravity anomalies are shown with a solid blue line. (B) Two-dimensional (2D) forward model illustrating the cross-sectional view of the lithospheric structure in southern Cameroon that best fit the observed Bouguer gravity anomalies of profile XX of Fig. 17. The white stars represent the Moho location of passive seismic stations of Tokam *et al.* (2010).

IV.1.5.1.2. Profile 2 (NW-SE: A-A')

Fig. 19B shows our 2D forward model, imaging the lithospheric structure beneath Cameroon and its surrounding that can contribute to better the understanding of the geodynamic and the lithosphere structure beneath the CASZ, the Benue trough, the CVL, the Congo craton and the Oubanguides fold belt and the relationship between them. Fig. 19B shows (1) the lithosphere is thicker in the cratonic lithospheric domain underneath the west Cameroon domain and above to the southern part of the Adamawa-Yade domain where the LAB depth is ~ 190 km, and thinner in the Panafrican lithospheric domain covering the vast part of the Adamawa-Yade domain, and the west Cameroon domain where the LAB depth is shallow as 110 km. The thinning underneath the most part of the Adamawa-Yade domain and the West Cameroon domain might be due to post-Precambrian tectonic events such as the eruption of the CVL and the uplift of the Adamawa plateau. (2) we injected several magmatic intrusions to cope with some high gravity anomaly representing the volcanic activities of the Cameroon volcanic line above the CASZ, while south of the CASZ represent some syn-to-post granitoids intruded into the crust resulting from the neoproterozoic orogenic event who happened resulting to the collision of the north-western edge of the Congo craton in Cameroon and the Oubanguides belt. (3) the southern part of the Adamawa-Yade domain is underlain by a dense (2.86 g/cm^3) material interpreted as the undertrusted metacratonized wedge of the Congo craton that was densified during the Pan-African orogenic event.

IV.1.5.1.3. Comparison between the currents two-dimensional (2D) forward gravity model, the (2D) tomography cross section and previous studies

The main observation between the (2D) forward modeling (Fig. 18B and 19B) and the seismic velocity 2 D cross section (Fig. 14F) is that, the slow S-wave velocity correspond to the area above the southern part of the Adamawa-Yade domain where a general mantle upwelling is observed (Fig. 18B).

The Cameroon crustal thickness and Moho depth have been subject to many geophysical studies using cross sections on contrary of the lithosphere thickness. Boukeke (1994) used gravity data to construct a series of N-S 2D forward models across the northern edge of the Congo craton, The Yaoundé domain and the southern part of the Adamawa-Yade domain.
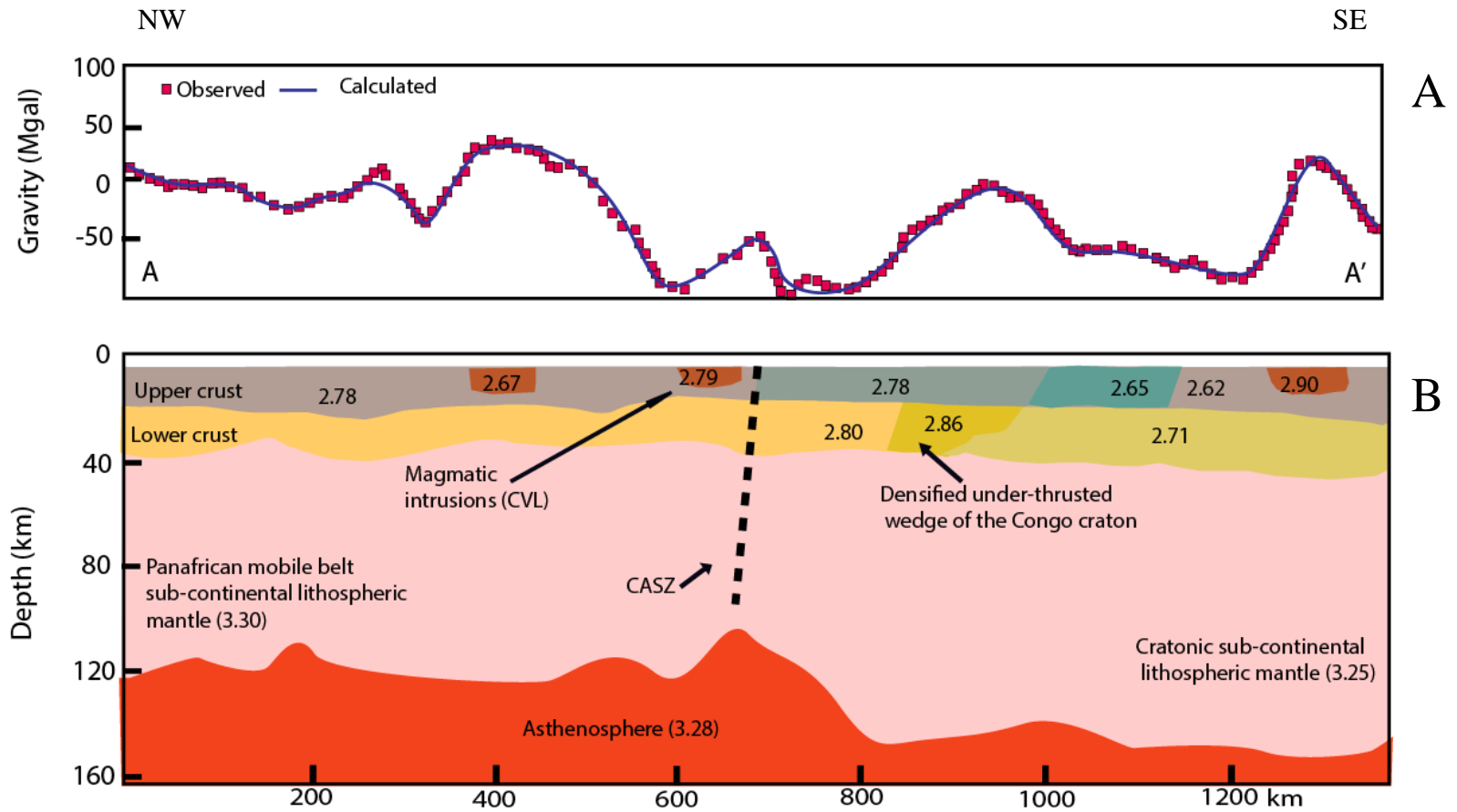
Figure 19: (A) Observed Bouguer gravity anomalies (red squares) extracted along a N-S profile flowing longitude 13°E from the World Gravity Map (WGM2012) data covering southern Cameroon and surrounding regions. Calculated Bouguer gravity anomalies are shown with a solid blue line. (B) Two-dimensional (2D) forward model illustrating the cross-sectional view of the lithospheric structure in Cameroon that best fit the observed Bouguer gravity anomalies along Profile AA' of Fig. 17. CASZ = Central African shear zone. CVL = Cameroon volcanic line.

Boukeke (1994) adopted a uniform Moho depth of ~42 km and used densities of 2.75 g/cm^3 for the Congo craton, 2.78 g/cm^3 for the Adamawa-Yade domain, and 3.3 gm/cm^3 for the SCLM. Boukeke (1994) used densities of 2.65 g/cm^3 and 2.70 g/cm^3 for the upper crust of the Congo craton and attributed this to the presence of granitic intrusions. Futher, Boukeke (1994) used density of 2.65 g/cm^3 for Yaoundé domain. Finally the southern part of the Adamawa-Yade domain, Boukeke (1994) introduced denser (2.83 g/cm^3 and 2.84 g/cm^3) under-plated bodies that extend from the Moho to a depth of ~20 km. Boukeke (1994) 2D forward model can't be compare with the current model due to the scale of the model however although the crust is divided in upper and lower crust en general,the present model (Fig. 16C) consider the presence of the under-plated bodies extending from the Moho to the base of the upper crust.

Tadjou *et al.* (2009) constructed 2D forward gravity models along NE-SW and E-W baselines that cross the northern part of the Cameroon craton and the Yaoundé domain on the one hand and the western side of the Cameroon craton on the other hand, respectively (shown with black dashed line labeled "Z1" and "Z2" in Fig. 17). Tadjou *et al.* (2009) initially used spectral analysis of the gravity data to constrain the average Moho depth to 38.6 ± 2.8 km for the NE-SW model (Profile "Z2" in Fig.17) 47.1 ± 4.2 km for the E-W model (Profile Z1 in Fig.17). Tadjou *et al.* (2009) concluded that the continental crust is denser within the terranes of the Oubangides orogenic belt (2.7 g/cm^3) and lighter within the Congo craton (2.67 g/cm^3).

Zanga-Amougou *et al.* (2013) used gravity data to model the upper crust in the south east of the study area (shown with pink dashed line labeled "N" in Fig.17). Zanga-Amougou *et al.* (2013) models results for 4 profiles N-S (shown with pink dashed line labeled "N" in Fig.17) mainly shown the presence of different rock bodies within the upper crust and their density within the upper crust of the Congo craton and the Oubanguides fold bed, and concluded that the upper crust underneath those profiles shows the gravity signature of the Congo craton and the Oubanguides fold belt.

Poudjom Djomani *et al.* (1995; 1997) used spectral analysis and forward modelling of gravity data to image the lithospheric structure beneath Cameroon (crust) and the Adamawa plateau (lithosphere thickness). They found that the crust was thicker beneath the Congo craton and thinner North of it. They also found that the lithosphere beneath the Adamawa plateau was ~ 80 km, and the correlation with the current crustal thickness is not good principally within the Adamawa Yade and west Cameroon domain where the crust is as shallowed as 22km comparing

to 33 km in the current work and the lithosphere thickness is 80 km compared to 70 - 117 km in this study. This discrepencie might be due to the resolution of the grid, the method and the quality of the data which in the current study is recent.

North of the current focus study area, Eyike and Ebbing (2015) with the Earth gravity model 2008 (EGM 2008) used three-dimensional (3D) gravity modeling and imaged the lithospheric structure of the west and central African rift system in Cameroon. Although Eyike and Ebbing (2015) works cover only one portion of our focus area, 3 out of their 4 modeled profiles are within the scope of this study (shown with black dash lines labeled "P1" "P2" and "P3" in Fig. 17). Eyike and Ebbing (2015) estimated in the west side of their profile "P1" (shown with black dash lines labeled P1 in Fig. 17) the lithosphere thickness as shallow as ~70km beneath the upper part of the Benue trough dipping westward up to ~110 km, with a sensibly constant crustal thickness. On their second profile "P2" (Fig. 17), the shallower lithosphere is observed in the middle part of the profile however the lithosphere thickness underneath the whole profile is < ~85 km. the third profile "P3" (Fig. 17) where the shallowest lithosphere is found in the central part of the profile (~75 km), the other parts staying as shallow as 110 km. There is a good correction with our current work, for the first and third profile.

IV.2. DISCUSSIONS

IV.2.1. Metacratonisation of the northern edge of the Congo craton

the 2D radially-averaged power spectral analysis and 2D forward modeling of the WGM 2012 was used to show that the southern part of the Adamawa-Yade domain is characterized by the presence of a pronounced positive gravity anomaly. The source of this positive gravity anomaly is a dense material beneath the southern part of the Adamawa-Yade domain. Also, this work has shown that the crust is generally thicker beneath the Congo craton and thinner north of it. The presence of denser material beneath the southern part of the Adamawa-Yade domain is explained as possibly due to densification of under-thrusted portion of the Congo craton that was modified possibly due to ascendance of asthenospheric material due to slab detachment during the Neoproterozoic Pan-African orogenic event (Fig. 20). Heating resulted in melting of the lower crust and upper mantle which resulted in wide spread emplacement of high-K granitoids during the Neoproterozoic, hence the metacratonization of most of the Adamawa-Yade domain and the northern edge of the Congo craton. The positive gravity anomaly has been previously linked to a Precambrian tectonic event, mostly the Neoproterozoic Pan African orogenic event and that it represents a deeper geological feature. For example, Boukeke (1994) used N-S 2D forward gravity models to suggest that the positive gravity anomaly is due to the emplacement of high-density material in the lower crust at depth greater than 20 km. Boukeke (1994) suggested that the high-density material was emplaced during the Neoproterozoic Pan-African orogenic event.

The densification of an under-thrusted portion of the Congo craton better explains the presence of the positive gravity anomaly. Toteu *et al.* (2004) showed that the trends of Precambrian foliation within the southern part of the Adamawa-Yade domain form a N-arching shape. Toteu *et al.* (2004) argued that this pattern developed from the deformation around the under-thrusted margin of the Congo craton. Further, Toteu *et al.* (2004) suggested that the positive gravity anomaly in the southern part of the Adamawa-Yade domain corresponds to the transition from denser crust in the north to a less dense crust to the south within the Congo craton. Toteu *et al.* (2004) used these observations to suggest that the northern edge of the positive gravity anomaly corresponds to the northern limit of the N-arching trend of the Precambrian foliation. It has been recognized that the Adamawa-Yade domain is a Paleoproterozoic crust (possibly of an Archean origin) that has been significantly remobilized during the Neoproterozoic especially through the

emplacement of high-K granitoids (Toteu *et al.*, 2001; 2004). Toteu *et al.* (2004) explain this remobilization as due to Neoproterozoic SCLM delamination that accompanied the collision between the Adamawa-Yade domain and the Congo craton. Upwelling of the asthenosphere that followed the SCLM delamination produced enough heat to melt the lower crust, hence the generation of felsic magma and subsequent emplacement of the voluminous high-K granitoids. The model proposed here (Fig. 20) agrees with the proposition of melting of the lower crust and upper SCLM through asthenospheric heating to generate the high-K granitoids. However, it can be suggested that the ascendance of the asthenospheric material through slab detachment is a plausible explanation. This is based on the fact that the positive gravity anomaly is elongated in an E-W direction suggesting zonal asthenospheric ascendance rather than a regional upwelling as what is expected for SCLM delamination.

It has also been suggested that the northern margin of the Adamawa-Yade domain has been metacratonized. Kwékam *et al.* (2010) proposed that the presence of a high-K plutonic complex that gave U-Pb zircon ages of 620+/- 3 Ma and 613 +/- 2 Ma which intrudes the Central African fold and thrust belt is associated with the metacratonic events that affected the northern edge of the Congo craton. Further, Kwékam *et al.* (2010) associated the metacratonization process to linear delamination of the SCLM along the Tchollire-Banyo shear zone (Fig. 20) which they referred to as the Central Cameroon shear zone system that developed after the Neoproterozoic Pan-African orogenic event. Additionally, Kwékam *et al.* (2010) advanced that delamination along the shear zone triggered partial melting of the lower crust and upper SCLM. The proposition of SCLM delamination along the Tchollire Banyo shear zone is in good agreement with results from a passive seismic study that showed thinner lithosphere along the shear zone (120 km along the shear zone and 190 km away from it) Plomerova *et al.* (1993). Further, Plomerova *et al.* (1993) attributed the lack of a positive gravity anomaly associated with the thinner lithosphere beneath the Tchollire Banyo shear zone as due to that the lithospheric thinning is only within a narrow belt that cannot be imaged by the spectral analysis of the gravity data that requires using at least ~110 km X 110 km sub-regions.

Metacratonization through continental subduction and subsequent SCLM delamination beneath major shear zones has been proposed by Liegeois *et al.* (2013) for the Moroccan Anti-Atlas. In this scenario, Liegeois *et al.* (2013) suggested that Neoproterozoic oblique collision between the West African craton in the south (equivalent to Congo craton in our model) and the

Peri-Gondwanan terranes (equivalent to West Cameroon domain) limited the depth of subduction of the craton margin. Subsequent transpressional and transtensional movement along shear zones dissected the northern margin of the West Africa craton, allowing for the emplacement of large magmatic bodies and converting the northern margin of the craton into the Anti-Atlas metacratonic boundary (equivalent to Adamawa-Yade domain).
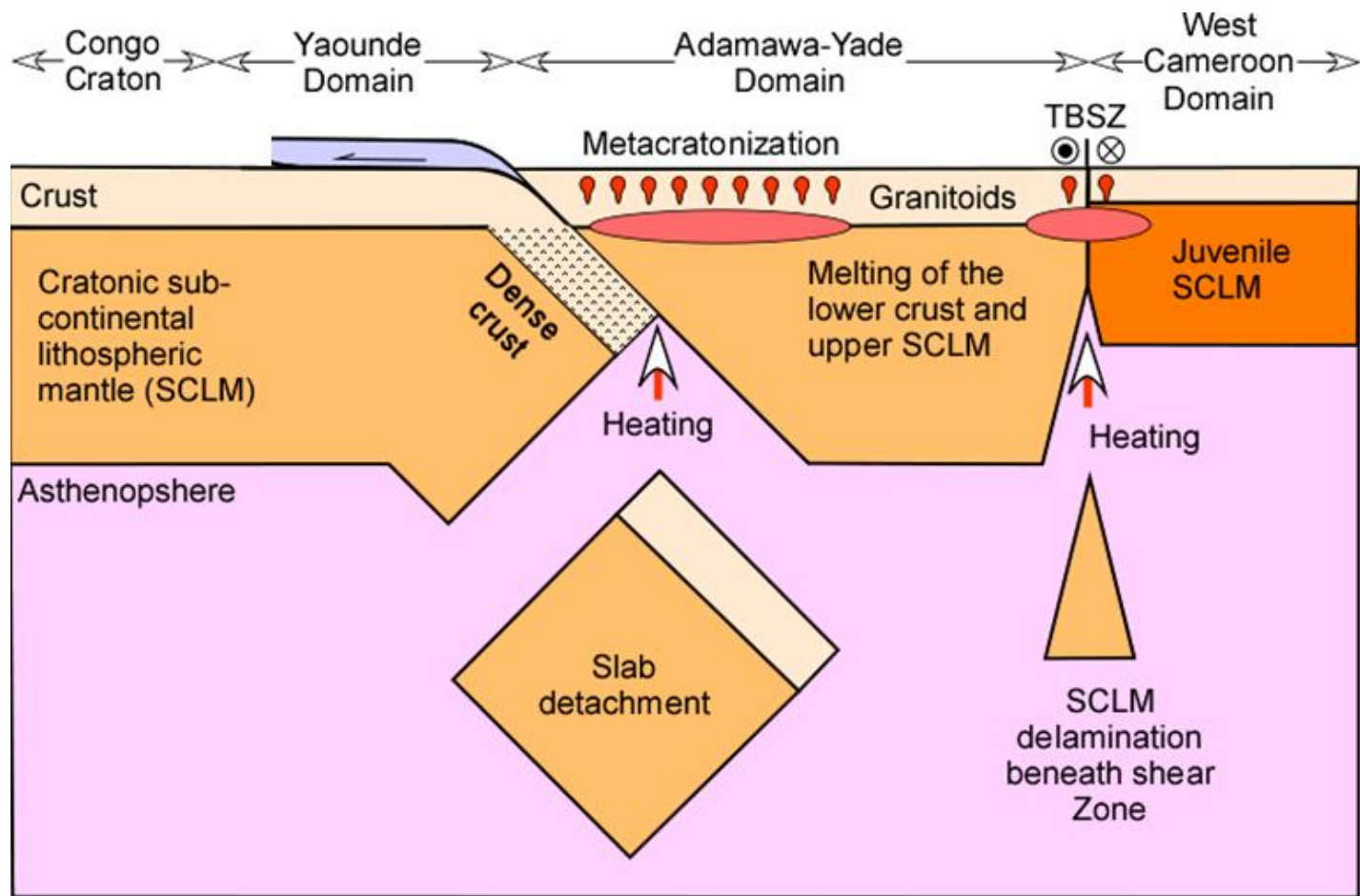
Figure 20 : Conceptual cross-section illustrating the metacratonization of the northern edge of the Congo craton and the Adamawa-Yade domain through melting of the lower crust and upper sub-continental lithospheric mantle (SCLM) through ascending asthenosphere, possibly due to slab detachment.

IV.2.2. Limit of the northwestern margin of the Congo craton in Cameroon

The results show that the crust and the SCLM beneath the northern part of the Adamawa-Yade domain, the West Cameroon domain and the Benue trough are thinner compared to those beneath the Congo craton and the Yaoundé domain (Figs. 21-B). These lithospheric structures suggest that, they are the result of a number of tectonic events that started in the Precambrian. Toteu *et al.* (2004) showed that the Adamawa – Yade domain is made-up of Archean – Paleoproterozoic crust which has been remobilized during the Neoproterozoic, dominantly through the injection of high-K granitoids. Toteu *et al.* (2004) interpreted the remobilization of the Adamawa – Yade domain by granitoid emplacement as the result of SCLM delamination that accompanied the collision between the Adamawa-Yade domain and the Congo craton. Heating of the lower crust by the ascending asthenosphere resulted in the generation of felsic magma and the emplacement of the high-K granitoids. Recently, Tchakounte *et al.* (2017) and Nkoumbou *et al.* (2014) proposed a model in which they considered the Adamawa – Yade as an Archean – paleoproterozoic micro-continent that was separated from the northern edge of the Congo craton in the early Neoproterozoic. Subsequently, this micro-continent was sutured back with the Congo craton as a result of collision between the two tectonic entities after the consumption of the oceanic basin separating them and the formation of a continental arc.

The model that advocated for Neoproterozoic collision between the Adamawa – Yade domain and the Congo craton (Nzenti *et al.*, 1988; Toteu *et al.*, 2004; Koumbou *et al.*, 2014 Tchakounte *et al.*, 2017) requires the presence of a Precambrian suture zone between the two tectonic entities (the vertical line labelled "?" in Fig. 22A), the upper crustal manifestation of which is represented by the Yaoundé domain. The results, especially the lithospheric thickness imaging does not support the presence of a lithospheric-scale suture zone between the Adamawa – Yade domain and the Congo craton (Figs; 14F, 15, 16, 19B and 22B). This is because the lithosphere beneath the Yaoundé domain has the same thickness as that of the Congo craton (Figs. 21A-B and 22B). Hence, the Adamawa – Yade domain can be consider as the northern edge of the Congo craton and that the Yaoundé domain is an allochthon that was thrust atop the Congo craton. Aternatively, the central Cameroon shear zone system and the Tcholire-Banyo shear is interpreted as the lithospheric-scale suture zone between the Congo craton (including the Adamawa – Yade domain) and the Western Cameroon domain (Fig. 22B). This interpretation is in good agreement

with the radial anisotropy analysis of Oko *et al.* (2017), which suggested that the Central Cameroon shear zone system and the Tchollire – Banyo shear zone represent the shallower crustal manifestation of a suture zone and that these structures have witnessed sub-horizontal strike-slip movement

The lithospheric thickness maps do not show any change in the thickness of the lithosphere across the Sanaga shear zone (Figs. 15 and 16). it suggests that the crust north of the Sanaga shear zone within the Adamawa – Yade domain is thinner than the crust to the south of the shear zone within the Congo craton and the Yaounde domain (Figs. 15 and 16). This might be due to modification during the remobilization of the Adamawa – Yade domain. Hence, this study proposes that the Congo craton and the Adamawa-Yade domain acted as a single and stable cratonic bloc until ~ 650 Ma as indicated by the U-Pb zironc ages obtain by Kwekam *et al.* (2010) for high-K Plutonic complex on the northern margin of the Adamawa-Yade domain. This cratonic bloc collided with the Neoproterozoic jugenile Western Cameroon domain during the Pan-African orogeny. This in turn resulted in the metacratonization of the northern margin of the cratonic block turning it into the Adamawa-Yade domain that is dominated by Archean-Paleoproterozoic crust that was highly injected by Neoproterozoic high-K granitoids (Toteu et al, 2001, 2004).

Those suggestions are also supported by evidences of Archean magmatic rocks found in Makenene and Nomale in the West of the Yaounde domain; for instance, Makenene migmatitic grey gneiss yielded a 2.55 Ga age (Figs. 21A-B) while the Nomale migmatitic gneiss has an upper intercept age at 2.98 ± 36 Ga (Tchakounte *et al.* 2017). Similar ages are found within the cratonic zone. In Sangmelima and Ebolowa area, charnockites and tonalities yielded U-Pb zircon ages at 2.86 ± 7 Ga (Toteu *et al.* 1994), Pb-Pb ages at 2.88 ± 11 Ga (Shang *et al.*, 2004) and 2.91 ± 1 Ga (Tchameni, 1997), and Sm-Nd and Rb-Sr isochron date in the range of 2.89-2.86 Ga (Figs. 21A-B ; Lasserre and Soba, 1976; Shang *et al.*, 2004). This interpretation agrees with Ganwa *et al.* (2016) regarding Meiganga, North of the Sanaga shear zone. They used zircon features and in-situ U-Th-Pb LA-MC-ICP-MS geochronology of a meta-sediments pyroxene-amphibole-bearing gneiss of the Meiganga area in the eastern part of the Adamawa-Yade domain and found that the pre-Panafrican history of Adamawa-Yade domain includes Meso (2900-2950 Ma)- to Neo-Archean (2741 ± 27 and 2551 ± 31 Ma) crustal accretion and associated magmatisme prior to the Paleoproterozoic event of Oubanguides belt (Figs. 21A-B).

It is also important to highlight that several works mentioned the presence of numerous outcrops with Archaean to Paleoproterozoic ages within the Oubanguides fold belt with some of them along the northern margin of the Adamawa Yade domain (Figs. 21A-B; Penaye *et al.*, 1989, 1993, 2004; Toteu *et al.*, 2001; Tchakounte *et al.* 2017), considered in the current study as the edge of the Congo craton in Cameroon. Similarly, geochemical evidence of magmatic arc setting of Andean-type had be found on the Sinassi batholith belonging to the West Cameroon domain and associated to a subduction environment (Bouyo *et al.* 2015; 2016). Additionnaly Tchouankoue *et al.* (2016) put in evidence a sudduction environment at the Bangante area locate at the southwestern margin of the West Cameroon domain (Fig. 21B). They used U-Pb ages and Hf-O isotopes of in sit zircon in Bangante area at the southwestern part of the west Cameroon domain to analyse Monzonites and syenites samples and found emplacement ages of 585 ± 4 Ma and 586 ± 4 Ma and suggested that those rocks were generated by partial melting of an enriched mantle sources metasomatized by previous subduction processes.

It can Therefore be suggested that the subduction of the Panafrican fold belt might have been happened along the northern margin of the Adamawa-Yade domain which followed approximatively the CASZ trend in some area (Fig.21A-B). This interpretation is also in good agreement with the model proposed by Kwekam *et al.* (2010) in which the Adamawa – Yade domain is considered to be the metacratonized northern edge of the Congo craton. Kwekam *et al.* (2010) used the presence of Neoproterozoic high-K granitoids along the CASZ Cameroon to suggest that the SCLM beneath the shear zone has been delaminated as that this resulted in partial melting of the lower crust and the upper SCLM. Further, Kwekam *et al.* (2013) obtained a U-Pb zircon age of ~575 Ma from a gabbro-norite complex that intruded into the Central Cameroon shear zone. Kwekam *et al.* (2013) considered the emplacement of the complex to be synchronous with dextral strike-slip movement along the shear zone. Kwekam *et al.* (2013) explained that the dextral strike-slip movement along the shear zone led to zonal delamination of the SCLM, which in turn led to metacratonization. It is not clear the extent and nature of the modification of the lithosphere beneath the CASZ by the Mesozoic rifting events especially the development of the Central African rift zone. It is obvious that the shear zone has influenced the development of the ENE-trending sedimentary basins in Chad and Central African Republic (Fig. 6A). These sedimentary basins have been interpreted as rift systems (Fairhead, 1988), which will require

additional thinning of the lithosphere beneath the CASZ. However, the alignment of these basins along the shear zone suggests their development as transtensional basins that do not require significant thinning as in the case of rift systems.
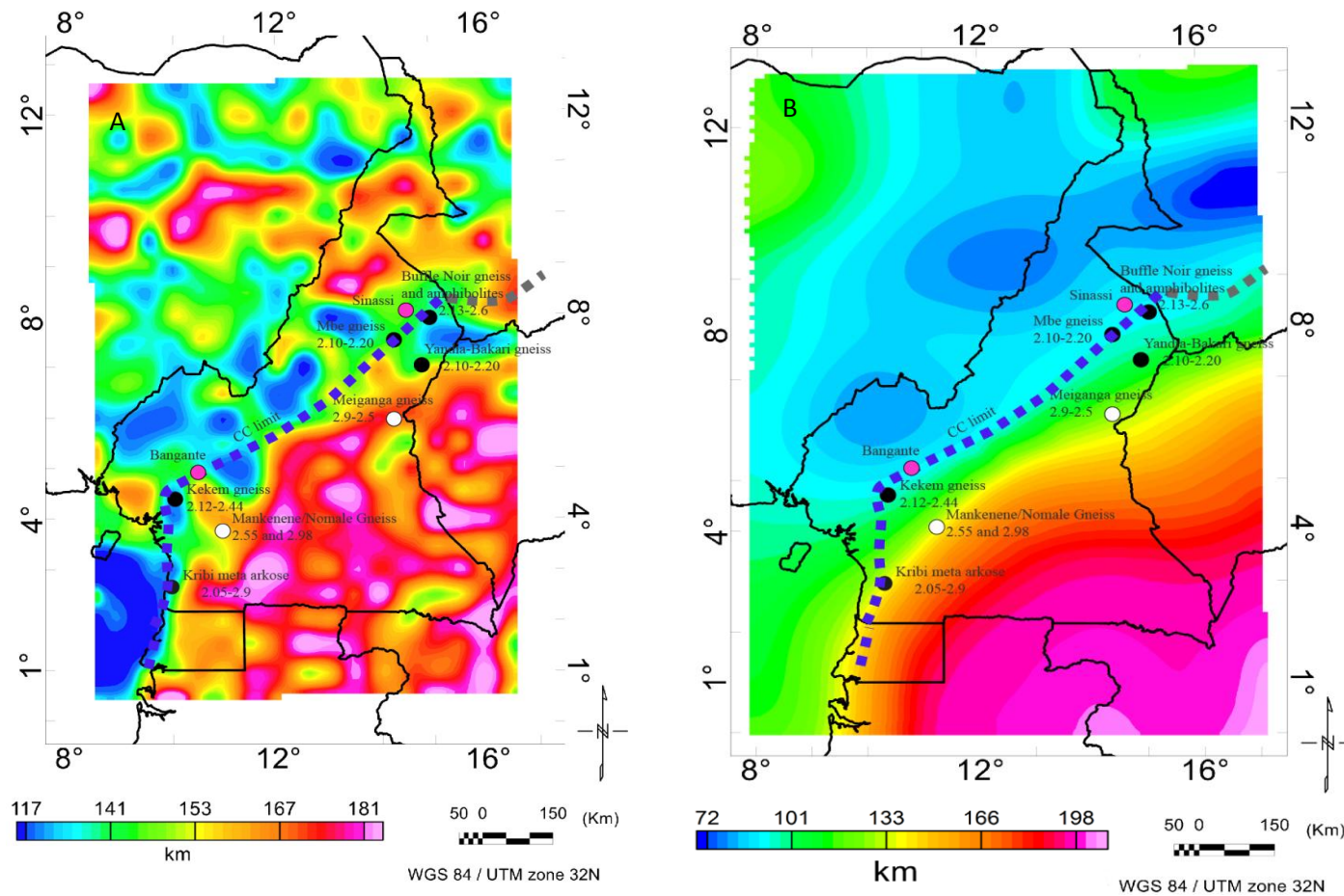
Figure 21: (A) Color-coded map showing lithosphere-asthenosphere (LAB)/Mid-lithosphere discontinuity (MLD) of Cameroon and its surrounding estimated from the World Gravity Map (WGM2012) data using two-dimensional (2D) radially-averaged power-spectrum analysis. CC = Congo craton. (B) Color code map showing Lithosphere - Asthenosphere Boundary (LAB) depth estimates for Cameroon and its surroundings obtained from the thermal inversion of seismic data. CC = Congo craton. The blue dash line represents the northwestern margin of the Congo craton (CC) and the grey dashed line the unconstrained CC limit. The black circle represents Palaeoproterozoic occurrences (Penaye *et al.* 2004). The white circle represents the Archaean occurences (Tchakounte *et al.* 2017 and Ganwa *et al.* 2016). The Pink circle represents the localization of Sinassi and Bangante where geochemical evidence subduction environment has been found (Tchouankoue *et al.*, 2016; Bouyo *et al.*, 2015; 2016).
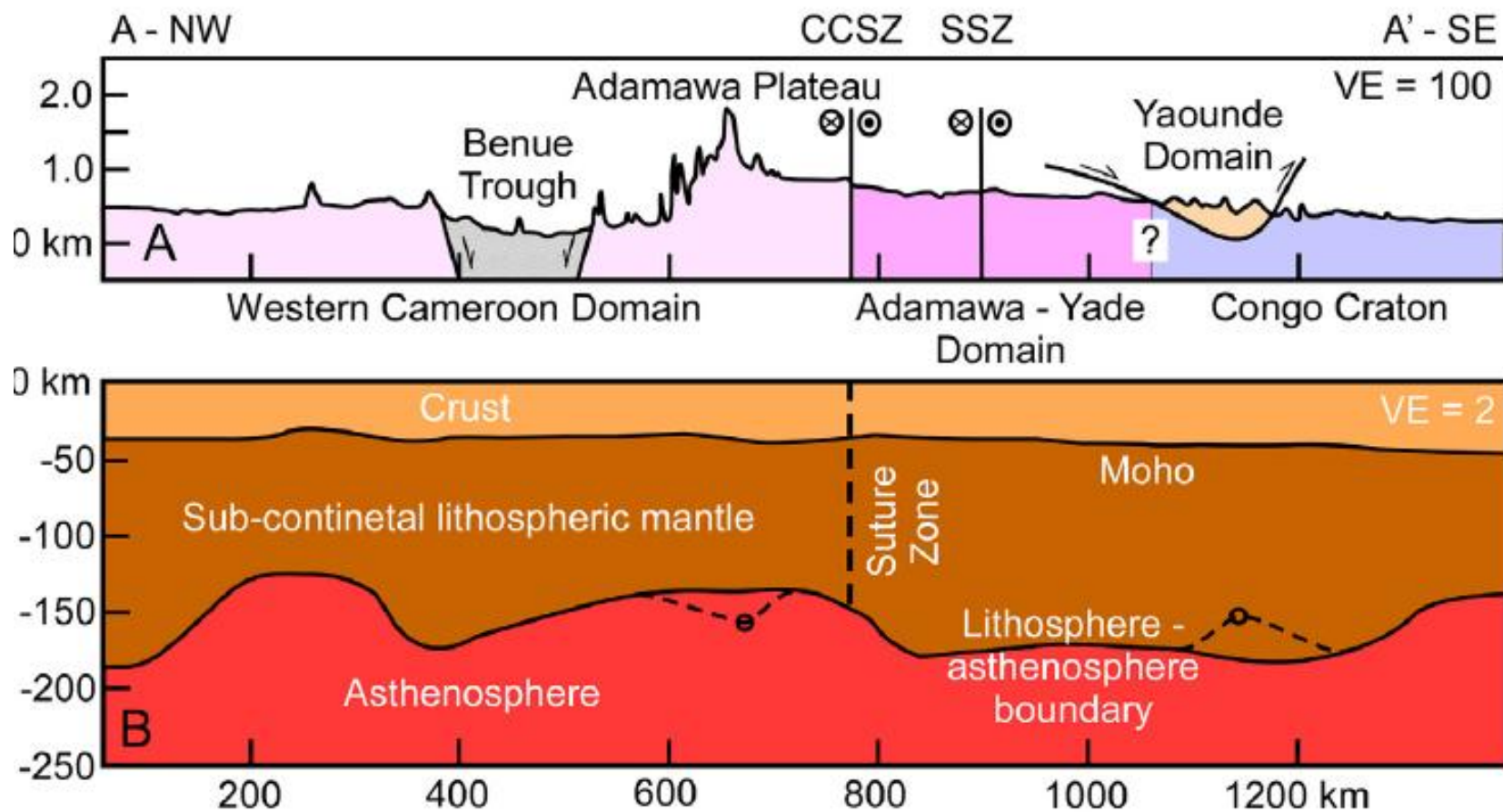
Figure 222: (A) NW-SE cross-section illustrating the major surface tectonic features of Cameroon and its surroundings. (B) Lithospheric-Scale cross-section along the the same trace in Fig. 22 A showing the Moho and lithosphere-asthenosphere boundary (LAB) depth variation. The depth values of the Moho and LAB are from the maps in Fig. 12A and 15. The dashed lines with small circles represent data points that are smoothed out because the anomalies are beyond the resolution of the analysis. CCSZ= Central Cameroon shear zone system. SSZ = Sanaga shear zone.

IV.2.3. Geological map of Cameroon

The geological map of Cameroon is plagued by major challenges. There is recent evidences of Archean inheritance within the Bafia group (Tchakounte *et al.*, 2017), and the meiganga area (Ganwa *et al.*, 2016) within the central Africa fold belt, Bouyo Houketchang *et al.* (2015; 2016) also found geochemical evidence of a continental magmatic arc setting of Andean-type on the Sinassi batholith (Adamawa pleateau; West Cameroon domain) and associated it to a subduction environment. Therefore, the suggested extension of Congo craton to the northern margin of the Adamawa-Yade domain challenges the Cameroon geologic map.

Table 2 shows Precambrian (Archean to Neoproterozoic) recurences in Cameroon within the Congo craton (Ntem complex, Nyong complex and Ayna unit), Yaounde domain, Adamawa-Yade domain and west Cameroon domain. The Ntem complex consists mainly of Archean lithologies (Toteu *et al.*, 1994; Talla Takam *et al.*, 2009: Ntomba *et al.*, 2016), while geochronogical ages within the Nyong complex and the understudied Ayna unit span from Archean to Paleoloproterozoic (Lerouge *et al.*, 2006; Poidevin and Pin, 1986). The Yaounde domain, except the Bafia group, is entirely composed of neoproterozoic formations (Toteu *et al.*, 1994; Penaye *et al.*, 1993 and Lassere and Soba, 1979: Owona *et al.*, 2012; Nzenti *et al.*, 2008) while the Bafia group consist of Paleoproterozoic to Neoproterozoic formations (Toteu *et al.*, 2004; Tchakounte *et al.*, 2007; 2017). Ages within the Adamawa-Yade span from Archean to Neoproterozoic (Toteu *et al.*, 2001; Ganwa *et al.*, 2016) while the west Cameroon domain contains no formations older than Neoproterozoic ages (Isseini *et al.*, 2012; Bouyo Houketchang *et al.*, 2016; Tagne Kamga 2003; Dawai *et al.*, 2013; 2017; Tchouankoue *et al.*, 2014: Ngalamo *et al.* 2017).

The Nyong complex, the Ayna unit, the Bafia Goup, the Adamawa Yade domain is interpreted as remobilized portions of the Congo craton that the Yaounde group was thrust upon (Fig. 22). Therefore Fig. 22 shows a new configuration of the geological map displaying the remobilized (metacratonized) Northwestern portion of the Congo craton in Cameroon. The Yokadouma serie and the lower Djo might be a remobilized portion of the Congo craton, but there are not enough geochronological evidences to support this suggestion (Fig. 22). The Yokadouma serie (Fig. 22) is not well understood and cannot not be considered in this study as a remobilized portion of the Congo craton. The nature of the contact between the Ntem complex, the Nyong complex and the Yokadouma and Dja series also need to be well defined (Fig. 22).

IV.2.4. Origin of magmatism in Central Africa

The thinning of the lithosphere above the northwestern margin of the Adamawa-Yade with a NE-SW trend might be a favourable factor for melting and /or delamination process at the base of the crust and within the upper mantle and this is exemplified by the high bouguer anomaly within the thin lithosphere zone (Fig. 23). The high bouguer anomaly might be due to underplate magmatic bodies beneath the Benue trough (Fig. 23; Poudjom Djomani *et al.* 1997; Ngalamo *et al.*, 2017) and the Chad basin (Fig. 23; Poudjom Djomani *et al.*, 1997). And the CVL is characterized by low gravity anomaly that can be associated with melt at the base of the crust and upper mantle (Ngalamo *et al.*, 2017).

The thin lithosphere is associated to the Central African magmatic corridor (CAMC; Figs. 24A and B) due to a zonal SCLM delamination during Precambrian collision in the assembly of Greater Gondwana along the northern margin of the Congo craton (represent in the current study as the northern margin of the Adamawa-Yade domain). This allowed for mantle flow channelization within the Central African magmatic corridor during the Phanerozoic and the Cenozoic with the formation of alkaline magmatism represented by anorogenic complex and vocanic magmatism reaching the surface in the thinnest places through reactivaction of Panafrican faults (Fig. 24B). The magmatism is exemplified in Cameroon by the Cameroon volcanic line which span in ages from Mezozoic (Tchouankoue *et al.*, 2014) to Cenozoic (Kamgang *et al.*, 2010; 2013; Nkono *et al.*, 2014; Tchouankoue *et al.*, 2012; 2014), and in Nigeria by the Benue trough which alkaline volcanism ages span from Mezozoic to Cenozoic, that is similar in composition and ages to the CVL (Nkono *et al.*, 2014; Tchouankoue *et al.*, 2014).

The uplift of the Adamawa plateau (Poudjom Djomani *et al.* 1997) is interpreted as a result of thrusting at the northern margin of the Congo craton during the Precambrian collision in the assembly of the greater Gondwana. Trusting is evident at the Adamawa plateau (within the Western Cameroon domain) specifically at the Sinasssi area where evidence of continental magmatic arc setting of Andean type has been found and associated to a subduction environment (Bouyo Houketchang *et al.*, 2015; 2016).

Table 2 : Summary table showing some available geochronological data within the West Cameroon domain, Adamwa-Yade domain, Yaounde domain, and the Congo craton in Cameroon. UI = Upper intercept; II = inferior intercept; CVL = Cameroon Volcanic line.

Geological domain		Rock types	Analytical method	Ages (Ma)	References
Congo craton	Ntem complex	Charnockites (Ebolowa)	U-Pb on zircon	2896 ± 7	Toteu *et al.*(1994)
		Tonalite (So'o)	U-Pb on zircon	2850 ±?	Toteu *et al.*(1994)
		Charnockite (Ebolowa)	Pb-Pb on signle Zircon	2912 ± 25	Pouclet *et al.*(2007)
		Gom charnockite	U-Pb on Zircon	2883 ± 11	Talla Takam *et al.* (2009)
		Akom Bikak charnockite	Pb-Pb on signle Zircon	3266 ± 5	Talla Takam *et al.* (2009)
		Adzap granite	U-Pb on Zircon	2853	Talla takam *et al.* (2009
		Ngoulemakong tonalite	U-Pb on zircon	2865 ± 4	Tchameni *et al.* (2010)
	Nyong complex	Sombong gneiss	U-Pb on zircon	2600 ± ?	Toteu *et al.* (1994)
		Metasedimentary rocks	U-Pb on zircon	2500-2900	Toteu *et al.* (2001); Lerouge *et al.* (2006)
		Metagranodiorite (Bonguen)	U-Pb on zircon	2066 ± 4	Toteu *et al.* (1994)
		Metasyenite	U-Pb on zircon	2836 ± 11	Lerouge *et al.* (2006)
	Ayna	Mbi Granodiorite	U-Pb on zircon	2070 ± 70	Poidevin and Pin (1986)
		Yobe granite	Rb-Sr on whole rock	1167 ± 61	Censier *et al.* (1989)
Yaounde Domain	Yaoundé group	Ngoa Ekele Orthogneiss	U-Pb on zircon	620 ± 20	Toteu *et al.* (1994)
		Metasédiment (Yaoundé)	U-Pb on zircon	620 ± 10	Penaye *et al.* (1993)
		Diorite (Yaoundé)	K-Ar	565 ± 22	Lassere and Soba (1979)
		Bibouba micaschist	Sm-Nd garnet-whole rock age	616	Toteu *et al.* (1994)
	Bafia serie	Gneiss (West of Bafia); Whole rock	U-Pb; Sm-Nd	1617 ± 16	Tchakounte *et al.* (2007)
		Makenene and Nomale Banded gneiss	**U-Pb on zircon**	**2980 ± 36**	**Tchakounte *et al.* (2017)**
		Ngaa Mbappe monzodiorite	U-Pb on zircon	600	Toteu *et al.* (2004)
		Makenene migmatites grey gneiss	**U-Pb on zircon**	**2535 ± 28**	**Tchakounte *et al.* (2017)**
		Maham diorite	U-Pb on zircon	2073 ± 20	Tchakounte *et al.* (2017)
		Bep granitic orthogneiss	U-Pb on zircon	643 ± 5	Tchakounte *et al.* (2017)

Geological domain	Rock types	Analytical method	Ages (Ma)	References
Adamawa-Yade domain	Amphibolite (Buffle noir)	U-Pb on zircon	2130 ± 20	Toteu *et al.* (2001)
	Granite (Ngaoundere)	U-Pb on zircon	2151 ± 10 (I.S); 660 ± 47 (I.I)	Toteu *et al.* (2001)
	Tchabal Granite	U-Pb on zircon	667 ± 40	Toteu *et al.* (2001)
	Tina granite	U-Pb on zircon	596.6 ± 7.5	Toteu *et al.* (2006)
	Dokayo and Kadei pluton	U-Pbl on zircon	596.6 ± 75	Soba *et al.*, (1991)
	Ngaoundere complex (Migmatitic othogneiss)	U-Pb on zircon	600	Toteu et a., 2001
	Meigagan gneiss	**U-Th-Pb on zircon**	**821 ± 50 (UI) – 2721 ± 24(II)**	**Ganwa *et al.* (2016)**
West Cameroon domain	Guider pluton	U-Pb	593 ± 4	Dawai *et al.* (2013)
	Sinassi Batholith (Nord Cameroon region; orthogneiss)	U-Pb on zircon	670 ; 677 and 686	Bouyo Houketchang *et al.* (2016)
	Fomepea complex (Monzodiorite) (West Cameroon region)	U-Pb on Zircon	613 ± 2	Kwekam *et al.* (2010)
	Ngondo plutonic complex (West Cameroon region)	U-Pb on zircon	602 ± 1.4	Tagne Kamga 2003
	Maham Basalt dykes (CVL)	40Ar/39Ar	404.22 ± 51	Tchouankoue *et al.* (2014)
	Dschang Basalt (CVL)	40Ar/39Ar	421.5 ± 3.5	Tchouankoue *et al.* (2014)
	Kendem (CVL)	40Ar/39Ar	192.10 ± 3.5	Tchouankoue *et al.* (2014)
	Gorge de Kolo orthogneiss	U-Pb on zircon	632 ± 4	Dawai *et al.* (2014)
	Mayo Punko metadiorite	U-Pb on zircon	633 ± 3	Toteu *et al.*(1987)
	Badjouma metadiorite	Pb-Pb	612 ± 1	Penaye *et al.* (2006)
	Mayo Kebi batholite- Pala granodiorite (Chad)	Pb-Pb on zircon	567 ± 10	Isseini *et al.* (2012)
	Bangante Monzonite	U-Pb on zircon	585 ± 4	Tchouankoue *et al.* (2016)
	Bangante sienyte	U-Pb on zircon	583 ± 4	Tchouankoue *et al.* (2016)

.
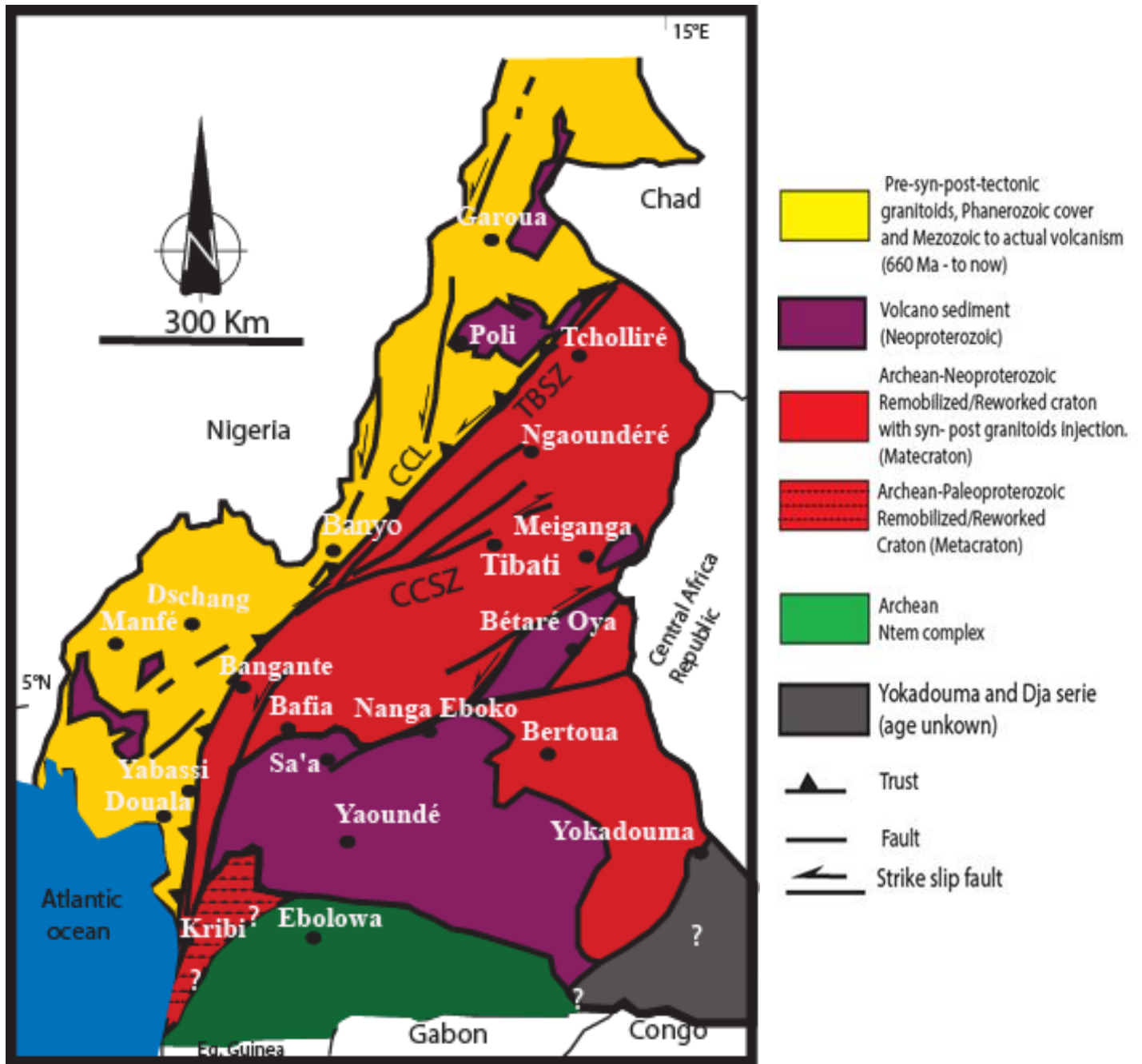
Figure 233: Geological map of Cameroon showing the remobilized (metacraton) portion of the Congo craton. CCSZ = Central Cameroon shear zone. CCL = Congo craton limit. TBSZ = Tchiollire-Banyo shear zone.

The origin of the Cameroon volcanic line proposed in the current study does not agree with the plume model (Morgan *et al.*, 1983), the proposal of the reworking of Precambrian fractures (Moreau *et al.*, 1987; Tchouakoue *et al.*, 2014), the plume and reactivation of preexisting fault model (Poudjom Djomani *et al.*, 1997) nor edge driving convection models (King and Ritsema, 2000; Mileni *et al.* 2012; Kock *et al.*, 2012). Instead this study proposes that the SCLM delamination at the northern edge of the Congo Craton might have allowed for mantle flow channelization during the Cenozoic and this resulted in the formation of the CVL and the uplift of the Adamawa plateau. This model is supported by results from shear wave splitting indicating the presence of faster velocities (Fig. 14A and B) correlated with the CAMC trend (Figs. 24 A and B). Koch *et al.* (2012) reported splitting parameters from averaging the data recorded by the CBSE stations. They observed NE-SW fast direction and splitting time of 0.7 s beneath the CVL. Koch *et al.* (2012) attributed this to variation in temperature between the Congo craton and the Oubanguides orogenic belt. De Plaen *et al.* (2014) used the same data from the CBSE stations to suggest a NNE-SSW fast direction with splitting time varies from 0.48 to 1.95 s and associated this to frozen anisotropy developed as a result of the Cretaceous rifting during the fragmentation of Gondwana. Elsheik *et al.* (2014) interpreted this as the result of channelized mantle flow at the base of the lithosphere originating from the NE-ward movement of the asthenosphere relative to the African plate which is the closest model to the conceptual model proposed in the current work (Fig. 25).
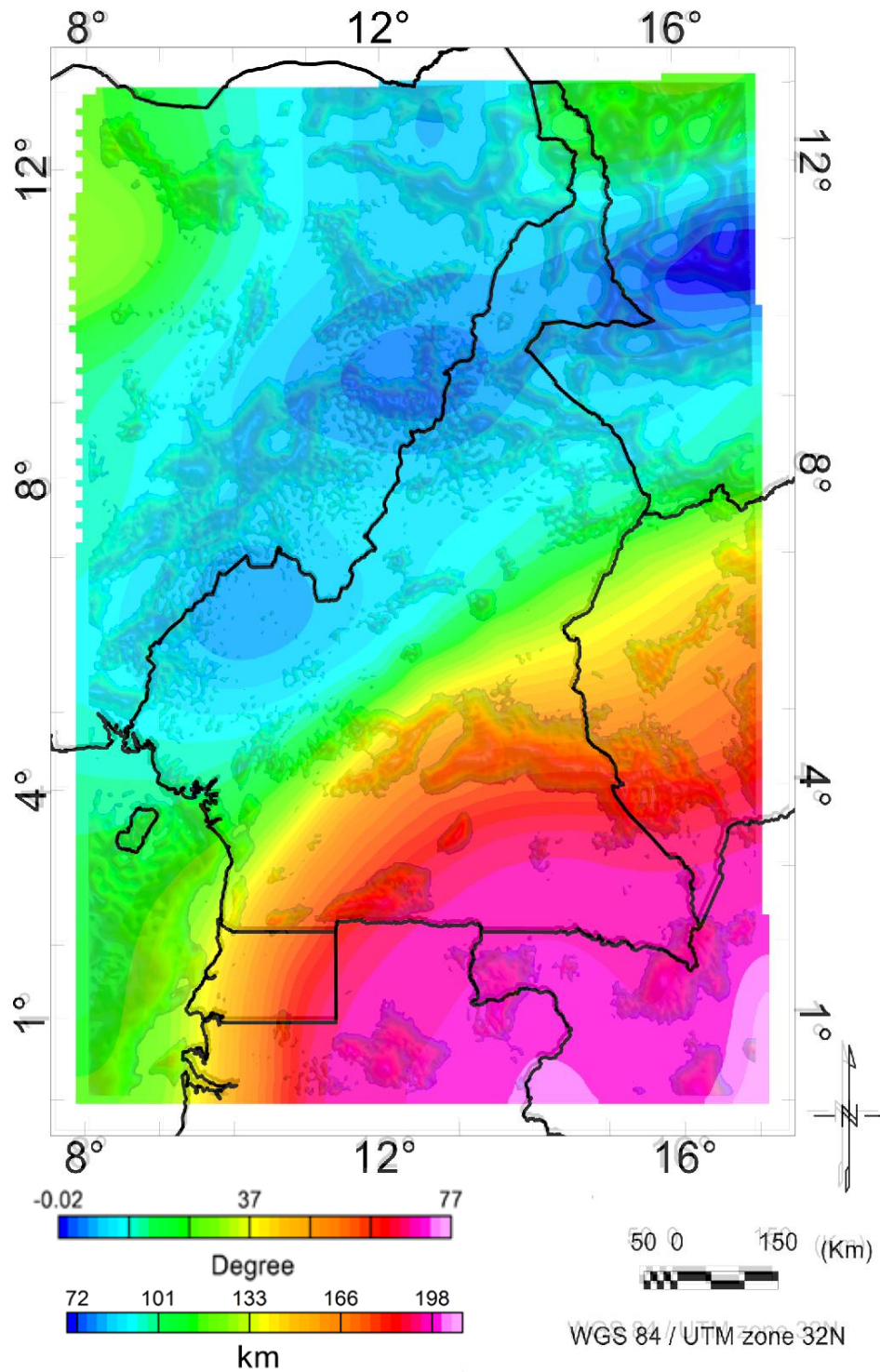
Figure 244: Color code map showing Lithosphere - Asthenosphere Boundary (LAB) depth estimates for Cameroon and its surroundings obtained from the thermal inversion of seismic data over lap by the color

code of positive anomalies of the vertical tilt derivative of the 2 km upward continuation of the Bouguer anomaly map.
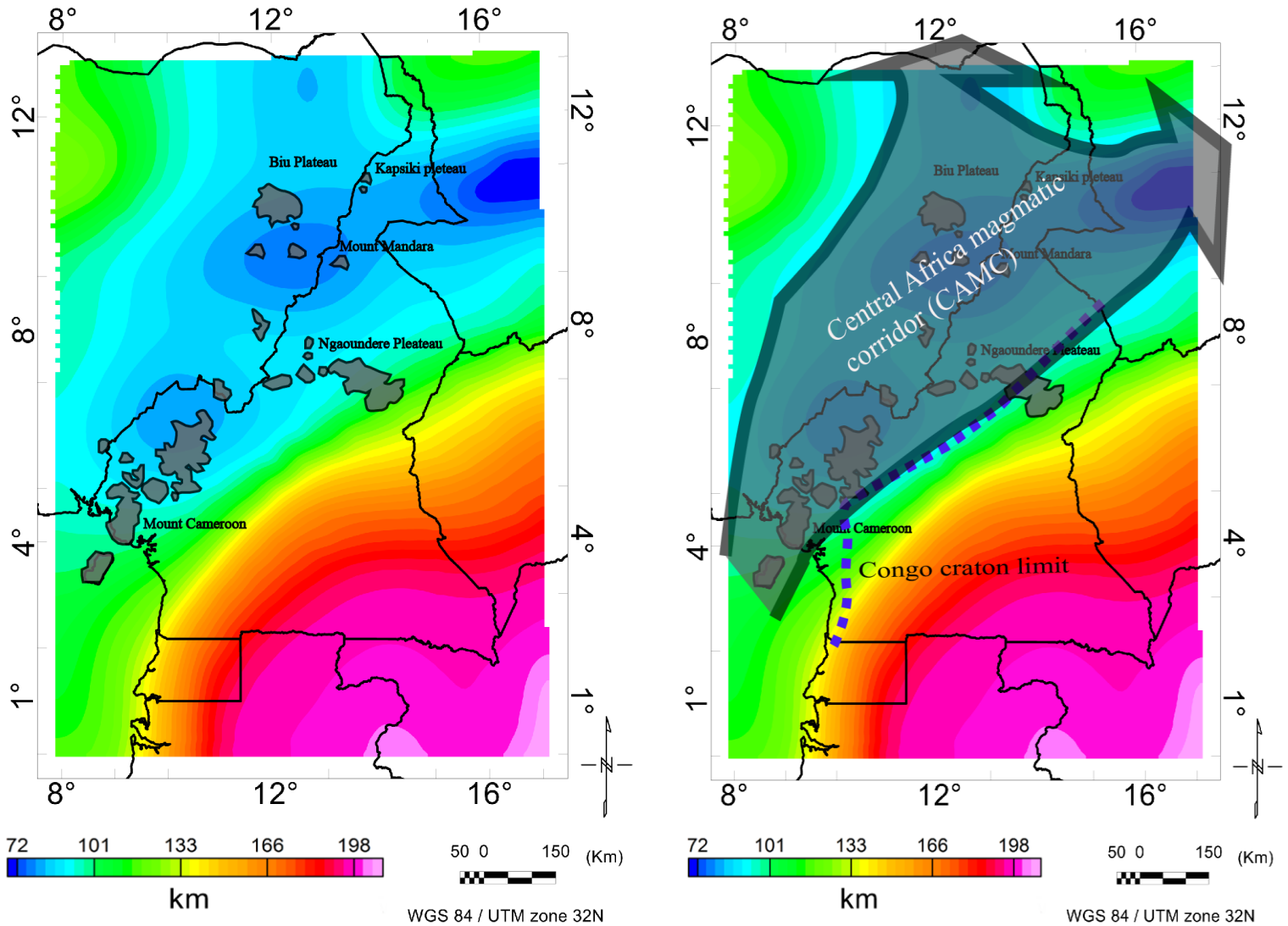
Figure 255: (A) Color code map showing Lithosphere - Asthenosphere Boundary (LAB) depth estimates for Cameroon and its surroundings obtained from the thermal inversion of the passive seismic tomography model of Fishwick (2010) overlap by the Cameroon volcanic line (Ngako *et al.* 2006). (B) Color code map showing Lithosphere - Asthenosphere Boundary (LAB) depth estimates for Cameroon and surroundings obtained from the thermal inversion of the passive seismic tomography model of Fishwick (2010). The blue dash line represents the northwestern margin of the Congo craton (CC).
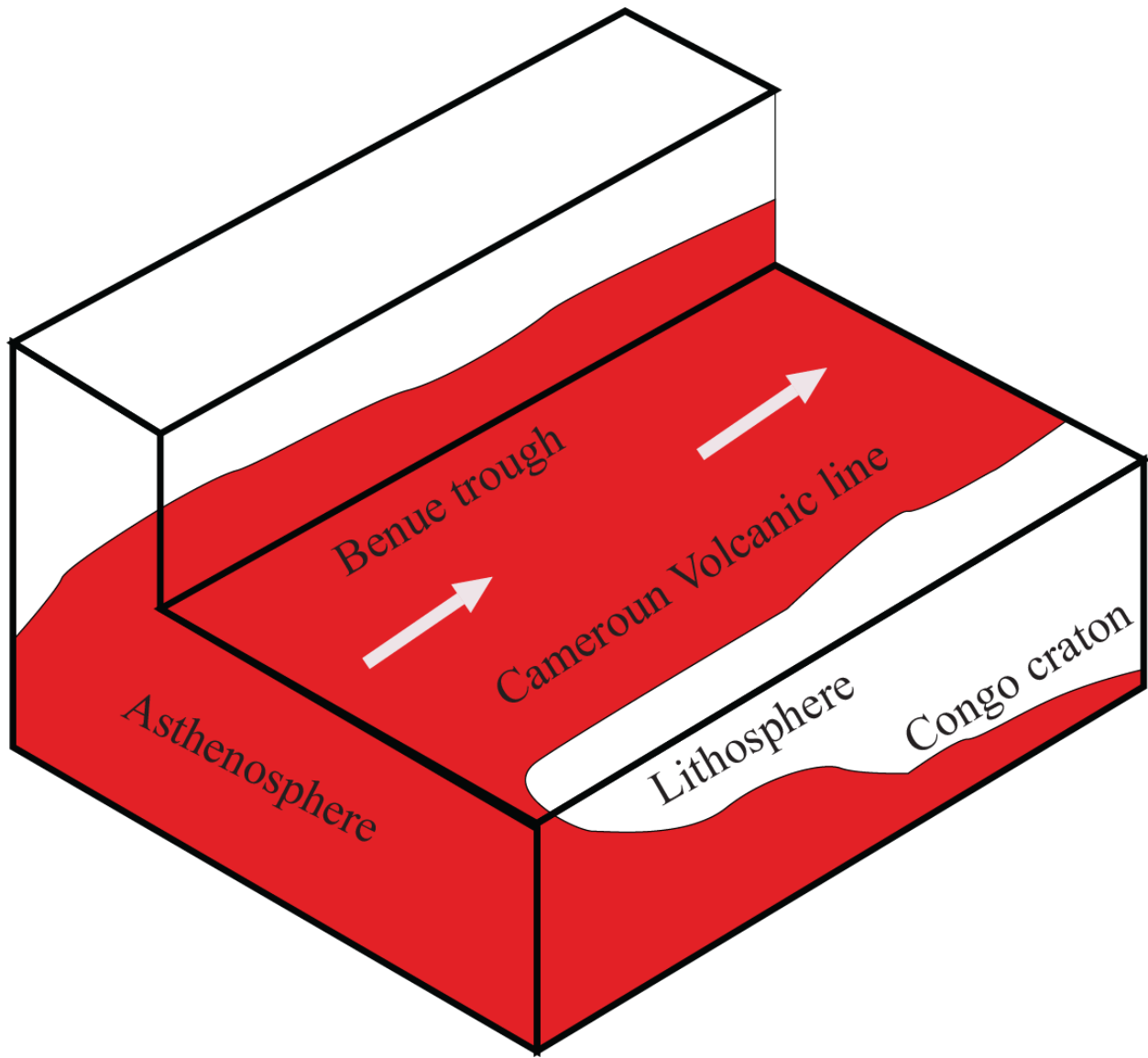
Figure 266: A schematic three-dimensional perspective view illustrates how the asthenospheric material flows beneath the Central African magmatic corridor covering the Cameroon volcanic line and the Benue trough (modified after Elsheikh *et al.*, 2014.

IV.2.5. Isostasy beneath Cameroon and its surroundings

Isostasy beneath Cameroon and its surroundings can be discussed indirectly using density depth relationship within the SCLM (Poudjom Djomani *et al.*, 2000). Poudjom Djomani *et al.* (2000) used information on composition, thermal state and petrological thickness to calculate the density of different types of subcontinental lithospheric mantle and also defined the isostasy condition for Archean SCLM, Proterozoic SCLM and Phanerozoic SCLM. Their results show that Archean section with lithosphere thickness ranges from 180-240 km cannot be delaminated by gravitational process alone and will tend to be preserved under a stable condition but can be disrupted and replaced if undergoing tectonic processes such as rifting. They also found that the Proterozoic SCLM less than 120 km thick is gravitationally unstable and that Phanerozoic sections less than 100 km thick are stable when the geotherms are still elevated but become unstable with delamination process as result once they have cooled to typical steady state of conductive geotherms. A brief analysis of the lithospheric thickness of Cameroon and its surroundings (Fig. 24A) shows that the northern margin of the Congo craton might have been partially under delamination process result of the Precambrian collision during the assembly of the greater Gondwana. Futhermore the Phanerozoic SCLM (West Cameroon domain) less than 120 km thick may have been gravitationally stable until the cooling period where gravitational instability and delamination processes followed.

CHAPTER V:

GENERAL CONCLUSION

Through the imaging of the Moho and LAB depth beneath Cameroon and surroundings using the 2D radially-average power spectrum analysis of the WGM 2012 and thermal inversion of passive seismic data the following was found: Through the evaluation of gravity anomaly characteristic, the 2D radially-average power spectral analysis, the 2D forward modeling of WGM 2012 satellite gravity data and thermal inversion of passive seismic data: 1) low gravity anomaly within the Congo craton, the Yaoundé domain, the southeastern part of the West Cameroon domain, and the northern part of the Adamawa-Yade domain. (2) a pronounced E-W trending high gravity anomaly within the southern part of the Adamawa-Yade domain. (3) a thicker crust beneath the Congo craton reaching 51 km. A deeper discontinuity at ~ 139 –199 km beneath the craton and interpreted as the LAB. (4) a thinner crust beneath the Precambrian orogenic belt (centered beneath the Adamawa plateau) reaching 32 km. A deeper discontinuity was also mapped, interpreted to represent the LAB, at ~ 104 km beneath the Precambrian orogenic belt and found that this anomaly closely coincides with the ENE-trend of the CASZ.

The denser material beneath the southern part of the Adamawa-Yade domain was interpreted as possibly due to the densification of an under-thrust portion of the Congo craton through metacratonization processes that accompanied collision between the craton and the Oubanguides orogenic terranes. This is interpreted as possibly due to slab detachment during the Neoproterozoic Pan-African orogenic event allowing for ascendance of asthenospheric material. Ascendance of the asthenosphere provided enough heat to partially melt the lower crust and upper SCLM producing felsic magma that was intruded in the form of high-K granitoids.

The deeper Moho and LAB beneath the Congo craton and the Yaounde domain reaching ~51 km and ~200 km, respectively and the shallow Moho and LAB beneath the CASZ, the Adamawa plateau, and the Benue trough reaching ~ 25 km and ~70 km, respectively is interpret as due to modification of the lithosphere by a number of tectonic events that started in the Precambrian. the shallower LAB zone called in the current study the Central African magmatic corridor is interpret as a favourable zone for melting and SCLM delamination during the Precambrian collision in the assembly of Greater Gondwana along the northern margin of the Congo craton. This allowed for mantle flow channelization during the Phanerozoic and the Cenozoic within the Central Africa magmatic corridor resulting in the formation of alkaline magmatism represented by anorogenic complex and vocanic magmatism reaching the surface in some place through reactivaction of some Panafrican faults and the uplift of the Adamawa plateau

Finaly the northwestern limit of thick lithosphere and LAB depth following partly the southern edge of the West Cameroon domain is interpreted as the northwestern edge of the Congo craton in Cameroon and that the Yaoundé domain is an allochthon that was thrust atop the Congo craton.

Future recommendations

Though this work has shown a high quality of the lithosphere structure underneath Cameroon and its surrounding, there is still room for further improvements to better the understanding of the geology, geodynamic and tectonic of the study area. A summary of open questions and recommendations for further researches is given below.

- The current research can be extended for the modeling of other interfaces, for instance the core mantle boundary zone. This can be achieved by a proper truncation of low-degree spherical harmonic coefficients and modeling of the inhomogeneities in the mantle.
- Model the thermal structure of the study area from surface, borehole and magnetic observations to support the interpretation of Gravity anomalies and passive seismic data.
- Dig futher into the state of the contact between the Archean Congo craton and the Nyong Complex?

REFERENCES

Abdelsalam, M.G. and Dawoud, A.S., 1991. The Kabus ophiolitic melange, Sudan, and its bearing on the western boundary of the Nubian Shield. Journal of the Geological Society, 148(1), 83-92.

Abdelsalam, M.G., Gao, S.S., Liégeois, J.P. 2011. Upper mantle structure of the Saharan Metacraton.Journal of African Earth Sciences 60,328-336.

Abdelsalam, M.G., Liégeois, J.P. and Stern, R.J., 2002. The saharan metacraton. Journal of African Earth Sciences, 34(3), 119-136.

Adams, A.N., Wiens, D.A., Nyblade, A.A., Euler, G.G., Shore, P.J. and Tibi, R., 2015. Lithospheric instability and the source of the Cameroon Volcanic Line: Evidence from Rayleigh wave phase velocity tomography. Journal of Geophysical Research: Solid Earth, 120(3), 1708-1727.

Airy, G.B., 1855. On the computation of the effect of the attraction of mountain-masses, as disturbing the apparent astronomical latitude of stations in geodetic surveys. Philosophical Transactions of the Royal Society of London, 145,101-104.

Aitken, A., Salmon, M., and Kennett, B. (2013). Australia's moho: A test of the usefulness of gravity modelling for the determination of moho depth. Tectonophysics, 609, 468–479.

Amante, C. and Eakins, B.W., 2009. ETOPO1 1 arc-minute global relief model: procedures, data sources and analysis (p. 19). Colorado: US Department of Commerce, National Oceanic and Atmospheric Administration, National Environmental Satellite, Data, and Information Service, National Geophysical Data Center, Marine Geology and Geophysics Division.

Anderson, O, B. (2010). The dtu10 gravity field and mean sea surface. Secondinternational symposium of the gravity field of the Earth, (IGFS2): Fairbanks, Alaska.

Anderson, O, B., Knudsen, P., and Berry, P. (2009). DNSC08 mean sea surface andmean dynamic topography models. Journal of geophysical research.

Archanjo, C.J., Launeau, P., Maria Helena B. M. Hollanda, M.H.B.M., Macedo, J.W.P., Liu, D., 2009. Scattering of magnetic fabrics in the Cambrian alkaline granite of Meruoca Cearà state, northeastern Brazil). International Journal Earth Sciences (Geol Rundsch), 98, 1793–1807.

Arthaud, M.H., Caby, R., Fuck, A., Dantas, E.L., Parente, C.V., 2008. Geology of the northern Borborema Province, NE Brazil and its correlation with Nigeria, NW Africa. In: Pankhurst, R.J., Trouw, R.A.J., Brito Neves, B.B., De Wit, M.J. (eds) West Gondwana: Pre-Cenozoic Correlations Across the South Atlantic Region. Geological Society, London, Special Publications, 294, 49-67.

Balmino, G., Vales, N., Bonvalot, S., Briais, A. 2012. Spherical harmonic modelling to ultra-high degree of Bouguer and isostatic anomalies. Journal of Geodesy 86, 499-520.

Balmino, G., Vales, N., Bonvalot, S., Briais, A. 2012. Spherical harmonic modelling to ultra-high degree of Bouguer and isostatic anomalies. Journal of Geodesy 86, 499-520.

Bassin, C., Laske, G., Masters, G., 2000. The current limits of resolution for surface wave tomography in North America. EOS. Transactions of the American Geophysical Union 81, F897.

Black, R. and Girod, M., 1970. Late Paleozoic to Recent igneous activity in West Africa and its relationship to basement structure. African magmatism and tectonics, 1(8), 5-2.

Black, R., Caby, R., Moussine-Pouchkine, A., Bayer, R., Bertrand, J.M., Boullie, A.M., Fabre, J., Lesquer, A. 1979. Evidence for lae Precambrian plate tectonics in West Africa. Nature 278, 223-227.

Boniface, N., Schenk, V., Appel, P., 2012. Paleoproterozoic eclogites of MORB-type chemistry and three. Proterozoic orogenic cycles in the Ubendian Belt (Tanzania): Evidence from monazite and zircon geochronology, and geochemistry. Precambrian Res. 192-195, 16-33.

Bonvalot, S., Balmino, G., Briais, A., M. Kuhn, Peyrefitte, A., Vales, Biancale, R., Gabalda, G., Moreaux, G., Reinquin, F., Sarraillh, M., 2012. World Gravity Map, 1:50,000,000. Editors: Bureau Gravimetrique International (BGI) – Commission for the Geological Map of the World (CGMW), Centre National d'Etudes Spatiales (CNES) – Institut de Reserche pour le Development (IRD), Paris.

Bonvalot, S., Balmino, G., Briais, A., M. Kuhn, Peyrefitte, A., Vales, Biancale, R., Gabalda, G., Moreaux, G., Reinquin, F., Sarraillh, M., 2012. World Gravity Map, 1:50,000,000. Editors: Bureau Gravimetrique International (BGI) – Commission for the Geological Map of the

World (CGMW), Centre National d'Etudes Spatiales (CNES) – Institut de Reserche pour le Development (IRD), Paris.

Boukeke, D.B., 1994. Structures crustales d'Afrique Centrale déduites des anomalies gravimétriques et magnétiques: le domaine précambrien de la République Centrafricaine et du Sud Cameroun (Doctoral dissertation, Paris 11).

Bouyo Houketchang, M., Toteu, S.F., Deloule, E., Penaye, J., Van Schmus, W.R., 2009. U-Pb and Sm-Nd dating of high-pressure granulites from Tcholliré and Banyo regions: Evidence for a Pan-African granulite facies metamorphism in northcentral Cameroon. Journal of African Earth Sciences. 54, 144–154.

Bouyo Houketchang, M., Zhao, Y., Penaye, J., Zhang, S.H., Njel, U.O., 2015.Neoproterozoic subduction-related metavolcanic and metasedimentary rocks from the Rey Bouba Greenstone Belt of north-central Cameroon in the Central African Fold Belt: new insights into a continental arc geodynamic setting. Precambrian Res. 261, 40-53.

Bouyo Houketchang Bouyo M., Penaye J., Njel U.O. Moussango A.P.I, Sep J.P.N., Nyama B.A., Wassouo W.J., Abate J.M.E., Yaya F., Mahamat A., Hao Ye, FeiWu, 2016. Geochronological, geochemical and mineralogical constraints of emplacement depth of TTG suite from the Sinassi Batholith in the Central African Fold Belt (CAFB) of northern Cameroon: Implications for tectonomagmatic evolution. Journal of African Earth Sciences 116, 9-41.

Braitenberg, C., Zadro, M., Fang, J., Wang, Y. and Hsu, H.T., 2000. The gravity and isostatic Moho undulations in Qinghai–Tibet plateau. Journal of Geodynamics, 30(5), 489-505.

Brinks, R.M. and Fairhead, J.D., 1992. A plate tectonic setting for Mesozoic rifts of West and Central Africa. Tectonophysics 213, 141-151.

Bullen, K. (1975). The Earth's density. Chapman and Hall. 2.1

Caby, R., 1989. Precambrian terranes of Benin-Nigeria and Northeast Brazil and the lateProterozoic South Atlantic fit. Geological Society America, Special Paper, 230: 145-158.

Caby, R., Sial, A.N., Arthaud, M.H., Vauchez, A., 1991. Crustal evolution and the Brasiliano Orogeny in Nort-east Brazil. In: Dallmeyer, R.D. and Lécorché, J.P. (eds) The West African Orogens and Circum-Atlantic Correlatives. Springer, Berlin, 373-397.

Cara, M. and Lévêque, J.J., 1987. Waveform inversion using secondary observables. Geophysical Research Letters, 14(10), 1046-1049.

Castaing, C., Feybesse, J.A., Thiéblemont, D., Triboulet, C. and Chevremont, P., 1994. Palaeogeographical reconstructions of the Pan-African/Brasiliano orogen: closure of an oceanic domain or intracontinental convergence between major blocks? Precambrian Research, 69(1-4), 327-344.

Castaing, C., Triboulet, C., Feybesse, J.L., Chèvremont, P., 1993. Tectonometamorphic evolution of the Ghana, Togo and Benin in the light of the Pan-African/Brasiliano orogeny. Tectonophysics, 218, 323-342.

Chen and Tenzer (2014). Harmonic coefficients of the earth's spectral crustal model 180-escm180. Earth Scie Inf, sum.

Censier C., Dynamique sédimentaire d'un système fluvuatile diamantifère mésozoïque. La formation de Carnot (République centrafricaine), thèse, université de Bangui, 1989.

Coulon, C., Vidal, P., Dupuy, C., Baudin, P., Popoff, M., Maluski, H. & Hermitte, D., 1996. The Mesozoic to early Cenozoic magmatism of the Benue Trough (Nigeria): geochemical evidence for the involvement of the St. Helena plume, J. Petrol., 37, 1341–1358.

Da Silva Amaral, W., dos Santos, T.J.S., Wernick, E., de Araújo Nogueira Neto, J., Dantas, E.L., Matteini, M., 2012. High-pressure granulites from Cariré, Borborema Province, NE Brazil: Tectonic setting, metamorphic conditions and U-Pb, Lu-Hf and Sm-Nd geochronology. Gondwana Research.

Dada, S.S., 2008. Proterozoic evolution of the Nigeria-Boborema province. In: R.J. Pankhurst, R.A.J. Trouw, B.B. Brito Neves and M.J. De Wit (eds), West Gondwana: Pre-Cenozoic Correlations Across the South Atlantic Region, Geological Society, London, Special Publications, 294, 121-136.

Daouda Dawaï D., Bouchez J. L., Paquettec J. L., Tchameni R., 2013. The Pan-African quartz-syenite of Guider (north-Cameroon): Magnetic fabric and U–Pb dating of a late-orogenic emplacement. Journal of African Earth Sciences. 236, 132– 144.

Dawaï D., Tchameni R., Bascou J., Awe Wangmene S., Fosso Tchunte P. M., Bouchez J. L., 2017. Microstructures and magnetic fabrics of the Ngaound_er_e granite pluton (Cameroon): Implications to the late-Pan-African evolution of Central Cameroon Shear Zone. Journal of African Earth Sciences. 129, 887-897.

De Plaen, R.S.M., Bastow, I.D., Chambers, E.L., Keir, D., Gallacher, R.J. and Keane, J., 2014. The development of magmatism along the Cameroon Volcanic Line: evidence from seismicity and seismic anisotropy. Journal of Geophysical Research: Solid Earth 119, 4233-4252.

De Wit, M.J., Stankiewicz, J., Reeves, C., 2008. Restoring Pan-African–Brasiliano connections: more Gondwana control, less Trans-Atlantic corruption. In: R.J. Pankhurst, R.A.J. Trouw, B.B. Brito Neves, M.J. De Wit (eds), West Gondwana: Pre-Cenozoic Correlations Across the South Atlantic Region, Geological Society, London, Special Publications, 294, 399-412.

Delhal J. & Ledent L. (1975). – Données géochronologiques sur le complexe calcomagnésien du Sud Cameroun. – Musée Royal d'Afrique Centrale (Belgique), Rapp. Annuel, 71-75.

Deruelle B., Ngounouno, I. & Demaiffe, D., 2007. The Cameroon Hot Line (CHL): a unique example of active alkaline intraplate structure in both oceanic and continental lithospheres, C. R. Geosci., 339, 589–600.

Deruelle B., Nkoumbou, C., Kambou, R., Lissom, J., Njongfang, E., Ghogomu, R.T. & Nono, A., 1991. The Cameroon Line: a review, in Magmatism in Extensional Structural Settings. The Phanerozoic African Plate, Vol. 79, 274–327, eds Kampunzu, A.B. & Lubala, R.T., Springer-Verlag, Berlin.

Dorbath, C., Dorbath, L., Fairhead, J.D. and Stuart, G.W., 1986. A teleseismic delay time study across the Central African Shear Zone in the Adamawa region of Cameroon, West Africa. Geophysical Journal International, 86(3), 751-766.

Dos Santos, T.J.S., Fetter, A.H., Neto, J.A.N., 2008. Comparisons between the northwestern Borborema Province, NE Brazil, and the southwestern Pharusian Dahomey Belt, SW Central Africa. Geological Society, London, Special Publications, 294, 101-120.

Drinkwater, K.F., Belgrano, A., Borja, A., Conversi, A., Edwards, M., Greene, C.H., Ottersen, G., Pershing, A.J. and Walker, H., 2003. The response of marine ecosystems to climate variability associated with the North Atlantic Oscillation (211-234). American Geophysical Union.

Dziewonski, A.M. and Anderson, D.L., 1981. Preliminary reference Earth model. Physics of the earth and planetary interiors, 25(4), 297-356.

Dziewonski, A.M., Hales, A.L. and Lapwood, E.R., 1975. Parametrically simple earth models consistent with geophysical data. Physics of the Earth and Planetary Interiors, 10(1), 12-48.

Ebinger C.J. & Sleep, N.H., 1998. Cenozoic magmatism throughout east Africa resulting from impact of a single plume, Nature, 395, 788–791.

Ekwueme, B. N. & Kröner, A. (1998) Single zircon evaporation ages from the Oban Massif, southeastern Nigeria. Journal of African Earth Sciences, 26, 195-205.

Ekwueme, B. N. & Kröner, A. (2006) Single zircon ages of migmatitic gneisses and granulites in the Obudu Plateau: Timing of granulite-facies metamorphism in southeastern Nigeria. Journal of African Earth Sciences, 44, 459-469.

Elsheikh, A.A., Gao, S.S. and Liu, K.H., 2014. Formation of the Cameroon Volcanic Line by lithospheric basal erosion: Insight from mantle seismic anisotropy. Journal of African Earth Sciences100, 96-108.

Eyike, A. and Ebbing, J., 2015. Lithospheric structure of the West and Central African Rift System from regional three-dimensional gravity modelling. South African Journal of Geology, 118(3), 285-298.

Fairhead, J. D. and Okereke, C.S., 1987. A regional gravity study of the West African rift system in Nigeria and Cameroon and its tectonic interpretation. Tectonophysics, 143(1-3),141-159.

Fairhead, J.D. & Binks, R.M., 1991. Differential opening of the central and south-atlantic oceans and the opening of the West African Rift System, Tectonophysics, 187(1–3), 191–203.

Fairhead, J.D. and Girdler, R.W., 1972. The seismicity of the East African rift system. Tectonophysics, 15(1), 115-122.

Fairhead, J.D., 1988. Mesozoic plate tectonic reconstructions of the central South Atlantic Ocean: The role of the West and Central African Rift System. Tectonophysics 155, 181-191.

Ferré, E.C., Galland, O., Montanari, D., Kalakay, T.J., 2012. Granite magma migration and emplacement along thrusts. International Journal of Earth Sciences (Geol Rundsch).

Ferre, E.C., Caby, R., Peucat, J.J., Capdevila, R., Monie, P., 1998. Pan-African, postcollisional, ferro-potassic granite and quartz-monzonite plutons of eastern Nigeria. Lithos 45, 255e279.

Fishwick, S. and Bastow, I.D., 2011. Towards a better understanding of African topography: a review of passive-source seismic studies of the African crust and upper mantle. Geological Society, London, Special Publications, 357(1), 343-371.

Fitton, J.G., 1987. The Cameroon line, West Africa: a comparison between oceanic and continental alkaline volcanism. Geological Society, London, Special Publications, 30(1), 273-291.

Floberghagen, R., Fehringer, M., Lamarre, D., Muzi, D., Frommknecht, B., Steiger, C., Piñeiro, J. and Da Costa, A., 2011. Mission design, operation and exploitation of the gravity field and steady-state ocean circulation explorer mission. Journal of Geodesy, 85(11), 749-758.

Foerste, C., Flechtner, F., Schmidt, R., Stubenvoll, R., Rothacher, M., Kusche, J., Neumayer, H., Biancale, R., Lemoine, J.M., Barthelmes, F. and Bruinsma, S., 2008, April. EIGEN-GL05C-A new global combined high-resolution GRACE-based gravity field model of the GFZ-GRGS cooperation. In Geophysical Research Abstracts (Vol. 10, pp. EGU2008-A).

Foerste C., Bruinsma S., Shako R., Marty J.C., Flechtner F., Abrikosov O., Dahle C., Lemoine J.M., Neumayer K.H., Biancale R., Barthelmes F., Koenig R. and Balmino G., 2011, EIGEN-6 – a new combined global gravity öeld model including GOCE data from the collaboration of GFZ-Potsdam and GRGS-Toulouse, Geophys. Res. Abs., 13, EGU2011-3242-2.

Förste, C., Bruinsma, S., Flechtner, F., Marty, J.C., Dahle, C., Abrykosov, O., Lemoine, J.M., Neumayer, H., Barthelmes, F., Biancale, R. and König, R., 2013, April. EIGEN-6C2-A new combined global gravity field model including GOCE data up to degree and order 1949 of GFZ Potsdam and GRGS Toulouse. In EGU general assembly conference abstracts(Vol. 15).

Gallacher, R.J. and Bastow, I.D., 2012. The development of magmatism along the Cameroon Volcanic Line: Evidence from teleseismic receiver functions. Tectonics, 31(3).

Ganade, C.E., Cordani, U.G., Agbossoumounde, Y., Caby, R., Basei, M.A.S., Weinberg, F., Sato, K., 2016. Tightening-up NE Brazil and NW Africa connections: new UePb/LueHf zircon data of a complete plate tectonic cycle in the Dahomey belt of the West Gondwana Orogen in Togo and Benin. Precambrian Res. 276, 24-42.

Ganwa, A.A., Klötzli, U.S., Hauzenberger, C., 2016. Evidence for Archean inheritance in the pre-Panafrican crust of Central Cameroon: Insight from zircon internal structure and LA-MC-ICP-MS U-Pb ages. Journal of African Earth Sciences. 120, 12–22.

Genik, G. J., 1992. Regional framework, structural and petroleum aspects of rift basins in Niger, Chad and the Central African Republic (CAR). Tectonophysics, 213(1-2), 169-185.

Genik, G.J., 1993. Petroleum geology of the Cretaceous – Tertiary rift basins in Niger, Chad, and Central African Republic. American Association of Petroleum Geologists Bulletin 73, 153 – 168.

Gibb, R.A., Thomas, M.D., Kearey, P. and Tanner, J.G., 1978. Gravity anomalies at structural province boundaries of the Canadian Shield: products of Proterozoic plate interaction. GeoSkrifter, 10, 21-57.

Gibb, R.A., Thomas, M.D., Lapointe, P.L. and Mukhopadhyay, M., 1983. Geophysics of proposed Proterozoic sutures in Canada. Precambrian Research, 19(4), 349-384.

Gómez-Ortiz, D., Tejero-López, R., Babín-Vich, R. and Rivas-Ponce, A., 2005. Crustal density structure in the Spanish Central System derived from gravity data analysis (Central Spain). Tectonophysics, 403(1), 131-149.

Grad, M. and Tiira, T., 2009. The Moho depth map of the European Plate. Geophysical Journal International, 176(1), 279-292.

Green, D.H., Falloon, T.J., Eggins, S.M. and Yaxley, G.M., 2001. Primary magmas and mantle temperatures. European Journal of Mineralogy, 13(3), 437-452.

Griffing, W.L., Ryan, C.G., Kaminsky, F.V., O'Reilly, S.Y., Natapov, L.M., Win, T.T., Kinny, P.D. and Ilupin, I.P., 1999b. The Siberian lithosphere traverse: mantle terranes and the assembly of the Siberian Craton. Tectonophysics, 310(1), 1-35.

Guiraud, R. & Maurin, C.J., 1992. Early cretaceous rifts of Western andCentral Africa, Tectonophysics, 213, 153–168.

Hayford, J.F. and Bowie, W., 1912. Geodesy: The Effet of Topography and Isostatic Compensation Upon the Intensity of Gravity (No. 10). US Govt. Print. Off.

Hayford, J.F., 1909a. Geodesy: The Figure of the Earth and Isostasy from Measurements in the United States (No. 82). US Government Printing Office.

Heiskanen, W.A. and Moritz, H., 1967. Physical geodesy. Bulletin Géodésique (1946-1975), 86(1), 491-492.

Heiskanen, W.A. and Vening Meinesz, F.A., 1958. The Earth and its Gravity Field. McGraw-Hill, New York.

Hinze, W.J., 2003. Bouguer reduction density, why 2.67. Geophysics, 68(5), 1559-1560.

Hussein, M., Mickus, K., Serpa, L.F. 2013. Curie point depth estimates from aeromagnetic data from Death Valley and surrounding regions, California. Pure and Applied Geophysics 170, 617-632.

Isseini, M., 2011. Croissance et différenciation crustales au Néoprotérozoïque. Exemple du domaine panafricain du Mayo Kebbi au sud-ouest du Tchad. Unpubl. Thesis, Univ. Lorraine, Nancy, 342p.

Isseini, M., André-Mayer, A.S., Vanderhaeghe, O., Barbey, P., Deloule, E., 2012. A-type granites from the Pan-African orogenic belt in south-western Chad constrained using geochemistry, Sr-Nd isotopes and U-Pb geochronology. Lithos 153, 39–52.

Isseini, M., André-Mayer, A.S., Vanderhaeghe, O., Barbey, P., Deloule, E., 2012. A-type granites from the Pan-African orogenic belt in south-western Chad constrained using geochemistry, Sr–Nd isotopes and U–Pb geochronology. Lithos 153, 39– 52.

Kaban, M.K., Schwintzer, P. and Tikhotsky, S.A., 1999. A global isostatic gravity model of the Earth. Geophysical Journal International, 136(3), 519-536.

Kaban, M.K., Schwintzer, P. and Tikhotsky, S.A., 1999. A global isostatic gravity model of the Earth. Geophysical Journal International, 136(3), 519-536.

Kaban, M.K., Tesauro, M., Mooney, W.D. and Cloetingh, S.A., 2014. Density, temperature, and composition of the North American lithosphere—New insights from a joint analysis of seismic, gravity, and mineral physics data: 1. Density structure of the crust and upper mantle. Geochemistry, Geophysics, Geosystems, 15(12), 4781-4807.

Kalsbeek, F., Affaton, P., Ekwueme, B., Frei, R., Thrane, K., 2012. Geochronology of granitoid and metasedimentary rocks from Togo and Benin, West Africa: Comparisons with NE Brazil. Precambrian Research, 196-197, 218- 233.

Kamgang, P., Njonfang, E., Nono, A., Gountie, D.M., Tchoua, F., 2010. Petrogenesis of a silicic magma system: geochemical evidence from Bamenda Mountains, NW Cameroon, Cameroon Volcanic Line. Journal of African Earth Sciences 58, 285–304.

Kamgang P., Gilles Chazot G., Njonfang D., Tchuimegnie Ngongang N. B.,Tchoua F. M., 2013. Mantle sources and magma evolution beneath the Cameroon Volcanic Line: Geochemistry of mafic rocks from the Bamenda Mountains (NW Cameroon Gondwana Research 24, 727–741.

Kellogg, O. D. (1929). Foundations of Potential Theory. Berlin Verlag Von Julius Springer.

King, S.D. & Ritsema, J., 2000. African hot spot volcanism: small-scale convection in the upper mantle beneath cratons, Science, 290, 1137–1140.

King, S.D., Anderson, D.L., 1995. An alternative mechanism of flood basalt formation. Earth Planet. Sci. Lett. 136, 269–279.

King, S.D., Anderson, D.L., 1998. Edge-driven convection. Earth Planet. Sci. Lett. 160, 289–296.

Koch, F.W., Wiens, D.A., Nyblade, A.A., Shore, P.J., Tibi, R., Ateba, B., Tabod, C.T. and Nnange, J.M., 2012. Upper-mantle anisotropy beneath the Cameroon Volcanic Line and Congo Craton from shear wave splitting measurements. Geophysical Journal International 190, 75-86.

Kustowski, B., Ekström, G. and Dziewoński, A.M., 2008. Anisotropic shear-wave velocity structure of the Earth's mantle: A global model. Journal of Geophysical Research: Solid Earth, 113(B6).

Kwékam, M., Liégeois, J.P., Njonfang, E., Affaton, P., Hartmann, G. and Tchoua, F., 2010. Nature, origin and significance of the Fomopéa Pan-African high-K calc-alkaline plutonic complex in the Central African fold belt (Cameroon). Journal of African Earth Sciences, 57(1), 79-95.

Kwekam, M., Liegois, J.P., Njonfang, E., Affaton, P., Hartmann, G., Tchoua, F., (2009). Nature, origin and significance of the Fomopéa Pan-African high K calc-alkaline plutonisme complex in the central African Fold Belt (Cameroon).

Kwékam, M., Affaton, P., Bruguier, O., Liégeois, J.P., Hartmann, G. and Njonfang, E., 2013. The Pan-African Kekem gabbro-norite (West-Cameroon), U–Pb zircon age, geochemistry and Sr–Nd isotopes: Geodynamical implication for the evolution of the Central African fold belt. Journal of African Earth Sciences, 84, pp.70-88.

Laske, G., Masters, G., Ma, Z. and Pasyanos, M., 2013, April. Update on CRUST1. 0—A 1-degree global model of Earth's crust. In Geophys. Res. Abstracts (Vol. 15, abstrEGU).

Lasserre, M. and Soba, D., 1976. Age Libérien des granodiorites et des gneiss à pyroxènes du Cameroun Méridional. Bull. BRGM, 2(1), 17l32.

Lasserre, M., Soba, D., 1979. Migmatisation d'âge panafricain au sein des formations camerounaises appartenant a la zone mobile d'Afrique Centrale. Comptes Rendus sommaires de la Société Geologies de France 2, 64–68.

Lee, D.C., Halliday, A., Fitton, J.G.&Poli, G., 1994. Isotopic variations with distance and time in the Volcanic Islands of the Cameroon line: evidence for a mantle plume origin, Earth planet. Sci. Lett., 123(1–4), 119–138.

Leseane, K., Atekwana, E.A., Mickus, K.L., Abdelsalam, M.G., Shemang, E.M., Atekwana, E.A. 2015. Thermal perturbations beneath the incipient Okavango Rift Zone, northwest Botswana. Journal of Geophysical Research: Solid Earth 120, 1210-1228.

Lerouge, C., Cocherie, A., Toteu, S.F., Penaye, J., Milési, J.P., Tchameni, R., Nsifa, E.N., Fanning, C.M. and Deloule, E., 2006. Shrimp U–Pb zircon age evidence for Paleoproterozoic sedimentation and 2.05 Ga syntectonic plutonism in the Nyong Group, South-Western Cameroon: consequences for the Eburnean–Transamazonian belt of NE Brazil and Central Africa. Journal of African Earth Sciences, 44(4-5), pp.413-427.

Liégeois, J.P., Latouche, L., Boughrara, M., Navez, J. and Guiraud, M., 2003. The LATEA metacraton (Central Hoggar, Tuareg shield, Algeria): behaviour of an old passive margin during the Pan-African orogeny. Journal of African Earth Sciences, 37(3), 161-190.

Maden, N. 2010. Curie-point depth from spectral analysis of magnetic data in Erciyes stratovolcano (Central Turkey). Pure and Applied Geophysics 167, 349-358.

Mader, K. (1951). Das Newtonsche raumpotential prismatischer Körper und seine ableitungen bis zur dritten Ordnung. Sonderheft 11 der Österreichischen Zeitschrift für Vermessungswesen. Österreichischer Verein für vermessungswesen, wien. Pages.

Magdala, T., Kaban, M., Sierd, and A., P., L. C. (2008). Eucrust-07: A new reference model for the european crust. Geophysical research letters, 35.

Makris, J., Henke, C.H., Egloff, F. and Akamaluk, T., 1991. The gravity field of the Red Sea and East Africa. Tectonophysics, 198(2-4), 369-381.

Mariani, Patrizia, Braitenberg, C., and Ussami, N. (2013). Explaining the thick crust in paraná basin, brazil, with satellite goce gravity observations. Journal of South American Earth Sciences, 45, 209–223.

Mathur, S.P., 1974. Crustal structure in southwestern Australia from seismic and gravity data. Tectonophysics, 24(1-2), 151-182.

Maurizot P., Abossolo, A., Feybesse, A., Johan, J.L. & Lecomte, P., 1986. Etude et prospection minière du Sud-Ouest Cameroun. Synthèse des travaux de 1978 a 1985, Rapport B.R.G.M, 85, CMR 066, Janvier 1986, 274.

Meier, U., Curtis, A., and Trampert, J. (2007). Fully nonlinear inversion of fundamentalmode surface waves for a global crustal model. GEOPHYSICAL RESEARCHLETTERS, 34, L16304.

Meyers, J.B., Rosendahl, B.R., Harrison, C.G.A., Ding, Z.-D., 1998. Deep-imaging seismic and gravity results from the offshore Cameroon Volcanic Line, and speculation of African hotlines. Tectonophysics 284, 31–63.

Milelli, L., Fourel, L., Jaupart, C., 2012. A lithospheric instability origin for theCameroon Volcanic Line. Earth Planet. Sci. Lett. 335–336, 80–87.

Mohorovicic, A. (1910). Earthquake of 8 October 1909 (English translation of "Potres of 8.X.1909", Godišnje izvješce zagrebackog meteorološkog opservatorija, 9(4/1),1-56). Geofizika, 1–56.

Mohorovicic, A. (1992). Earthquake of 8 October 1909 (English translation of "Potres of 8.X.1909", Godišnje izvješce zagrebackog meteorološkog opservatorija, 9(4/1), 1-56). Geofizika, 9:3–56.

Montes-Lauar, C.R., Trompette, R., Melfi, A. J., Bellieni, G., de min, A., Bea, A., Piccirillo, E.M., Affaton, P., Pacca, I. G. (1997). Panafrican Rb-Sr ages of magmatic rocks from northern Cameroon. Preliminary results. South-American Symposium on Isotope Geology-Brazil, June 1997.

Mooney, W.D., Laske, G. and Masters, T.G., 1998. CRUST 5.1: A global crustal model at 5×5. Journal of Geophysical Research: Solid Earth, 103(B1), 727-747.

Mooney, W.D., Laske, G. and Masters, T.G., 1998. CRUST 5.1: A global crustal model at 5×5. Journal of Geophysical Research: Solid Earth, 103(B1), 727-747.

Morgan, W.J., 1983. Hotspot tracks and the early rifting of the Atlantic. Tectonophysics 94, 123–139.

Moreau, C., Regnoult, J.M., Deruelle, B., Robineau, B., 1987. A new tectonic model for the Cameroon Line, Central-Africa. Tectonophysics 141, 317–334.

Moritz, H. (2006). Physical geodesy. Springer-Verlag Wien Austria

Mvondo, H., Den Brok, S.W.J. and Ondoa, J.M., 2003. Evidence for symmetric extension and exhumation of the Yaounde nappe (Pan-African fold belt, Cameroon). Journal of African Earth Sciences, 36(3), 215-231.

Mvondo O. J., 2009. Caractérisation des évènements tectoniques dans le domaine sud de la chaine panafricaine au Cameroun : styles tectoniques et géochronologie des séries de Yaoundé et de Bafia. Thèse de Doct/Ph. D, Univ. Ydé I, 170p.

Mvondo, H., Owona, S., Ondoa, J. M. and Essono, J., 2007. Tectonic evolution of the Yaounde segment of the Neoproterozoic Central African orogenic belt in southern Cameroon. Canadian Journal of Earth Sciences 44, 4, 433-444.

Narain, H. and Subrahmanyam, C., 1986. Precambrian tectonics of the South Indian shield inferred from geophysical data. The Journal of Geology, 94(2), 187-198.

Nataf, H.C. and Ricard, Y., 1996. 3SMAC: an a priori tomographic model of the upper mantle based on geophysical modeling. Physics of the Earth and Planetary Interiors, 95(1-2), 101-122.

Nédélec a., Macaudière j., Nzenti j.p. & Barbey p. (1986). – Evolution structurale et métamorphique des schistes de Mbalmayo (Cameroun). Implication pour la structure de la zone mobile d'Afriquecentrale au contact du craton. – C.R. Acad. Sci., Paris, 303, sér. II, 75-80.

Nédélec a., Nsifa N.E. & Martin H. (1990). – Major and trace element geochemistry of the Archaean Ntem plutonic complex (South Cameroon): petrogenesis and crustal evolution. – Precambrian Res., 47, 35-50.

Nédélec, A. and NSIFA, E., 1987. Le complexe du Ntem (Sud-Cameroun): une série tonalito-trondhémitique archéenne typique. In Colloquium on African geology. 14, 3-6.

Nédélec, A., Minyem, D. and Barbey, P., 1993. High-P—high-T anatexis of Archaean tonalitic grey gneisses: the Eseka migmatites, Cameroon. Precambrian Research, 62(3), 191-205.

Nédélec, A., Nsifa, E.N. and Martin, H., 1990. Major and trace element geochemistry of the Archaean Ntem plutonic complex (South Cameroon): petrogenesis and crustal evolution. Precambrian Research, 47(1), 35-50.

Nedelec, A., Nsifa, E.N., Martin, H., 1989. Major and trace element geochemistry of the Archean Ntem plutonic complex (South Cameroon): petrogneiss and crustal evolution. Precambrian Res. 47, 35-50.

Negue, E.N., Tchameni, R., Vanderhaeghe, O., Fengyue, S., Barbey, P., Tekoum, Lé.,Fosso, P.M., Eglinger, A., Fouotsa, N.A.S., 2017. Structure and LA-ICP-MS zircon U-Pbdating of syntectonic plutons emplaced in the Pan-African Banyo-Tcholliré shear zone (central north Cameroun), Journal of African Earth Sciences.

Neves S. P., Monié P., Bruguier O., da Silva J. M. R., 2012. Geochronological, thermochronological and thermobarometric constraints on deformation, magmatism and thermal regimes in eastern Borborema Province (NE Brazil). Journal of South American Earth Sciences 38, 129-146.

Neves, P.S., 2003. Proterozoic history of the Borborema province (NE Brazil): Correlations with neighbouring cratons and Pan-African belts and implications for the evolution of western Gondwana. Tectonics, 22: 1031.

Ngako, V., Affaton, P. and Njonfang, E., 2008. Pan-African tectonics in northwestern Cameroon: implication for the history of western Gondwana. Gondwana Research, 14(3), 509-522.

Ngako, V., Njonfang, E., Aka, F.T., Affaton, P., Nnange, J.M., 2006. The North–SouthPaleozoic to Quaternary trend of alkaline magmatism from Niger–Nigeria toCameroon: complex interaction between hotspots and Precambrian faults. J.Afr. Earth Sci. 45, 241–256.

Ngalamo, J. F.G., Bisso, D., Abdelsalam, M.G., Atekwana, E.A., Katumwehe, A.B. and Ekodeck, G.E., 2017. Geophysical imaging of metacratonizaton in the northern edge of the Congo craton in Cameroon. Journal of African Earth Sciences, 129, 94-107.

Ganwa, A.A., Klotzli U. S., Hauzenberger C., 2016. Evidence for Archean inheritance in the pre-Panafrican crust of Central Cameroon: insigh from zircon internal structure and LA-MC-ICP-MS U-Pb ages. Journal of African Earth Sciences 120, 12-22.

Ngnotué, T., Ganno, S., Nzenti, J. P., Schulz B., Tchaptchet Tchato D., Suh Cheo E. 2012. Geochemistry and geochronology of Peraluminous High-K granitic leucosomes of Yaoundé

series (Cameroon): evidence for a unique Pan-African magmatism and melting event in North Equatorial Fold Belt. International Journal of Geosciences, 3, 525-548.

Njonfang, E., 1998. Contribution à l'étude de la relation entre la "Ligne du Cameroun" et la direction de l'Adamaoua : 1. Pétrologie, Géochimie et Structure des Granitoïdes Panafricains de la zone de cisaillement Foumban-Bankim (Ouest-Cameroun et Adamaoua). 2. pétrologie et géochimie des formations magmatiques tertiaires associées (Thèse de Doctorat d'_Etat). Université de Yaoundé I, Cameroun, 392.

Njonfang, E., Ngako, V., Kwekam, M., Affaton, P., 2006. Les orthogneiss calcoalcalins de Foumban-Bankim : témoins d'une zone interne de marge active panafricaine en cisaillement. Comptes Rendus Geosci.338, 606-616.

Njonfang, E., Ngako, V., Moreau, C., Affaton, P., Diot, H. (2008). Restraining bends in high temperature shear zones: "The Central Cameroon Shear Zone", Central Africa. Journal of African Earth Sciences 52, 9-20.

Nkono C., Féménias O., b, Daniel Demaiffe D., 2014. Geodynamic model for the development of the Cameroon Hot Line (Equatorial Africa). Journal of African Earth Sciences. 100, 626–633.

Nkoumbou, C., Barbey, P., Yonta-Ngouné, C., Paquette, J.L., Villiéras, F., 2014. Precollisional geodynamic context of the southern margin of the Pan-African fold belt in Cameroon. Journal of African Earth Sciences 99, 245–260.

Nkoumbou, C., Barbey, P., Yonta-Ngouné, C., Paquette, J.L., Villiéras, F., 2014. Precollisional geodynamic context of the southern margin of the Pan-African fold belt in Cameroon. Journal of African Earth Sciences. 99, 245–260.

Nkoumbou, C., Barbey, P., Yonta-Ngouné, C., Paquette, J.L., Villiéras, F., 2014. Precollisional geodynamic context of the southern margin of the Pan-African fold belt in Cameroon. Journal of African Earth Sciences. 99, 245–260.

Nnange, J.M., Ngako, V., Fairhead, J.D. and Ebinger, C.J., 2000. Depths to density discontinuities beneath the Adamawa Plateau region, Central Africa, from spectral analyses of new and existing gravity data. Journal of African Earth Sciences, 30(4), 887-901.

Ntomba, S. M., Ndong B. F., Messi Ottou J. E., Goussi Ngalamo F. J, Bisso, D., Magnekou Takamte C. R., Mvondo Ondoa J., 2016. Phlogopite compositions as an indicator of both the geodynamic context of the granitoids and the metallogeny aspect in Membe'ele Archean Area, northwestern Congo craton. Journal of African Earth Sciences. 18, 231-244.

Nwankwo, C. N. and Ekine, A., 2009. Geothermal gradients in the Chad Basin, Nigeria, from bottom hole temperature logs.

Nyblade, A., Dirks, P., Durrheim, R., Webb, S., Jones, M., Cooper, G. and Graham, G., 2008. AfricaArray: developing a geosciences workforce for Africa's natural resource sector. The Leading Edge 27, 1358-1361.

Nzenti, J. P., Barbey, P., Jegouzo, P, Moreau, C. (1984). Un nouvel exemple de ceinture granulitique dans une chaîne protérozoïque de collision : les migmatites de Yaoundé au Cameroun. C.R. Académie des Sciences Paris 299, 1197-1199.

Nzenti, J.P., 1998. Neoproterozoic alkaline meta-igneous rocks from the Pan-African North Equatorial Fold Bel (Yaounde, Cameroon): biotitites and magnetite rich pyroxenites. Journal of African Earth Sciences, 26(1), 37-47.

Nzenti, J.P., Barbey, P., Macaudiere, J. and Soba, D., 1988. Origin and evolution of the late Precambrian high-grade Yaounde gneisses (Cameroon). Precambrian Research, 38(2), 91-109.

Nzolang, C., 2005. Crustal evolution of the Preacambrian basement in west Cameroon: inference from geochemistry, Sr–Nd and experimental investigation of some granitoids and metamorphic rocks. Ph.D. Thesis. Graduate School of Science and Technology, Niigata University, Japan, 207.

Ojo, A.O., Ni, S., Li, Z., 2017. Crustal radial anisotropy beneath Cameroon from ambient noise tomography. Tectonophysics 696–697, 37–51.

Oliveira, E.P., Toteu, S.F., Araújo, M.N.C., Carvalho, M.J., Nascimento, R.S., Bueno, J.F., McNaughton, N. and Basilici, G., 2006. Geologic correlation between the Neoproterozoic

Sergipano belt (NE Brazil) and the Yaoundé belt (Cameroon, Africa). Journal of African Earth Sciences, 44(4), 470-478.

Owona, S., Schulz, B., Ratsbacher, L., Mvondo-Ondoa, J., Ekodeck, G.E., Tchoua, F., Affaton, P., 2011. Pan-African metamorphic evolution in the southern Yaounde Group (Oubanguides Complex, Cameroon) as revealed by EMP-monazite dating and thermobarometry of garnet metapelites. Journal of African Earth Sciences. 59, 125–139.

Pasyanos, M., Masters, G., Laske, G., and Ma, Z. (2012). Litho1.0 -an updated crust and lithospheric model of the earth developed using multiple data constraints. Fall Meeting, AGU, San Francisco, Calif., Abstract:3–7 Dec. 2012.

Pavlis, N.K., Holmes, S.A., Kenyon, S.C. and Factor, J.K., 2008. An earth gravitational model to degree 2160: EGM2008. EGU General Assembly 4, 4-2.

Penaye, J., Kröner, A., Toteu, S.F., Van Schmus, W.R. and Doumnang, J.C., 2006. Evolution of the Mayo Kebbi region as revealed by zircon dating: An early (ca. 740Ma) Pan-African magmatic arc in southwestern Chad. Journal of African Earth Sciences, 44(4), 530-542.

Penaye, J., Toteu, S.F., Michard, A., Bertrand, J.M., Dautel, D. (1989). Reliques granulitiques d'âge Protérozoïque inférieur dans la zone mobile Panafricaine d'Afrique Centrale au Cameroun; Géochronologie U – Pb sur zircon. C.R. Académie des Sciences Paris 309, 315-318.

Penaye, J., Toteu, S.F., Tchameni, R., Van Schmus, W.R., Tchakounté, J., Ganwa, A., Minyem, D. and Nsifa, E.N., 2004. The 2.1 Ga West central African belt in Cameroon: extension and evolution. Journal of African Earth Sciences, 39(3), 159-164.

Penaye, J., Toteu, S.F., Van Schmus, W.R. and Nzenti, J.P., 1993. U-Pb and Sm-Nd preliminary geochronologic data on the Yaoundé series, Cameroon: re-interpretation of the granulitic rocks as the suture of a collision in the centrafrican belt. Comptes rendus de l'Académie des sciences. Série 2, Mécanique, Physique, Chimie, Sciences de l'univers, Sciences de la Terre, 317(6), 789-794.

Pin, c. & Poidevin, J. L. (1987). U-Pb zircon evidence for Pan-African granulite facies metamorphism in Central African Republic. A new interpretation of the high-grade series of the northern border of the Congo craton. Precambrian Research, 36, 303-312.

Plomerova, J., Babuška, V., Dorbath, C., Dorbath, L. and Lillie, R. J., 1993. Deep lithospheric structure across the Central African shear zone in Cameroon. Geophysical Journal International 115, 2, 381-390.

Poidevin J.-L., Pin C. 1986. 2 Ga U–Pb zircon dating of Mbi granodiorite (Central African Republic) and its bearing on the chronology of the Proterozoic of Central Africa, Journal of African Earth Sciences. 5–6, 581–587.

Pouclet, A., Tchameni, R., Mezger, K., Vidal, M., Nsifa, E., Shang, C. and Penaye, J., 2007. Archaean crustal accretion at the northern border of the Congo Craton (South Cameroon). The charnockite-TTG link. Bulletin de la Société géologique de France, 178(5), pp.331-342.

Poudjom Djomani, Y., Nnange, J., Diament, M., Ebinger, C., Fairhead, J. 1995. Effective elastic thickness and crustal thickness variations in west central Africa inferred from gravity data. Journal of Geophysical Research: Solid Earth 100, 22047-22070.

Poudjom Djomani, Y.P., Diament, M., Wilson, M. 1997. Lithospheric structure across the Adamawa plateau (Cameroon) fromgravity studies. Tectonophysics 273, 317-327.

Poudjom Djomani, Y. P., O'Reilly, S. Y., Griffin, W. L., Morgan, P., 2000. The density structure of subcontinental lithosphere through time. Earth and Planetery Science Letters 184, 605-624.

Pratt, J.H., 1855. On the attraction of the Himalaya Mountains, and of the elevated regions beyond them, upon the plumb-line in India. Philosophical Transactions of the Royal Society of London, 145, pp.53-100.

Priestley, K. and McKenzie, D., 2006. The thermal structure of the lithosphere from shear wave velocities. Earth and Planetary Science Letters, 244(1), 285-301.

Princivalle F., Salviulo, G., Marzoli, A. & Piccirillo, E.M., 2000. Clinopyroxene of spinel-peridotite mantle xenoliths from Lake Nji (Cameroon Volcanic Line, W Africa): crystal chemistry and petrological implications, Contrib. Mineral. Petrol., 139, 503–508.

Reigber, C., Lühr, H. and Schwintzer, P., 2002. CHAMP mission status. Advances in Space Research 30, 2, 129-134.

Reigber, C., Schwintzer, P. and Luehr, H., 1996. CHAMP–a challenging mini-satellite payload for geoscientific research and application. Erste Geodaetische Woche, Stuttgart 7, 12, 4.

Reusch, A.M., Nyblade, A.A., Tibi, R., Wiens, D.A., Shore, P.J., Bekoa, A., Tabod, C.T. and Nnange, J.M., 2011. Mantle transition zone thickness beneath Cameroon: evidence for an upper mantle origin for the Cameroon Volcanic Line. Geophysical Journal International, 187(3), 1146-1150.

Ritsema, J. & Allen, R.M., 2003. The elusive mantle plume, Earth planet. Sci. Lett., 207, 1–12.

Sanchez-Rojas, J. and Palma, M., 2014. Crustal density structure in northwestern South America derived from analysis and 3-D modeling of gravity and seismicity data. Tectonophysics, 634, 97-115.

Schubert, G., 2001. Mantle convection in the Earth and planets. Cambridge University Press

Shang, C.K., Satir, M., Nsifa, E.N., Liégeois, J.P., Siebel, W. and Taubald, H., 2007. Archaean high-K granitoids produced by remelting of earlier Tonalite–Trondhjemite–Granodiorite (TTG) in the Sangmelima region of the Ntem complex of the Congo craton, southern Cameroon. International Journal of Earth Sciences, 96(5), 817-841.

Shang, C.K., Satir, M., Siebel, W., Nsifa, E.N., Taubald, H., Liégeois, J.P. and Tchoua, F.M., 2004. TTG magmatism in the Congo craton; a view from major and trace element geochemistry, Rb–Sr and Sm–Nd systematics: case of the Sangmelima region, Ntem complex, southern Cameroon. Journal of African Earth Sciences, 40(1), 61-79.

Simmons, N.A., Forte, A.M., Boschi, L. and Grand, S.P., 2010. GyPSuM: A joint tomographic model of mantle density and seismic wave speeds. Journal of Geophysical Research: Solid Earth, 115(B12).

Stein, C.A. and Cochran, J.R., 1985. The transition between the Sheba Ridge and Owen Basin: rifting of old oceanic lithosphere. Geophysical Journal International, 81(1), 47-74.

Stuart, G.W., Fairhead, J.D., Dorbath, L. and Dorbath, C., 1985. A seismic refraction study of the crustal structure associated with the Adamawa Plateau and Garoua Rift, Cameroon, West Africa. Geophysical Journal International, 81(1), 1-12.

Subrahmanyam, C., 1978. On the relation of gravity anomalies to geotectonics of the Precambrian terrains of the south Indian shield. Geological Society of India, 19(6), 251-263.

Tadjou, J.M., Nouayou, R., Kamguia, J., Kande, H.L. and Manguelle-Dicoum, E., 2009. Gravity analysis of the boundary between the congo graton and the pan-africal belt of cameroon. Austrian journal of earth sciences, 102(1).

Talla Takam, Makoto, A., Kokonyangi, J., Dunkley, D.J., Nsifa, E.N., 2009. Paleoarchean charnockite in the Ntem Complex, Congo Craton, Cameroon: insights from SHRIMP zircon U-Pb ages. J. Mineral. Petrol. Sci. 104, 1-11.

Tapley, B.D., Bettadpur, S., Watkins, M. and Reigber, C., 2004. The gravity recovery and climate experiment: Mission overview and early results. Geophysical Research Letters, 31(9).

Tchakounte J., Eglinger A., Toteu S. F., Zeh A., Nkoumbou C., Mvondo-Ondoa J., Penaye J., de Wit M., Barbey P., 2017. The Adamawa-Yade domain, a piece of Archaean crust in the Neoproterozoic Central African Orogenic belt (Bafia area, Cameroon). doi.org/10.1016/j.precamres.

Tchakounté Numbem, J., Toteu, S. F., Van Schmus, W. R., Penaye, J., Deloule, E., Mvondo Ondoua, J., Bouyo Houketchang, M., Ganwa, A. A., White, W. M., 2007. Evidence of ca. 1.6-Ga detrital Zircon in the Bafia Group (Cameroon): Implication for the chronostratigraphy of the Pan-African Belt north of the Congo craton. Comptes Rendus de l'Académie des Sciences 339, 132-142.

Tchakounté, J.N., Toteu, S.F., Van Schmus, W.R., Penaye, J., Deloule, E., Mvondo- Ondoa, J., Bouyo Houketchang, M., Ganwa, A.A., White, W., 2007. Evidence of ca 1.6-Ga detrital zircon in the Bafia Group (Cameroon): Implication for the chronostratigraphy of the Pan-African Belt north on the Congo craton. C.R. Geoscience 339, 132–142.

Tchameni, R., 1997. Géochimie et géochronologie des formations de l'Archéen et du Paléoprotérozoïque du Sud-Cameroun (Groupe du Ntem, Craton du Congo) (Doctoral dissertation).

Tchameni, R., Mezger, K., Nsifa, N.E. and Pouclet, A., 2000. Neoarchaean crustal evolution in the Congo Craton: evidence from K rich granitoids of the Ntem Complex, southern Cameroon. Journal of African Earth Sciences, 30(1), 133-147.

Tchameni, R., Mezger, K., Nsifa, N.E. and Pouclet, A., 2001. Crustal origin of Early Proterozoic syenites in the Congo craton (Ntem complex), South Cameroon. Lithos, 57(1), 23-42.

Tchameni, R., Lerouge, C., Penaye, J., Cocherie, A., Milesi, J.P., Toteu, S.F., Nsifa, N.E., 2010. Mineralogical constraint for metamorphic conditions in a shear zone affecting the Archean Ngoulemakong tonalite, Congo Craton (Southern Cameroon) and retentivity of U-Pb SHRIMP zircon dates. Journal of African Earth Sciences. 58, 67-80.

Tchameni, R., Sun, F., Dawaï, D., Danra, G., Tékoum, L., Negue, E.N., Vanderhaeghe, O., Nzolang, C. and Dagwaï, N., 2016. Zircon dating and mineralogy of the Mokong Pan-African magmatic epidote-bearing granite (North Cameroon). International Journal of Earth Sciences, 105(6), pp.1811-1830.

Tchouankoue J. P., Wambo, S. N. A., Dongmo K. A., Li X. H., 2014. 40Ar/39 Ar dating of basaltic dykes swarm in western Cameroon; Evidence of late paleozoic and Mesozoic magmatism in the corridor of the Cameroon Line. Journal of African Earth Sciences, 93, 133-147.

Tchouankoue, J. P., Li X. H., Ngo Belnoun, R. N., Mouafo L.,Valderez Pinto Ferreira v., P., 2016. Timing and tectonic implications of the Pan-African Bangangte syenomonzonite, West Cameroon: Constraints from in-situ zircon U-Pb age and Hf-O isotopes. Journal of African Earth Sciences 124, 94-103.

Pierre Tchouankoue, J., Wambo, N.A.S., Dongmo, A.K. and Wörner, G., 2012. Petrology, geochemistry, and Geodynamic implications of basaltic Dyke Swarms from the southern Continental part of the Cameroon volcanic line, Central Africa. The Open Geology Journal, 6(1), pp.72-84.

Tedla, G.E., Van Der Meijde, M., Nyblade, A.A. and Van Der Meer, F.D., 2011. A crustal thickness map of Africa derived from a global gravity field model using Euler deconvolution. Geophysical Journal International, 187(1), 1-9.

Tenzer, R., Gladkikh, V., Novák, P. and Vajda, P., 2012. Spatial and spectral analysis of refined gravity data for modelling the crust–mantle interface and mantle-lithosphere structure. Surveys in Geophysics, 33(5).

Theunissen, K., Lenoir, J.L., Liegois, J.P., Delvaux, D. and Mruma, A., 1992. Empreinte Pan-Africaine majeure dans la chaîne ubendienne de Tanzanie Sud-occidentale : géochronologie U-Pb sur zircon et contexte structural. Comptes rendus de l'Académie des sciences. Série 2, Mécanique, Physique, Chimie, Sciences de l'univers, Sciences de la Terre, 314(12).

Tokam, A.P.K., Tabod, C.T., Nyblade, A.A., Julià, J., Wiens, D.A. and Pasyanos, M.E., 2010. Structure of the crust beneath Cameroon, West Africa, from the joint inversion of Rayleigh wave group velocities and receiver functions. Geophysical Journal International, 183(2).

Torge, W. (1991). Geodesy. De Gruyter.

Toteu, S. F., 1990. Geochemical characterization of the main petrographical and structural units of Northern Cameroon: implications for Pan-African evolution. Journal of African Earth Sciences (and the Middle East) 10, 4, 615-624.

Toteu, S.F., Michard, A., Bertrand, J.M. and Rocci, G., 1987. U/Pb dating of Precambrian rocks from northern Cameroon, orogenic evolution and chronology of the Pan-African belt of central Africa. Precambrian Research, 37(1), 71-87.

Toteu, S.F., Penaye, J. and Djomani, Y.P., 2004. Geodynamic evolution of the Pan-African belt in central Africa with special reference to Cameroon. Canadian Journal of Earth Sciences, 41(1), 73-85.

Toteu, S.F., Penaye, J., Deloule, E., Van Schmus, W.R. and Tchameni, R., 2006b. Diachronous evolution of volcano-sedimentary basins north of the Congo craton: insights from U–Pb ion microprobe dating of zircons from the Poli, Lom and Yaoundé Groups (Cameroon). Journal of African Earth Sciences, 44(4), 428-442.

Toteu, S.F., Van Schmus, W.R., Penaye, J. and Michard, A., 2001. New U–Pb and Sm–Nd data from north-central Cameroon and its bearing on the pre-Pan African history of central Africa. Precambrian Research, 108(1), 45-73.

Toteu, S.F., Van Schmus, W.R., Penaye, J. and Nyobe, J.B., 1994. U-Pb and Sm-Nd edvidence for Eburnian and Pan-African high-grade metamorphism in cratonic rocks of southern Cameroon. Precambrian Research, 67(3), 321-347.

Toteu, S.F., Yongue Fouateu, R., Penaye, J., Tchakounté, J., Seme Mouangue, A.C., Van Schmus, W.R., Deloule, E., Stendal, H. (2006a). U-Pb dating of plutonic rocks involved in the nappe tectonic in southern Cameroon: consequence for the Pan-African orogenic evolution of the central African fold belt. Journal of African Earth Sciences 44, 479-493.

Trabant, C., Hutko, A., Bahavar, M., Karstens, R., Ahern, T., and Aster, R. (2012).Data products at the iris dmc: stepping-stones for research and other application,.Seism Res Lett, 83(6), 846–854.

Trompette, R (1994). Geology of Western Gondwana (2000-500 Ma). Pan-African- Brasiliano aggregation of South America and Africa. A.A. Balkema edition, Rotterdam:350p.

Tselentis, G. A., Drakopoulos, J., Dimtriads, K. 1988. A spectral approach to Moho depths estimation from gravity measurement in Epirus (NW Greece), Journal of the Physics of the Earth 36, 255–266.

Tugume, F., Nyblade, A., Julià, J. and van der Meijde, M., 2013. Precambrian crustal structure in Africa and Arabia: evidence lacking for secular variation. Tectonophysics, 609, 250-266.

Vail, J.R., 1972. Jebel Marra, a dormant volcano in Darfur Province, Western Sudan. Bulletin of Volcanology 36, 251-265.

Van der Lee, S. and Nolet, G., 1997. Seismic image of the subducted trailing fragments of the Farallon plate. Nature, 386(6622).

Van der Meijde, M., Julià, J. and Assumpção, M., 2013. Gravity derived Moho for South America. Tectonophysics, 609, 456-467.

Van Schmus, W.R., de Brito Neves, B.B., Hackspacher, P. and Babinski, M., 1995. UPb and SmNd geochronologic studies of the eastern Borborema Province, Northeastern Brazil: initial conclusions. Journal of South American Earth Sciences, 8(3-4), 267-288.

Van Schmus, W.R., Oliveira, E.P., Da Silva Filho, A.F., Toteu, S.F., Penaye, J. and Guimarães, I.P., 2008. Proterozoic links between the Borborema Province, NE Brazil, and the Central African Fold Belt. Geological Society, London, Special Publications, 294(1), 69-99.

Vicat, J.P., Leger, J.M., Nsifa, E., Piguet, P., Nzenti, J.P., Tchameni, R. and Pouclet, A., 1996. Distinction within the Congo craton in South-West Cameroon of two doleritic episodes initiating the Eburnean (Palaeoproterozoic) and Pan-African (Neoproterozoic) orogenic cycles. Comptes rendus de l academie des sciences serie ii fascicule a-sciences de la terre et des planetes, 323(7), 575-582.

Vicat, J.P., Moloto-A-Kenguemba, G., Pouclet, A., 2001. Les granitoïdes de la couverture protérozoïque de la bordure nord du craton du Congo (Sud-Est du Cameroun et Sud-Ouest de la République Centrafricaine), témoins d'une activité magmatique post-kibarienne à pré-panafricaine. Comptes Rendus de l'Académie des Sciences, Paris 332, 235–242.

Vicat, J.P., Pouclet, A., Nkoumbou, C., Seme Mouangue, A.C., 1997. Le volcanisme fissural néoprotérozoïque des séries du Dja inférieur, de Yokadouma (Cameroun) et de Nola (RCA) – signification géotectonique. Comptes Rendus de l'Académie des Sciences, Paris 325, 671–677.

Wellmann, 1978. Gravity evidence for abrupt changes in the mean crustal density at the junction of Australian crustal blocks. Buerue of Mineral Resources Journal of Australian Geology and Geophysics 3, 153-162.

Woollard, G. P. (1971). The Earth crust and upper Mantle. National academy of sciences- national research council publication.

Yonta-Ngouné, C., Nkoumbou, C., Barbey, P., Le Breton, N., Montel, J.M., Villiéras, F., 2010. Geological context of the Boumnyebel talcschists (Cameroon): inferences on the Pan-African belt of Central Africa. Comptes Rendus Geoscience 342, 108–115.

Zanga-Amougou, A., Ndougsa-Mbarga, T., Meying, A., Layu, D.Y., Bikoro-Bi-Alou, M. and Manguelle-Dicoum, E., 2013. 2.5 D Modeling of Crustal Structures along the Eastern Cameroon and Western Central African Republic Derived from Finite Element and Spectral Analysis Methods. Geophysica, 49.

APPENDIX

<div align="center">**APPENDIX I**</div>

Data Management Plan

I. Types of Data

Data used in this study included satellite gravity data from the World Gravity Model 2012 (WGM12) downloaded from the Bureau Gravimetrique International website and Seismological data obtained from the Department of Geoscience of Kiel University (Germany)

II. Data and Metadata Standards

The WGM12 model comprises of surface gravity measurements (from land, airborne and marine surveys), and satellite gravimetry (from the GRACE mission). The Bouguer gravity data were computed using the spherical correction instead of the regular slab correction. Passive seismic data was corrected from major noises.

III. Policies for Access and Sharing

The satellite gravity data can be downloaded from http://bgi.omp.obs-mip.fr/data-products/Toolbox/WGM2012-maps-vizualisation-extraction. The Seismoligical data can be obtained through the Department of Geoscience of Kiel University (Germany).

Any researcher seeking to perform repeatability of this project's tasks or manipulate the data for other processing schemes not included in this project proposal may do so by accessing freely online the data used during this research study.

IV. Policies and Provisions for Re-Use, Re-Distribution

The PIs will not put any restrictions on the use of the gravity data once publicly available. There are no economic, political or other embargoes that will be placed on the use of the data, nor privacy or ethical issues that will constrain the release of this data to the general public. Once published and made available in a publicly accessible data storage, the data can be used for any purpose deem fit by any user.

V. Plans for Archiving and Preservation of Access

Geophysical data and interpretations are available online upon request and in publications.

APPENDIX II

1. Ngalamo, J. F.G., Bisso, D., Abdelsalam, M.G., Atekwana, E.A., Katumwehe, A.B. and Ekodeck, G.E., 2017. Geophysical imaging of metacratonizaton in the northern edge of the Congo craton in Cameroon. Journal of African Earth Sciences, 129, pp.94-107.
2. Ngalamo, J.F.G., Sobh, M., Bisso, D., Abdelsalam, M.G., Atekwana, E. and Ekodeck, G.E., 2018. Lithospheric structure beneath the Central Africa Orogenic Belt in Cameroon from the analysis of satellite gravity and passive seismic data. Tectonophysics, 745, pp.326-337.